Phylogenetic Analyses of Postcranial Skeletal Morphology in Didelphid Marsupials

Author: Flores, David A.

Source: Bulletin of the American Museum of Natural History, 2009(320) : 1-81

Published By: American Museum of Natural History

URL: https://doi.org/10.1206/320.1

PHYLOGENETIC ANALYSES OF POSTCRANIAL SKELETAL MORPHOLOGY IN DIDELPHID MARSUPIALS

DAVID A. FLORES

Museo Argentino de Ciencias Naturales ''Bernardino Rivadavia''
Buenos Aires, Argentina
(dflores@macn.gov.ar)

BULLETIN OF THE AMERICAN MUSEUM OF NATURAL HISTORY
CENTRAL PARK WEST AT 79TH STREET, NEW YORK, NY 10024
Number 320, 81 pp., 40 figures, 8 tables
Issued March 17, 2009

 ISSN 0003-0090

CONTENTS

ABSTRACT

In this study I provide a phylogenetic hypothesis for didelphid Marsupials including a suite of 114 postcranial characters. The postcranial evidence was cladistically analyzed separately and concatenated with a nonmolecular data set previously published (71 cranio-dental-external characters). A combined analysis was done including published IRBP (interphotoreceptor retinoid binding protein, 1158 bp), DMP-1 (dentin matrix protein 1, 1176 bp), and RAG-1 (recombinase-activating gene, 2790 bp) sequences to the nonmolecular data set. In order to compare and evaluate the influence of the inclusion of postcranial morphology to previous hypotheses, the taxon sampling of didelphine ingroup was almost similar to the one used in recent series of papers on didelphid phylogeny. The postcranial information includes 48 characters from the axial skeleton, 37 from the anterior limb, and 29 from the posterior limb. I present anatomical descriptions for each postcranial character, adding details of different conditions observed among didelphine ingroup, as well as some functional implications. Different hypotheses that are discussed as polymorphic characters are alternatively treated as composite entries (CO) and transformation series (TS) in morphological and combined analyses. Different codings of polymorphic postcranial characters produce topologies that in general are not contradictory. The principal difference is the loss of resolution of trees in TS analysis, compared to CO analysis in postcranial evidence, whereas the support values were in general low in both codings. The topology obtained from postcranial evidence supported some already recovered relationships, such as the monophyly of the large opossums (*Didelphis*, *Philander*, *Chironectes*, *Lutreolina*, and *Metachirus*), and several polytypic groups such as *Didelphis*, *Monodelphis*, *Marmosops*, *Thylamys*, *Micoureus*, and *Philander*. Additionally, the intermediate position of *Hyladelphys* between calorumyines and didelphines is kept in CO analysis. The inclusion of the postcranial data set to previous nonmolecular evidence causes little incongruence, although some modifications in the topology and support values were detected. The effect of different codings of polymorphic characters was similar respect to the postcranial-only data set. In this case, the topology obtained with CO analysis was also notably better resolved than TS analysis. Similarly to the postcranial-only analysis, the topologies obtained in the total morphological evidence applying the two kinds of codings are highly congruent, but the TS treatment seemed not to contribute to retention of more phylogenetic information, since the CO analysis was better resolved. The relationships obtained adding the postcranial evidence to published combined data set (i.e., morphology, IRBP, DMP-1, and RAG-1 sequences) were mostly better resolved and supported in the CO coding than the morphological analyses, although the TS coding causes loss of resolution in the strict consensus. In this sense, some strong differences on deep branch topology can be detected depending on the treatment applied to polymorphic entries and partitioned analyses (e.g., phylogenetic condition of the mouse opossums, nodes C and B). Including the postcranial evidence in the total data set, I also recovered the intermediate position of *Hyladelphys*, but never the distantly related clades recently recovered by the inclusion of RAG-1 sequences (clades B + I *in* Gruber, K.F., R.S. Voss, and S.A. Jansa. 2007. Base-compositional heterogeneity in the RAG1 locus among didelphid marsupials: implications for phylogenetic inference and the evolution of GC content. Systematic Biology 56: 1–14). However, the position of *Metachirus nudicaudatus* and *Tlacuatzin canescens* is highly affected. Excluding the last gene, the partitioned combined analysis considering postcranial evidence was highly congruent with previous IRBP, morphology, and combined topologies, especially in the TS analysis, where all already defined nodes were recovered. The inclusion of postcranial evidence to the previous combined data set actually improves the support values when RAG-1 is eliminated. However, even when the topologies from both kinds of codings of polymorphic data were considerably congruent, the mouse opossums were clustered in CO analysis (although including *Metachirus* if RAG-1 sequences are included). The application of different criteria for the treatment of polymorphic data affects the relationships and phyletic condition of the mouse opossums. Finally, I discuss the postcranial morphology as evidence of didelphid phylogeny, as well as the new postcranial synapomorphies found in the monophyletic groups recovered in the didelphid crown group.

INTRODUCTION

Didelphid marsupials represent a living Neotropical radiation including around 85 species (Gardner, 2005) ranging from Canada to Patagonia. Through the past decades, the study of the New World living marsupials has been focused in diverse disciplines, resulting in an important amount of information available, ranging from systematics and taxonomy to anatomy, ontogeny, behavior, ecology, biogeography, physiology, and cytogenetics. As indicated by Voss and Jansa (2003), this interesting group represents the most diverse living radiation of the old endemic fauna that evolved in South America during the Tertiary isolation, and it is the only large radiation of metatherian mammals outside of Australia (Simpson, 1971; Patterson and Pascual, 1972).

In studies of marsupial evolution, didelphids were traditionally identified as ''primitive'' relative to the remaining marsupial families (Bensley, 1903; Gregory, 1910) and were thought to be models to extrapolations for Paleogene and Cretaceous metatherian biology (e.g., Crompton and Hiiemae, 1970; Crompton and Hylander, 1986; Crompton, 1989). Additionally, some modern studies placed either Didelphimorphia or Ameridelphia (i.e., Didelphimorphia + Paucituberculata) as the basal branch of the marsupial clade (see Horovitz and Sánchez-Villagra, 2003; Asher et al., 2004). However, it is widely recognized at present that living didelphids are not ''living fossils'', and even though they are considered basal relative to most of the Australasian living marsupials, they are derived relative to most Cretaceous and Paleogene metatherians (Clemens, 1968; Szalay, 1982, 1994; Reig et al., 1987; Wible, 1990; Goin, 1993; Horovitz and Sánchez-Villagra, 2003; Sánchez-Villagra et al., 2007).

In a morphological and distributional framework, didelphids have been traditionally diagnosed by plesiomorphies and biogeographical patterns, and some studies have demonstrated the failures of morphological characters to recover didelphids as a monophyletic group (see Kirsch and Archer, 1982; Wroe et al., 2000). The phylogenetic study by Horovitz and Sánchez-Villagra (2003) provides some unambiguous and unreversed postcranial synapomorphies for Didelphidae (e.g., calcaneal notch for cuboid present, or ridge on proximal articular facet of metacarpal I present). However, only two taxa representing the whole family were considered in that paper (*Didelphis* and *Monodelphis*), as the main scope was focused on a high-level marsupial relationship. In this sense, a more inclusive taxon sampling is neccesary for scoring most postcranial characters described in didelphids, detecting phylogenetic information in a family-level context as well. The same lack of a denser taxon sampling was noted for other morphological characters such as sperm morphology and mammary pattern (Jansa and Voss, 2005). On the contrary, IRBP (interphotoreceptor retinoid binding protein, 1158 bp) sequences provide strong evidence of didelphid monophyly, since the family is supported for 10 uniquely derived and unreversed transformations (Jansa and Voss, 2000, 2005) in the context of a higher taxonomic sample.

The study of the phylogenetic relationships in didelphids has been based on different points of view, resulting in occasionally well-supported hypotheses with evidence from diverse sources. For instance, the monophyly of the large $2n = 22$ opossums was recovered using different kinds of data (e.g. Creighton, 1984; Reig et al., 1987; Kirsch and Palma, 1995; Jansa and Voss, 2000, 2005; Flores, 2003; Voss and Jansa, 2003; Gruber et al., 2007), whereas in other cases there were conflicting patterns, as the paraphyletic condition of some genera of mouse opossums, currently considered as taxonomically valid (see Gardner, 2005). According to Voss and Jansa (2003), the incongruence among different hypotheses is likely caused by several factors, such as disparate taxon sampling, use of nonmonophyletic supraspecific taxa as terminals, discrepant scoring of the same character, different rooting criteria and algorithms, and voucher misidentifications.

Recently, the study of didelphid phylogeny has expanded markedly due to new knowledge and interpretations of the external and internal anatomy, new DNA sequence information from nuclear genes (e.g., IRBP, DMP-1 [dentin matrix protein 1, 1176 bp], RAG-1 [recombinase-activating gene, 2790

bp]), inclusion of a larger taxonomic sample, and taxonomic clarification of some polytypic groups. The ingroup relationships in didelphids obtained in previous papers were partially summarized by Jansa and Voss (2000) and Voss and Jansa (2003). The molecular evidence available for a higher didelphid taxonomic sample includes sequences of different nuclear genes, such as IRBP (Jansa and Voss, 2000; 2005), DMP-1 (Jansa and Voss, 2005; Jansa et al., 2006), and RAG-1 (Gruber et al., 2007). Additionally, the morphological evidence used in a cladistic background consists of craniodental, external anatomy, and karyotypes (see Voss and Jansa, 2003 and citations therein). In relation to this diverse array of evidence, interesting hypotheses based in combined analyses were recently obtained (Voss and Jansa, 2003; Jansa and Voss, 2005; Gruber et al., 2007), whose topologies show some stability, since in some cases they are congruent, independent of the type of characters employed. Additionally, the wide taxonomic sample available made possible the formulation of more inclusive phylogenetic hypotheses. In this sense, the recent addition of new taxa such as *Chacodelphys formosa* (Voss et al., 2004) or *Hyladelphys kalinowskii* (Jansa and Voss, 2005) in some cases has modified topologies or changed the support values in different clades.

The more recent hypothesis on didelphid phylogeny based on nonmolecular characters (Jansa and Voss, 2005: fig. 1C) included craniodental, external, and karyological characters. In the topology obtained, the large 2n = 22 opossums (i.e., *Didelphis*, *Philander*, *Lutreolina*, and *Chironectes*) were recovered as a monophyletic group, closely related to the monophyletic *Monodelphis* and the 2n = 14 *Metachirus*. The mouse opossums resulted in a paraphyletic group, of which only *Gracilinanus*, *Cryptonanus*, and *Marmosops* were recovered as monophyletic. The position of the monotypic *Chacodelphys* was basal to the *Lestodelphys* + *Thylamys* group, and *Hyladelphys* was placed basal to the whole didelphine crown group (i.e., intermediate between caluromyines and didelphines). The combination of the morphological data set with genetic information (i.e., IRBP, DMP-1, and RAG-1 sequences) caused a better resolution on the topologies obtained with morphology alone, and the support values of most nodes had ≥75% bootstrap support. In this scheme, the large opossums were equally recovered, as well as several mouse opossum genera (i.e., *Thylamys*, *Cryptonanus*, *Gracilinanus*, *Marmosops*, *Micoureus*, and *Monodelphis*), and the position of *Hyladelphys* was similar to the results from morphological data (i.e., basal to the didelphine group, except including RAG-1 sequences). It is clear that at present the phylogenetic relationships on didelphid groups are based on profuse evidence, which in general does not exhibit substantial conflict. As stated by Jansa and Voss (2000), the node-by-node comparison of different hypotheses obtained by different sources suggested that many cases of conflict do not reflect considerable incongruence of data.

Although the study of the postcranial morphology in metatherians has received notable attention, most of it was focused on functional, ontogenetic, and descriptive frames, but not phylogenetics (e.g., Coues, 1869; Flower, 1885; Elftman, 1929; Barnett and Napier, 1953; Mann-Fischer, 1953; Jenkins and Weijs, 1979; Klima, 1987; White, 1990; Pridmore, 1992; Marshall and Sigogneau-Russell, 1995; Lunde and Schutt, 1999; Argot, 2001, 2002, 2003a, 2003b, 2004a, 2004b; Martin and Mackay, 2003; Muizon and Argot, 2003; but see Szalay, 1994; Szalay and Sargis, 2001; Horovitz and Sánchez-Villagra, 2003). The study of Horovitz and Sánchez-Villagra (2003) contains numerous postcranial characters treated in high-level taxonomic categories that are interpreted in a cladistic context. Some characters described in that paper have shown some variability in the ingroup considered in this report, being parsimony informative in lower taxonomic levels. Additionally, several previous papers detected notable morphological variation in the postcranial skeleton of the taxa treated, in a descriptive or functional frame. In this sense, the identification and inclusion of postcranial characters in an appropriate taxonomic sample is significant in order to be analyzed in a cladistic framework. It is essential to know the influence of inclusion of the postcranial characters, identifying con-

gruences as well as incongruences among previous hypotheses based in other sorts of characters, and to integrate this evidence in a combined analysis to obtain hypotheses based on all available evidence of didelphid phylogeny.

In this study, I conducted a cladistic analysis of living didelphids based on postcranial characters, and I describe the postcranial character variations among 38 didelphid species, including most of those previously analyzed in other morphological frameworks (e.g., Voss and Jansa, 2003). Having considered practically the same taxonomic sample used in recent phylogenetic analyses (Voss and Jansa, 2003; Jansa and Voss, 2005; Voss et al. 2006; Jansa et al., 2006; Gruber et al., 2007) for comparative purposes, this data set was incorporated in the previous data set available (i.e., craniodental and external anatomy, karyology, plus IRBP, DMP-1, and RAG-1 sequences). I analyzed the postcranial and previously known morphological characters separately and in combination with the molecular data. I also explored the congruence and conflict between both kinds of data sets. The addition of postcranial characters to the known phylogenetic evidence is essential, since in some situations it could improve the support values on previously recognized monophyletic groups, although in other circumstances it could contradict those topologies. Furthermore, I provide additional character information in order to reach a comprehensive perception of the postcranial variation within the living didelphid group.

TABLE 1
Taxonomic Diversity of Extant Didelphid Genera (Sensu Gardner, 2005, Except in Taxa Indicated) and Number of Included Species per Taxon in the Postcranial Analysis

Genera	No. species	No. included species
Caluromysiops	1	1
Caluromys	3	2
Chironectes	1	1
Cryptonanus[a]	5	1
Didelphis	6	3
Glironia	1	1
Gracilinanus	6	2
Hyladelphys	1	1
Lestodelphys	1	1
Lutreolina	1	1
Marmosa	9	4
Marmosops[b]	14	5
Metachirus	1	1
Micoureus	6	3
Monodelphis[c]	20	3
Philander[d]	7	3
Thylamys	10	4
Tlacuatzin	1	1
Total	92	38

[a]Genus recently recognized by Voss et al. (2006); species previously included in *Gracilinanus*.

[b]Including *M. creightoni* (see Voss et al., 2004).

[c]Including *M. ronaldi* (see Solari, 2004) and *M. handleyii* (see Solari, 2007).

[d]Including *P. mondolfii*, *P. deltai* (see Lew et al., 2006), and *P. olrogi* (see Flores et al., 2008).

MATERIALS AND METHODS

Taxon Sampling

I analyzed the osteological postcranial morphology in 4 outgroups and 34 ingroup didelphid taxa (table 1; appendix I). In order to reach a viable comparison and combination with morphological and genetic data sets previously published in recent phylogenetic studies on didelphids (Voss and Jansa, 2003; Jansa and Voss, 2005; Jansa et al., 2006; Gruber et al., 2007), the outgroup considered is composed of a caluromyine group including *Glironia venusta* (root), two species of *Caluromys*, and *Caluromysiops irrupta*. The ingroup includes practically the same didelphine taxa as the ones in the cited papers. Postcranial samples for four species (*Chacodelphys formosa*, *Gracilinanus emiliae*, *G. aceramarcae*, *Marmosa lepida*, and *Cryptonanus chacoensis*) could not be examined in this analysis, since the material is apparently nonexistent in extant systematic collections. All polytypic groups were represented by several species in order to test the monophyletic condition of each supraspecific group (table 1). In general, I examined several adult specimens of both sexes per taxon in order to detect polymorphism (table 2). However, some species with scarce postcranial material deposited in systematic collections (e.g., *Glironia venusta*, *Hyladelphys kalinowskii*, *Philander mcilhennyi*, or *Marmosa rubra*) were represented by only one or two specimens (see appendix 1).

TABLE 2
Polymorphic Characters Observed on Postcranial Morphology in Didelphid Taxa
(For details, see character descriptions.)

Taxa	Character no.
Caluromys lanatus	35
Caluromysiops irrupta	15, 52
Chironectes minimus	35, 63, 87, 97
Cryptonanus unduaviensis	22
Didelphis virginiana	35, 47, 110
D. albiventris	35, 47, 66
D. marsupialis	35, 47, 59, 66, 110
Gracilinanus agilis	2, 17, 62, 63, 68, 77
Lutreolina crassicaudata	47
Micoureus demerarae	18, 60, 70
M. regina	17, 18, 20, 34, 88
M. paraguayanus	1, 2, 59, 60, 62, 66, 70, 77
Marmosops incanus	47
M. noctivagus	2, 17, 35, 40, 57
M. pinheiroi	40, 60
M. impavidus	22, 35
Marmosa mexicana	111
M. robinsoni	2, 13, 22, 35, 43, 47, 59, 66, 67, 68
M. murina	35, 47, 66, 77
Metachirus nudicaudatus	2, 8
Philander opossum	3, 47, 59, 102
P. frenatus	2, 87
Thylamys pallidior	22
T. pusillus	1, 2, 57, 66
T. venustus	4, 20, 22, 40
Tlacuatzin canescens	11, 47

Postcranial Character Scoring

The parsimony analysis of didelphid species-level relationships is based on a suite of new and partially scored postcranial characters (see character descriptions and appendix 2) and the comparison and combination with the morphological data matrix previously defined by Voss and Jansa (2003). Australasian and American nondidelphid taxa were not considered part of the outgroup. Consequently, several postcranial characters that could define the didelphid position with respect to nondidelphid marsupials (see Szalay, 1994; Szalay and Sargis, 2001; Horovitz and Sánchez-Villagra, 2003) were not incorporated, as they are apparently invariant in the didelphid ingroup considered here. On the other hand, some characters described in the previous cladistic analysis of Horovitz and Sánchez-Villagra (2003) illustrated significant variation when a didelphid denser taxon sampling was included, and thus they were reanalyzed in this context of didelphid systematics. The complete morphological data set is composed of 185 characters (table 3), of which 114 are new and reanalyzed postcranial characters: 48 from the axial skeleton, 37 from anterior limbs, and 29 from posterior limbs. The remaining 71 characters were described by Voss and Jansa (2003) and include craniodental, external, and karyological evidence. In this way, the taxonomically variable postcranial characters come mainly from direct observation of the material under study and from reinterpretation of characters previously defined in studies with taxonomic, systematic, or a functional-descriptive perspective (e.g., Flower, 1885; Elftman, 1929; Barnett and Napier, 1953; Mann-Fischer, 1953; Jenkins and Weijs, 1979; Szalay, 1982, 1994; Marshall and Sigogneau-Russell, 1995; Muizon, 1998; Argot, 2001, 2002, 2003a, 2003b, 2004a, 2004b; Szalay and Sargis, 2001; Horovitz and Sánchez-Villagra, 2003; Muizon and Argot, 2003).

In a few cases, postcranial elements were incomplete, destroyed, or in bad condition. In such cases, published descriptions or drawings were consulted to assess the correct character state. Due to the absence of information in some cases, I scored the relevant matrix cells as missing (“?”). Those that resulted from unsuitable comparisons (table 4) were scored as inapplicable (“–”).

In the postcranial data matrix, I defined both binary and multistate characters, where three or more alternative conditions were observed. In some cases, multistate characters could be logically ordered in a transformation series, but in other situations no compelling justification for ordering could be found (see the character descriptions). In the analyses, I included both parsimony informative characters and few autapomorphies (table 3). The latter were not eliminated because of reasons mentioned by Voss and Jansa (2003); that is, scoring autapomorphies is required to preserve the homologies in unordered multistate characters that contain parsimony informative characters, such scoring facilitates the recovery of taxon diagnoses from the data matrix, and some autapomorphies can be parsimony informative in a

TABLE 3
Comparison of Three Data Set Characteristics of Nonmolecular Data Matrix
(See text for explanation of combined nonmolecular data set.)

	Jansa and Voss (2005)	Postcranial	Combined nonmolecular data set
No. terminal taxa[a]	44	38	44
No. cells	3124	4332	8140
Missing	109 (3%)	85 (2%)	871 (11%)
Inapplicable	33 (1%)	44 (1%)	77 (1%)
No. characters	71	114	185
Parsimony-informative characters	67 (94%)	106 (93%)	173 (94%)
Autapomorphic characters	4 (6%)	8 (7%)	12 (7%)
Binary characters	53 (75%)	66 (58%)	119 (64%)
Ordered multistate characters	12 (17%)	47 (41%)	59 (32%)
Unordered multistate characters	6 (8%)	1 (0.9%)	7 (4%)

[a]The postcranial data set does not include *Chacodelphys formosa*, *Cryptonanus chacoensis*, *Gracilinanus aceramarcae*, *G. emiliae*, *Marmosa lepida*, and *Monodelphis emiliae*, but they are included in the combined nonmolecular data set (coded "?" for postcranial characters).

more denser taxon sampling and could be used in future analyses. On the other hand, to consider autapomorphies in the ingroup might eventually serve as synapomorphies for clades represented by a single taxon in the present analysis (Weksler, 2006). Proper polarity of characters was determined after rooting the trees.

The treatment of polymorphic characters was done following two methods in order to detect the influence of different criteria in the topology and support values. In the first mode, I considered the polymorphic condition as composite states (CO) in a transformation series or in a binary character (i.e., polymorphic conditions between two character states 0 and 1, coded as {01} for a taxon with states 0 and 1 observed among its exemplars). Alternatively, the polymorphic condition was considered as an intermediate character state in a transformation series (TS), and the series is treated as ordered (see Campbell and Frost, 1993; Wiens, 1999, 2000; Voss and Jansa, 2003; Weksler, 2006). The binary character with the polymorphic condition takes the form of a multistate character with an ordered transformation series, and the intermediate condition represents the polymorphism. With the intermediate character state representing the polymorphism, the transformations $0 \leftrightarrow 1$ and $1 \leftrightarrow 2$ each were weighed to 0.5 relative to the unit weight (1.0) assigned to the transformation $0 \leftrightarrow 1$ in a binary character without polymorphism. Obviously, polymorphism does not always occur in a binary character. In multistate characters, the polymorphism is included as a transitional state between two different conditions observed (whose weight is assigned with the same procedure mentioned above) so that it adds one condition to the ordered transformation series, and the multistate character is assumed as ordered.

The postcranial data matrix presented herein was composed in order to analyze the internal didelphid relationships and compare and combine with recent data sets including a denser taxon sampling (Voss and Jansa, 2003; Jansa and Voss, 2005). For this reason, it is not situable to define nondidelphid marsupial relationships. The position of didelphids and their relationships in a supraordinal context are beyond the scope of this report, but a postcranial data matrix including several nondidelphid Australasian, American, and some fossil taxa is in preparation as part of a subsequent report.

Phylogenetic Analysis

I performed parsimony analyses of postcranial evidence both separately and in combination with the nonmolecular data set (craniodental and external) devised by Jansa and Voss (2005), as well as in the supermatrix obtained by combining all the nonmolecular evidence, with IRBP, DMP-1, and RAG-1 sequences. The sequences can be aligned

TABLE 4
Postcranial Data Completeness for Didelphid Terminal Taxa

	Inapplicable	Missing	% Complete
Glironia venusta	3	0	97
Caluromysiops irrupta	1	0	99
Caluromys lanatus	2	0	98
C. philander	2	0	98
Metachirus nudicaudatus	0	0	100
Philander opossum	1	0	99
P. franatus	1	0	99
P. mcilhenyii	1	3	96
Didelphis virginiana	1	0	99
D. albiventris	1	0	99
D. marsupialis	1	0	99
Lutreolina crassicaudata	2	3	96
Chironectes minimus	0	0	100
Tlacuatzin canescens	0	2	98
Thylamys pallidior	1	0	99
T. pusillus	1	2	97
T. venustus	2	4	94
T. macrurus	1	1	98
Monodelphis brevicaudata	1	1	98
M. adusta	0	10	91
M. theresa	2	0	98
Micoureus paraguayanus	0	12	89
M. regina	0	1	99
M. demerarae	0	0	100
Marmosa rubra	2	3	95
M. robinsoni	1	0	99
M. mexicana	1	0	99
M. murina	0	3	97
Marmosops impavidus	1	1	98
M. parvidens	2	0	98
M. pinheiroi	1	2	97
M. noctivagus	2	1	97
M. incanus	2	0	98
Lestodelphys halli	1	13	88
Cryptonanus unduaviensis	3	1	96
Gracilinanus agilis	1	0	99
G. microtarsus	1	13	88
Hyladelphys kalinowskii	3	1	96

unambiguously among didelphids (Jansa and Voss, 2000; Jansa et al., 2006; Grueber et al., 2007). In both morphological and combined analyses, the characters were equally weighted. All of the postcranial, total morphology, and combined matrices were analyzed with two different coding for polymorphic entries explained in the ''Postcranial Character Scoring'' section; that is, CO and TS analyses, respectively. For all parsimony analyses I used the program TNT (Goloboff et al., 2004) to search for optimal trees under equal weights. I conducted heuristic, unconstrained searches for optimal trees using tree bisection-reconnection (TBR) branch-swapping in each of 100 replications of random taxon addition sequences, keeping up to 10 trees per replication. A second TBR round was applied to each of the optimals in order to increase the confidence of finding all topologies of minimum length. Zero-length branches were collapsed and strict consensus trees were generated. Clade support was estimated using both absolute Bremer support (Bremer, 1994) and character resampling (Goloboff et al., 2003). Values of absolute Bremer support were calculated following the approach of Giannini and Bertelli (2004) in order to prevent overestimation of support values. Specifically, they implemented a strategy for obtaining suboptimal trees in seven successive stages in which <2000 suboptimal trees were saved in each stage. First, I saved suboptimal trees that were one step longer than the optimals. Next, searches saved trees up to two to seven steps longer than the optimals. Thus, in the analysis a sample of $\geq 14{,}000$ suboptimal trees was used to calculate absolute Bremer support. In this way, I sampled several suboptimal trees that could be overlooked in a less careful selection of suboptimals, which would lead to overestimated support values. On the other hand, the resampling technique used was a variant of the jackknife implemented by Goloboff et al. (2003). Group frequency (based on unbiased symmetric resampling) was calculated on the basis of 2000 replications.

I combined the postcranial data set with the previously defined nonmolecular characters (Voss and Jansa, 2003; Jansa and Voss, 2005). Additionally, IRBP, DMP-1, and RAG-1 sequences were included, resulting in a supermatrix analyzed using the same parsimony procedures as described above. Finally, the patterns of congruence and conflict among separate analyses (i.e., postcranial only, total morphology, and com-

bined analysis) were evaluated by direct inspection of tree topologies and values of nodal support.

RESULTS

Postcranial Character Description

In this section I describe the variations observed on the skeletal morphology of the taxa included in the analysis. In most cases, some brief descriptions and comments about evolutionary or functional features were added to the character description, and the character state observed in the taxonomic sample is also reported. The 114 postcranial characters are listed by different skeletal sections as follows: atlas, axis, posterior cervical vertebrae, thoracic vertebrae, lumbar vertebrae, sacrum and caudal vertebrae, ribs and sternum, scapula, humerus, radius and ulna, pelvis and epipubic bones, femur, tibia and fibula, carpus and metacarpus, and tarsus. For the osteological and muscular terminology, I followed several works that treated skeletal and muscular morphology in mammals (e.g., Maynard Smith and Savage, 1955; Taylor, 1974, 1976; Evans, 1993; Gilbert, 1994; Sargis, 2002; Bezuidenbout and Evans, 2005; Whitehead et al., 2005) and specifically in marsupials (e.g. Elftman, 1929; Szalay, 1994; Marshall and Sigogneau-Russell, 1995; Muizon, 1998; Argot, 2001, 2002, 2003a, 2003b, 2004a, 2004b; Szalay and Sargis, 2001; Horovitz and Sánchez-Villagra, 2003).

Atlas

Character 1: Atlantal foramen: (0) absent; (1) present. In caluromyines and large opossums (*Didelphis*, *Philander*, *Chironectes*, *Lutreolina*, and *Metachirus*) the foramen is present, whereas in the mouse opossums in general this foramen is absent (except *Marmosa rubra*). Horovitz and Sánchez-Villagra (2003: ch. 1) reported asymmetry in the presence/absence of this character in some taxa such as *Monodelphis domestica*, *Dasyuroides*, and *Dromiciops*. I also found the same asymmetry in some specimens of *Thylamys pusillus* and *Micoureus paraguayanus*, and the taxa are treated as polymorphic (coded {01}).

Character 2: Atlas transverse foramen: (0) absent; (1) present. Although Horovitz and Sánchez-Villagra (2003: ch. 3) coded *Didelphis* as polymorphic, I did not see any specimen in the sample with the atlas transverse foramen completely closed. Notable ontogenetic variation was observed in *Metachirus*: in subadults and young specimens, the foramen is not completely closed, but shows a small ossified process that tends to close the foramina. This foramen is present in *Caluromysiops*, *Caluromys*, *Marmosa murina*, and *M. rubra*, but it is absent in most of the didelphid taxa included here. In the sample, individual variation is observed in *Philander frenatus*, *Metachirus*, *Thylamys pusillus*, *Marmosa robinsoni*, *Marmosops noctivagus*, and *Gracilinanus agilis* (coded {01}).

Character 3: Posterior extension of the transverse processes: (0) absent; (1) present. In the same way as Horovitz and Sánchez-Villagra (2003: ch. 4), I coded this character as present when the transverse processes extend caudally beyond the caudal facets for the axis articulation. Although Horovitz and Sánchez-Villagra (2003) coded *Didelphis* as polymorphic, in almost the complete sample analyzed here, *Didelphis* was scored as present. Only in young and subadult specimens is the extension absent, and one specimen of *D. virginiana* (AMNH 70082) exhibits the transverse process extended to the same level or almost posterior to the caudal facets for the axis. In general, *Philander opossum* exhibits the condition 0, but some specimens (e.g., AMNH 190446, 210408) show the processes barely extended beyond the caudal facets (coded {01}).

Character 4: Cranial facets shape: (0) only concave; (1) dorsal edge curved. Although the position of the occipital condyle shows variation in didelphids (Argot, 2003a), I did not note discrete interespecific variation of the atlas cranial facet shape. Here, this character is modified from Horovitz and Sánchez-Villagra (2003: ch. 5), because there are no taxa in the sample with the dorsal edges enveloping the occipital condyle, as shown in some Australasian groups. The dorsal border curved is the most common condition present in the didelphid crown group, although in *Thylamys pallidior*, *Tlacuatzin*, and *Hyladelphys* the cranial facet is only concave, and the polymorphic condition is evidenced in *Thylamys venustus*.

Character 5: Development of ventral tubercle: (0) without tubercle; (1) tubercle as a small protuberance, almost absent; (2) tubercle developed; (3) tubercle well developed, laminar shape. The ventral tubercle is a process on the ventral region of the vertebral body. Some muscles implied in neck flexion (such as m. longus colli and m. longus capitis) insert in this structure (Argot, 2003a; see Evans, 1993: fig. 6–31). In didelphids, this tubercle has several degrees of development. For instance, in *Philander* (state 2) this structure appears more developed than in *Didelphis* (state 1), whereas in *Gracilinanus*, *Metachirus*, *Chironectes*, and *Marmosa rubra* the tubercle is well developed and triangular in shape (state 3). In *Glironia*, *Caluromys*, *Caluromysiops*, *Lutreolina*, *Tlacuatzin*, and most species of *Marmosa* the tubercle is present but small. No information is currently available about this character for *Thylamys macrurus* (coded "?"). Since I observed intermediate conditions on the development of this structure, the character is treated as ordered ($0 \leftrightarrow 1 \leftrightarrow 2 \leftrightarrow 3$) in all analyses.

Character 6: Dorsal portion of the caudal articular fovea: (0) caudal articular fovea not posteriorly extended; (1) caudal articular fovea posteriorly extended. The caudal articular fovea appears caudally extended in most of the didelphid species considered here, although it is absent in *Didelphis* and *Caluromysiops*, where the fovea is short and not posteriorly extended.

Character 7: Caudal articular fovea shape: (0) caudal fovea oval in shape; (1) caudal fovea round in shape. The caudal articular fovea consists of two cavities that form a freely movable articulation with the second vertebra (Evans, 1993), and it provides for most cranial mobility (Argot, 2003a, 2003b). For this reason, the shape of the fovea has deep implications on head movements. The overall outline is round in shape in several taxa, such as *Glironia*, *Caluromysiops*, *Caluromys*, *Philander*, *Chironectes*, *Monodelphis*, *Gracilinanus*, *Micoureus*, *Cryptonanus unduaviensis*, *Marmosa robinsoni*, *M. murina*, *Lestodelphys*, and *Thylamys pusillus*. In contrast, it is oval in shape in *Didelphis*, *Metachirus*, *Marmosops*, *Marmosa rubra*, *Thylamys pallidior*, and *T. venustus*.

Character 8: Transverse process craniocaudal length with respect to the hemal arches craniocaudal length: (0) longer; (1) equal; (2) shorter. In this character, I compared the craniocaudal development of the transverse process in relation to the dorsal portion of hemal arches, independent of the transverse process posterior extension described in character 3. Several important muscles implied in head movements (e.g., Mm. obliquus capitis caudalis, obliquus capitis cranialis, splenius, and rectus capitis dorsalis minor) are related to the transverse process and the dorsal portion of the hemal arch (Coues, 1869; Filan, 1990; Evans, 1993; Argot, 2003a). Variations in development of hemal arches in some didelphids were evidenced by Argot (2003a: figs. 1, 4). In *Didelphis* and *Philander* the transverse process is notably larger than the craniocaudal dimension of the hemal arches, whereas in *Chironectes* and *Lestodelphys* there is similar development of both structures. Most of the remaining taxa included here exhibit a small transverse process with respect to the hemal arches. In this pattern, *Metachirus* exhibits the hemal arches very developed craniocaudally in relation to the transverse process (Argot, 2003a: fig. 1b). Since I observed an intermediate condition in the craniocaudal length of the transverse process with respect to the craniocaudal length of the hemal arches, this character is treated as ordered ($0 \leftrightarrow 1 \leftrightarrow 2 \leftrightarrow 3$) in all analyses.

Character 9: Lateral extension of the transverse process with respect to the lateral extension of the cranial articular fovea: (0) extended laterally beyond the cranial articular fovea; (1) extended laterally to the same level of the cranial articular fovea. The general pattern in didelphids is the condition 0. Thus, in most groups considered in this report, the transverse process is more laterally expanded with respect to the cranial articular fovea. To the contrary, a not very laterally expanded transverse process is present in some mouse opossums such as *Marmosops pinheiroi Thylamys* (except *T. macrurus*), and *Gracilinanus*.

Axis

Character 10: Posterior spinous process extension: (0) absent; (1) present (fig 1).

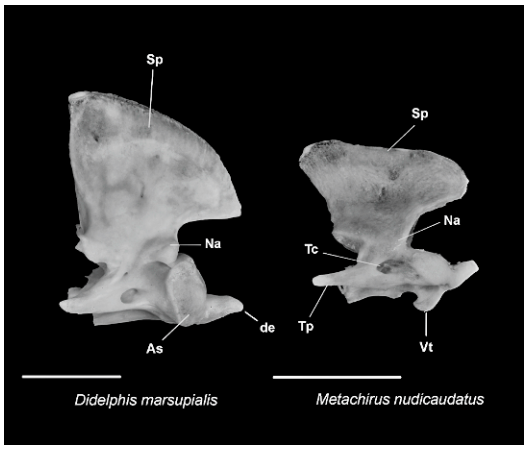

Fig. 1. *Didelphis marsupialis* (AMNH 21439) and *Metachirus nudicaudatus* (AMNH 244617), axis in lateral view. The spinous process (Sp) in *Metachirus* is posteriorly extended (ch. 10[1]), whereas in *Didelphis* it is not extended beyond the neural arches (Na) (ch. 10[0]). In *Didelphis*, the anterior extension of the dens (de) is barely anterior to the anterior tip of the spinous process (ch. 11[0]), whereas in *Metachirus* the dens is cranialy extended (ch. 11[2]). The ventral tubercle (Vt) is a uniform crest in *Didelphis* (ch. 14[0]), whereas in *Metachirus* it forms two protruding lobes (ch. 14[1]). Other abbreviations: As, articular surface; Tc, transverse canal; Tp, transverse process. Scale bars: 10 mm.

Similar to Horovitz and Sánchez-Villagra (2003: ch. 10), I coded this character as present when the neural spine extends posteriorly beyond the vertebral arches. Important muscles implied in the head movements, such as Mm. rectus capitis posterior, obliquus capitis caudalis, and spinalis capitis, originate in the axis spinous process (Coues, 1869; Filan, 1990; Evans, 1993; Sargis, 2001; Muizon and Argot, 2003; Argot, 2004a, 2004b). According to Muizon and Argot (2003) and Muizon (1998), the development of the occipital crest in the skull and the craniocaudal extension of the axis spinous process are indicative of a strong musculature of the neck, which is related to predatory habits. In didelphids, the axis spinous process does not show significant variation, since the process is posteriorly extended beyond the neural arches in most taxa included here, except for *Didelphis* and *Hyladelphys*, where the posterior extension of the spinous process is absent.

Character 11: Dens cranial extension relative to the cranial tip of the spinous process: (0) to the same level or barely anterior; (1) notably anterior (fig. 1). In head movements, where the atlantoaxial articulation is involved, the dens is used as a pivot (Argot, 2003a). On the other hand, a notable cranial extension of the axis spinous process would restrict neck mobility by contact with the caudal tip of the atlas (Evans, 1993; Sargis, 2001). Some large opossums such as *Caluromysiops*, *Caluromys*, *Didelphis*, and *Philander* exhibit the dens to the same level or barely anterior with respect to the anterior tip of the spinous process. Most of the remaining taxa show condition 1, and *Tlacuatzin* is scored as polymorphic for this character (coded {01}). No information is currently available about this character for *Marmosa murina* and *Gracilinanus microtarsus* (coded "?").

Character 12: Axis caudal articular surface fovea shape: (0) rounded shape; (1) oval shape. The caudal articular surface shape is rounded in some taxa, such as *Caluromysiops*, *Philander*, *Metachirus*, *Chironectes*, *Thylamys pallidior*, *T. venustus*, *Micoureus regina*, *Marmosa robinsoni*, *Marmosops*, and *Lestodelphys*. Instead, an oval caudal articular surface is observed in *Glironia*, *Caluromys*, *Didelphis*, *Lutreolina*, *Thylamys pusillus*, *Monodelphis*, *Marmosa rubra*, *Micoureus demerarae*, *Tlacuatzin*, and *Gracilinanus agilis*. No information is currently available about this character for *Marmosa murina*, *Gracilinanus microtarsus*, and *Hyladelphys* (coded "?").

Character 13: Inferior portion of neural arches shape in lateral view: (0) narrow; (1) wide (fig. 1). The contact of the neural arches with the vertebral body exhibits two different morphological patterns on the axis. On the one side, a very thin inferior portion of neural arches is observed in several taxa, such as *Glironia*, *Chironectes*, *Thylamys*, *Marmosa*, *Monodelphis*, *Marmosops*, *Gracilinanus*, and *Lestodelphys*. In contrast, in *Caluromysiops*, *Caluromys*, *Didelphis*, *Lutreolina*, *Philander*, *and Metachirus*, the inferior portion of neural arches is notably craniocaudally wide. Polymorphism is observed only in *Marmosa robinsoni*, which usually shows the condition 1, but some specimens (e.g.,

AMNH 257209, 206597, 140332) show the condition 0 (coded {01}).

Character 14: Ventral tubercle shape: (0) uniform crest; (1) two separate lobes; (2) without crest or lobe (fig. 1). The ventral tubercle of the axis exhibits different patterns in the taxa analyzed here. In some of them, such as *Caluromysiops*, *Caluromys*, *Didelphis*, *Philander*, *Chironectes*, *Micoureus*, *Marmosa murina*, and *Gracilinanus agilis* the ventral tubercle is simply an anteroposteriorly elongated uniform crest. A more complex shape is observed in *Glironia*, *Metachirus*, *Lutreolina*, *Thylamys*, *Monodelphis*, some species of *Marmosa*, *Marmosops*, and *Lestodelphys*, where the ventral tubercle takes the form of two separate lobes anteroposteriorly aligned. Finally, no trace of a crest or lobe is observed in *Tlacuatzin*. No information is currently available about this character for *Gracilinanus microtarsus* (coded "?"). As none of the conditions of the ventral tuberlcle morphology appears to be intermediate to the others, I treated this character as unordered.

Character 15: Neural arch cranial notch shape: (0) narrow; (1) wide. The notch in the cranial border of neural arch exhibits different morphologies in the taxa analyzed here. *Caluromys*, *Philander*, *Didelphis*, *Lutreolina*, *Micoureus demerarae*, *Marmosops impavidus*, and *M. noctivagus* show the notch narrow. In other groups, such as *Glironia*, *Chironectes*, *Metachirus*, *Thylamys*, *Tlacuatzin*, *Monodelphis*, *Micoureus regina*, *Marmosa*, *Gracilinanus*, *Marmosops parvidens*, *M. pinheiroi*, *Cryptonanus*, and *Lestodelphys*, the notch is notably wide. In the limited postcranial sample of *Caluromysiops* (see appendix 1), I observed polymorphism in this character, because in one specimen (AMNH 208101) the notch is wide, while in the other (AMNH 244364) the notch is markedly narrow (coded {01}).

Posterior Cervical Vertebrae

Character 16: C5 and T1 craniocaudal body length: (0) C5 and T1 craniocaudal body length subequal; (1) C5 craniocaudal body length shorter than T1. This character was described by Horovitz and Sánchez-Villagra (2003: ch. 18). The C5 and T1 body length determines the gap between vertebrae in the cervico-thoracic junction, a functionally important area where changes in the skeletal configuration occur during locomotion (Herbin et al., 2000). Most didelphids have the C5 craniocaudal body length subequal to or longer than T1. *Marmosa rubra* is autapomorphic in this character, because it shows the C5 body shorter than the T1 body.

Character 17: C6 spinous process shape: (0) absent; (1) protuberance; (2) lamina (fig. 4). The shape and development of the spinous process in posterior cervical vertebrae are important because it is where part of the deep musculature of the neck attaches, such as Mm. spinalis cervicis and multifidus cervicis (Mann Fischer, 1956; Argot, 2003a, 2003b; Evans, 1993). The shape variations of the C6 spinous process were described by Horovitz and Sánchez-Villagra (2003: ch. 20). In didelphids, different conditions in the C6 spinous process are present. *Caluromys*, *Caluromysiops*, *Didelphis*, *Philander frenatus*, *P. mcilhennyi*, *Metachirus*, *Lutreolina*, *Marmosa robinsoni*, *M. murina*, *Marmosops fuscatus*, and *Lestodelphys* show the C6 spinous process as laminar. Only a small protuberance is observed in *Glironia*, *Philander opossum*, *Mamrosa rubra*, *Thylamys pallidior*, *T. macrurus*, *Monodelphis*, *Micoureus demerarae*, *Marmosa mexicana*, and *Marmosops* (except *M. noctivagus*). Lastly, the spinous process in C6 is completely absent in *Tlacuatzin*, *Thylamys pusillus*, *T. venustus*, *Cryptonanus unduaviensis*, and *Gracilinanus microtarsus*. Additionally, polymorphism is observed in *Micoureus regina*, *Gracilinanus agilis*, and *Marmosops noctivagus*, as in some specimens the process is absent, whereas in others there is a small protuberance (coded {01}). As I observed an intermediate condition in the C6 spinous process shape, this character is treated as ordered ($0 \leftrightarrow 1 \leftrightarrow 2$) in all analyses.

Character 18: C7 transverse foramen: (0) absent; (1) present. This character is modified from Horovitz and Sánchez-Villagra (2003: ch. 21), since here I did not observe any taxa with the C7 transverse foramen incipient. The C7 transverse foramen is present in *Glironia*, *Caluromysiops*, *Caluromys*, *Didelphis*, *Philander opossum*, *P. frenatus*, *Chironectes*, *Marmosa rubra*, and *Monodelphis adusta*. This foramen is absent in *Philander mcilhennyi*,

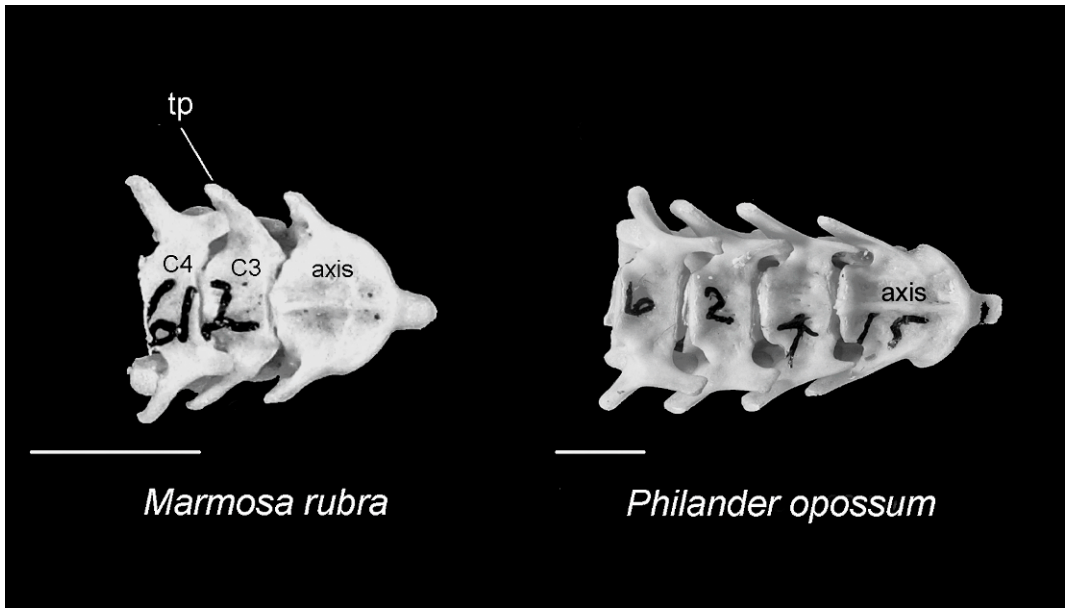

Fig. 2. *Marmosa rubra* (FMNH 124612) and *Philander opossum* (AMNH 262415), anterior cervical vertebrae in ventral view. In *Marmosa rubra*, the transverse process (Tp) on the third cervical (C3) has one head (ch. 21[0]), but in *Philander* it shows an anterior head (h) (ch. 21[1]). In both species the fourth cervical (C4) has two heads (ch. 22[1]). Scale bars: 5 mm.

Lutreolina, *Tlacuatzin*, *Thylamys*, *Monodelphis brevicaudata*, *M. theresa*, *Marmosa robinsoni*, *M. mexicana*, *M. murina*, *Marmosops*, *Gracilinanus*, *Cryptonanus*, and *Lestodelphys*. The polymorphic condition is present in *Metachirus*, *Micoureus demerarae*, and *M. regina* (coded {01}).

Character 19: C3–C7 spinous process size with respect to the spinous process of the axis: (0) lesser; (1) subequal (figs. 3, 4, 6). In general, didelphids show the spinous process of posterior cervical vertebrae shorter than that of the axis. Condition 1 is exhibited only in *Didelphis*, which has a rigid neck related with the hypertrophy of the spinous processes, and the particularly strong articulation in cervical vertebrae. This special morphology prevents the dorsiflexion and lateral movements of the neck, but it is difficult to relate it to any diet or locomotor specialization in *Didelphis* (Argot, 2003a).

Character 20: Relative size between C6 and C7 spinous process: (0) C7 spinous process taller than C6 spinous process; (1) C6 and C7 spinous process of similar size (fig. 4). I observed the C7 spinous process to be taller than C6 spinous process in *Glironia*, *Caluromysiops*, *Caluromys*, *Philander*, *Lutreolina*, *Tlacuatzin*, *Thylamys pusillus*, *Marmosa robinsoni*, *M. rubra*, *Marmosops parvidens*, *Cryptonanus unduaviensis*, *Gracilinanus agilis*, and *Lestodelphys*. In contrast, C6 and C7 spinous processes have a similar size in *Didelphis*, *Metachirus*, *Chironectes*, *Thylamys pallidior*, *T. macrurus*, *Monodelphis*, *Micoureus*, *Marmosa mexicana*, *M. murina*, *Marmosops* (except *M. parvidens*), and *Gracilinanus microtarsus*. In the sample of *Thylamys venustus*, I found a specimen (AMNH 261245) with a small C7 spinous process and another (AMNH 261253) without this process. Similarly, *Micoureus regina* exhibits the polymorphic condition, as a male specimen has the C7 spinous process taller than the C6 spinous process, whereas in a female specimen the spinous processes of both vertebrae are similar in size (coded {01}). No information is currently available about this character for *Marmosops pinheiroi* (coded "?").

Character 21: C3 transverse process heads: (0) one head; (1) two heads (fig. 2). The anterior part of the transverse process (called inferior lamellae) is present in some cervical

vertebrae in didelphids. Some essential muscles related with neck flexion, such as Mm. longus colli (pars cervicalis), longissimus cervis, intertransversarii dorsales cervicis, and intertransversarii ventrales cervicis (see Evans, 1993: figs. 6–28, 6–30; Argot, 2003a: fig. 4a), originate in this structure. In C3, the anterior portion of the transverse process is present in several taxa, such as *Caluromysiops*, *Caluromys*, *Didelphis*, *Philander*, *Chironectes*, *Metachirus*, and *Lutreolina*. On the other hand, in *Glironia* and mouse opossums this structure is absent.

Character 22: C4 transverse process heads: (0) one head; (1) two heads (fig. 2). The lamellae in the C4 transverse process are present in most species treated here. However, in some small opossums, such as *Thylamys pusillus*, *T. macrurus*, *Monodelphis adusta*, *M. theresa*, *Lestodelphys*, and *Hyladelphys*, the lamellae on C4 are absent. Individual variation in this character is common in *Thylamys pallidior*, *Marmosops impavidus*, *and Thylamys venustus*, *Marmosa robinsoni*, and *Cryptonanus unduaviensis* (coded {01}).

Character 23: C7 transverse process direction: (0) lateral; (1) ventrolateral. According to Argot (2003a), the C7 transverse process is anteriorly oriented in some taxa such as *Metachirus*. However, the variation of this process in didelphids is focused here on a lateral or ventrolateral C7 transverse process orientation. In some taxa, such as *Glironia*, *Caluromys*, *Caluromysiops*, *Didelphis*, *Thylamys pallidior*, *T. macrurus*, *Marmosa rubra*, and *M. mexicana*, the process is ventrolateral. On the other hand, in *Metachirus*, *Philander*, *Lutreolina*, *Chironectes*, *Tlacuatzin*, *Thylamys pusillus*, *T. venustus*, *Monodelphis*, *Micoureus*, *Lestodelphys*, *Marmosa murina*, *Marmosops*, *Gracilinanus*, *Cryptonanus*, and *Hyladelphys*, the process is laterally oriented.

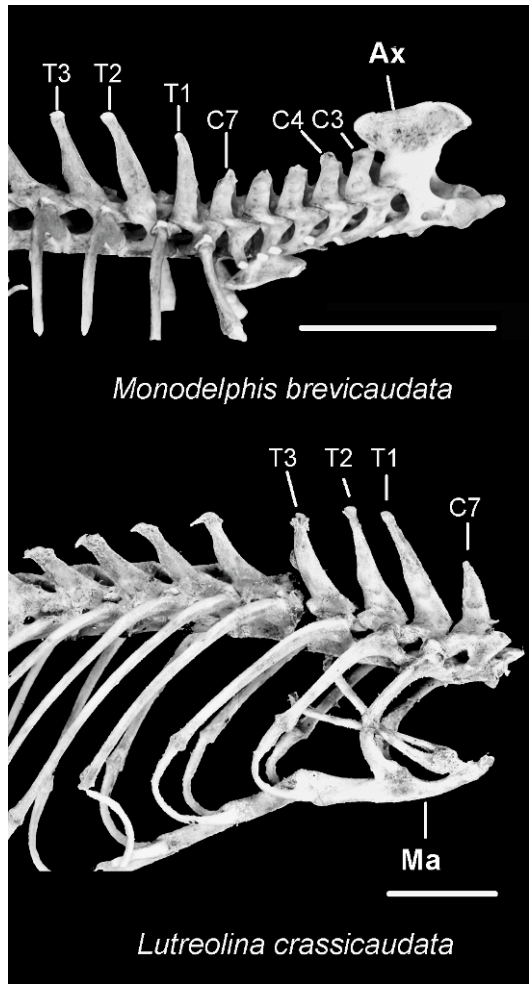

Fig. 3. *Monodelphis brevicaudata* (AMNH 257203) and *Lutreolina crassicaudata* (AMNH 133250), partial vertebral series in lateral view. In *Monodelphis*, C3–C5 spinous processes are lower than the axis spinous process (ch. 19[0]). The first thoracic vertebra with tall spinous process relative to other vertebrae is placed in the T2 position in *Monodelphis* (ch. 24[1]), but it is in the T1 position in *Lutreolina* (ch 24[0]). Abbreviation: Ma, manubrium of sternum. Scale bars: 10 mm.

Thoracic Vertebrae

Character 24: First thoracic vertebra with a tall spinous process relative to other vertebrae: (0) T1; (1) T2 (fig. 3). The muscular system that is located in the first two thoracic vertebrae is complex (Mann-Fischer, 1956; Filan, 1990). The M. splenius (which is involved in the support and movements of the head) originates in the spinous process of T1 (Argot, 2003a: fig. 4a; Evans, 1993). This character is modified from Horovitz and Sánchez-Villagra (2003: ch. 26), because it appears as multistate, with a third condition indicating the spinous process tall in T3. However, according to their published

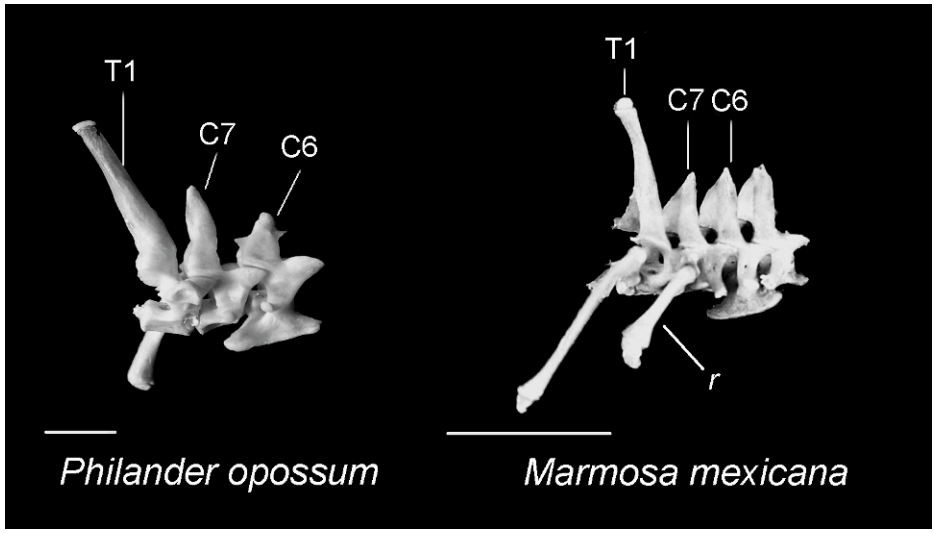

Fig. 4. *Philander opossum* (AMNH 262415) and *Marmosa mexicana* (ROM 99608), last cervical vertebrae and first thoracic vertebra in lateral view. In *Philander*, the C7 spinous process is taller than the C6 process (ch. 20[0]), whereas in *Marmosa mexicana* the C6 and C7 spinous processes are similar in size (ch. 20[2]). Note the C6 spinous process resembling a protuberance in both species (ch. 17[2]). Abbreviation: r, rib. Scale bars: 5 mm.

data matrix, there are not terminals with this condition. In the same work, the authors reported polymorphism in *Didelphis virginiana*, although in the sample examined, I did not find evidence of any individual variation in this species. All didelphid groups show spinous process of T1 tall relative to other vertebrae, except for *Monodelphis brevicaudata* and *M. theresa*, where the first tall spinous process is placed in T2.

Character 25: First thoracic vertebra with prezygapophysis facing laterally: (0) T2; (1) T3. This character was defined by Horovitz and Sánchez-Villagra (2003: ch. 27). All didelphid groups display T3 with prezygapophysis facing laterally, except for *Caluromys* and *Caluromysiops*, where the first prezygapophysis facing laterally is in T2. This condition is common in some Autralidelphians, such as *Dromiciops*, diprotodontians, and the dasyurid *Myoictis* (Horovitz and Sánchez-Villagra, 2003).

Character 26: T1 body craniocaudally extended in dorsal view: (0) absent; (1) present (fig. 5). The vertebral body extended craniocaudally in T1 occurs only in *Caluromysiops* and *Didelphis*.

Character 27: Position of the first thoracic vertebra with a low and craniocaudally expanded spinous process: (0) T10; (1) T11; (2) T12; (3) T13. The spinous process is low and craniocaudally enlarged in the posterior thoracic vertebrae, casually coincident with the position of the diaphragmatic vertebra. A short and wide spinous process restricts spinal mobility by decreasing intervertebral space (Sargis, 2001). In most taxa included in this analysis, the location of this kind of spinous process starts on T10. However, some species show variations departing from the most common condition. In *Glironia*, *Philander frenatus*, *Marmosa robinsoni*, *Marmosops noctivagus*, *M. incanus*, *M. parvidens*, *M. pinheiroi*, *Cryptonanus unduaviensis*, and *Gracilinanus microtarsus*, the process starts on T11; in *Lestodelphys* and *Tlacuatzin*, it starts on T12, whereas in *Chironectes* and *Hyladelphys* it starts on T13. The posterior position of this kind of spinous process in *Chironectes* indicates freer movements of the vertebral spine on the anterior portion, perhaps related to the particular swimming characteristic of this species. However, the specific mode of locomotion in *Hyladelphys*

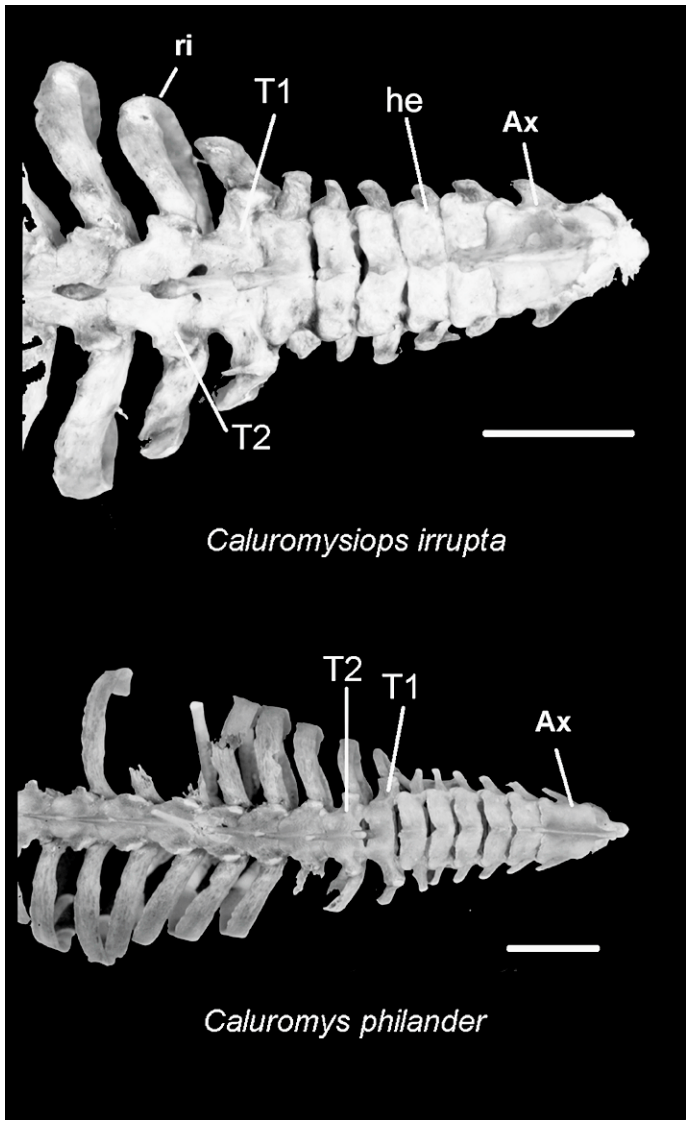

Fig. 5. *Caluromysiops irrupta* (AMNH 208101) and *Caluromys philander* (AMNH 267001), cervical and thoracic vertebrae in dorsal view. The T1 body in *Caluromysiops* is lengthened craniocaudally (ch. 26[1]), whereas this condition is not observed in *Caluromys* (ch. 26[0]). However, in both taxa the hemal arches in T1 are notably shorter than hemal arches in T2 (ch. 32[1]). Note the ribs (ri) flattened and craniocaudally expanded in both taxa (ch. 49[0]). Other abbreviations: Ax, axis; he, hemal arch. Scale bars: 10 mm.

is unknown. Due to the fact that *Lutreolina* does not show this kind of vetebra, I scored it as inapplicable ("–") for this character. Because I observed intermediate conditions in the position of the first thoracic vertebra with a low and craniocaudally expanded spinous process, this character is treated as ordered (0 ↔ 1 ↔ 2 ↔ 3) in all analyses.

Character 28: Position of the diaphragmatic vertebra: (0) T8; (1) T10; (2) T11; (3) T12; (4) T13. The mammillary process in the region is more developed in the posterior vertebrae. The diaphragmatic vertebrae represent a point of transition in the vertebral column, where the articulation displays a different articular mode, and therefore it

becomes functionally distinct (Argot, 2003a). Posterior to the diaphragmatic vertebra, the thoracic vertebrae become morphologically lumbarlike (Argot, 2003a). In this point, the contact between facets is more obliquely oriented, and therefore it reduces lateral bending and log-axis rotation of the vertebral column, allowing a sagittal flexion-extension of the spine (Rockwell et al., 1938; Washburn and Buettner-Janush, 1952; Pridmore, 1992; Shapiro and Jungers, 1994). The mammillary process of the diaphragmatic and postdiaphragmatic vertebrae is the point of origin of tendons for M. longissimus dorsi, a powerful extensor of the back (Argot, 2003a), and M. multifidus thoracis, which (along with other dorsal back muscles) fixes the vertebral column, especially in bilateral action (see Evans, 1993: fig. 6–30). Thus, the position of the diaphragmatic vertebra has an important functional significance.

I found a high variation in the location of the diaphragmatic vertebra among didelphids. In *Caluromys lanatus*, *Caluromysiops*, *Philander opossum*, and *P. frenatus*, the position is in T10. In *Glironia*, *Caluromys philander*, *Metachirus*, *Philander mcilhennyi*, *Lestodelphys*, *Lutreolina*, *Chironectes*, *Marmosa rubra*, *Thylamys pusillus*, *T. macrurus*, *Monodelphis brevicaudata*, *M. adusta*, *Micoureus demerarae*, and *Marmosops incanus*, the position is in T11. In *Tlacuatzin*, *Thylamys pallidior*, *T. venustus*, *Monodelphis theresa*, *Marmosa robinsoni*, *M. mexicana*, *M. murina*, *Marmosops impavidus*, *M. noctivagus*, *M. pinheiroi*, *Cryptonanus unduaviensis*, and *Gracilinanus*, this vertebra is in T12. Only *Micoureus regina* shows this vertebra in T13, and in *Didelphis* it is placed in T8, although according to Argot (2003a), this element is placed in the T9 position. Because I observed intermediate conditions in the position of the diaphragmatic vertebra, this character is treated as ordered ($0 \leftrightarrow 1 \leftrightarrow 2 \leftrightarrow 3 \leftrightarrow 4$) in all analyses.

Character 29: Position of the anticlinal vertebra: (0) T10; (1) T11; (2) L4; (3) L5; (4) L6; (5) S1. According to most previous definitions, the anticlinal vertebra is the element in which the orientation of the spinous process reverses from posterior to anterior (Mann Fischer, 1953; Evans, 1993; Shapiro, 1995; Muizon and Argot, 2003; Kurz, 2005). This morphology is a consequence of the tractions exerted by the common epaxial musculature, whose fibers insert on the tip of these processes (Mann Fischer, 1953; Muizon and Argot, 2003). This pattern is part of a functional complex that points toward the sagittal flexibility required for quadrupedal locomotion (Rockwell et al., 1938; Howell, 1965; Shapiro, 1995). According to Argot (2003a), there is no anticlinal vertebra in *Caluromys* and *Philander*, because all spinous process are posteriorly oriented. This is a general pattern evidenced in most didelphids (except for *Metachirus* and some species of *Marmosops*). However, and following the criterion of Evans (1993), I consider the anticlinal vertebra that in which the spinous process is nearest perpendicular to the long axis of the vertebral body, independent of the orientation of the spinous process on the posterior vertebrae. In this sense, an anticlinal vertebra is exhibited in didelphids, but its position is highly variable.

In some taxa, the anticlinal vertebra is placed posteriorly in the lumbar region, as in *Caluromys* and *Monodelphis theresa*, where it is observed on L6; or *Philander*, *Tlacuatzin*, *Thylamys pusillus*, *T. macrurus*, *Marmosops pinheiroi*, *Micoureus*, and *Cryptonanus*, where the anticlinal vertebra is on L5. The anticlinal vertebra is in L4 in *Hyladelphys*, *Lestodelphys*, *Marmosops parvidens*, *Thylamys venustus*, and *T. pallidior*. Other groups, such as *Didelphis*, *Metachirus*, *Monodelphis adusta*, *Marmosa robinsoni*, *M. mexicana*, *Marmosops incanus*, and *Gracilinanus microtarsus*, have the anticlinal vertebra in T11. The last group, which is composed of *Chironectes*, *Monodelphis brevicaudata*, *Marmosa murina*, *Marmosops imavidus*, and *M. noctivagus*, has the anticlinal vertebra located in T10. According to Argot (2003a), this element is in the third lumbar vertebra in *Metachirus*, but I observed that vertebra in the T11 position. As I observed intermediate conditions in the position of the anticlinal vertebra, this character is treated as ordered ($0 \leftrightarrow 1 \leftrightarrow 2 \leftrightarrow 3 \leftrightarrow 4 \leftrightarrow 5$) in all analyses.

Character 30: Position of the first vertebra where the accessory process is differentiated from the transverse process: (0) T6; (1) T7; (2) T8; (3) T9. The accessory process (called

anapophysis by some authors) appears in the posterior thoracic vertebrae. The accessory processes protrude posteriorly and lock the articulation with the following vertebra, restricting lateral flexibility. The transverse and accessory processes are completely separated in different vertebral positions. In *Caluromys* and *Philander mcilhennyi* the position is in T9, whereas in *Didelphis*, *Philander opossum*, *P. frenatus*, *Metachirus*, *Lutreolina*, *Monodelphis theresa*, *Micoureus regina*, *Marmosa robinsoni*, *M. mexicana*, *Marmosops impavidus*, *M. noctivagus*, *Cryptonanus unduaviensis*, and *Gracilinanus agilis*, the position is in T8. A third condition includes *Caluromysiops*, *Chironectes*, *Tlacuatzin*, *Thylamys*, *Monodelphis brevicaudata*, *M. adusta*, *Micoureus demerarae*, *Marmosa murina*, *M. rubra*, *Marmosops incanus*, *M. parvidens*, *M. pinheiroi*, and *Gracilinanus microtarsus*, where the position is in T7. Lastly, only *Lestodelphys* and *Glironia* show this vertebra in the T6 position. As I observed intermediate conditions in the position of the first vertebra where the accessory process is differentiated from the transverse process, this character is treated as ordered (0 ↔ 1 ↔ 2 ↔ 3) in all analyses.

Character 31: Caudal enlargement of the postzygapophysis in thoracic vertebrae 2–8: (0) absent; (1) present. In dorsal view, the postzygapophysis of the thoracic vertebrae 2–8 appears caudally enlarged only in *Glironia* and in the majority of small opossums (*Tlacuatzin*, *Marmosa*, *Micoureus*, *Marmosops*, *Thylamys*, *Monodelphis*, *Gracilinanus*, *Cryptonanus*, and *Lestodelphys*).

Character 32: Hemal arches in T1 notably shorter (craniocaudally) than hemal arches in T2: (0) absent; (1) present (fig. 5). Most of the taxa treated exhibit condition 0, except for *Glironia*, *Caluromys*, and *Caluromysiops*, in which the hemal arches in T1 are craniocaudally shorter than the hemal arches in T2.

Character 33: Spinous process posterior to the anticlinal vertebra cranially oriented: (0) absent; (1) present. As mentioned for character 29, the anticlinal vertebra is the element in which the orientation of the spinous process is almost perpendicular in relation to the horizontal plane of the body. The most common pattern evidenced in didelphids is that in which the spinous process of the postanticlinal vertebra does not change its orientation. Only in *Metachirus*, *Marmosops parvidens*, and *M. pinheiroi* are the spinous processes in postanticlinal vertebrae anteriorly oriented.

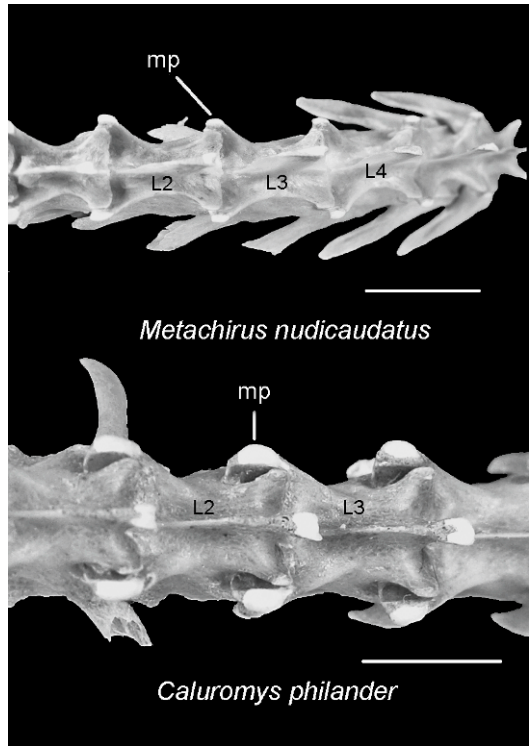

Fig. 6. *Metachirus nudicaudatus* (AMNH 267009) and *Caluromys philander* (AMNH 267001), lumbar vertebrae in dorsal view. In *Metachirus* the mammillary process (mp) of L3 is not anteriorly extended beyond the articulation with L2 (ch. 34[0]), whereas in *Caluromys* it is extended (ch. 34[1]). Scale bars: 10 mm.

Lumbar Vertebrae

Character 34: Extension of mammillary process in L3: (0) not beyond the anterior vertebra; (1) scarcely beyond the anterior vertebra (fig. 6). This character is modified from Horovitz and Sánchez-Villagra (2003: ch. 30) in which I consider different levels of anterior extension in the mammillary process (called metapophysis in the referenced work). The mammillary process in L3 is barely extended anteriorly in *Glironia*, *Caluromys*,

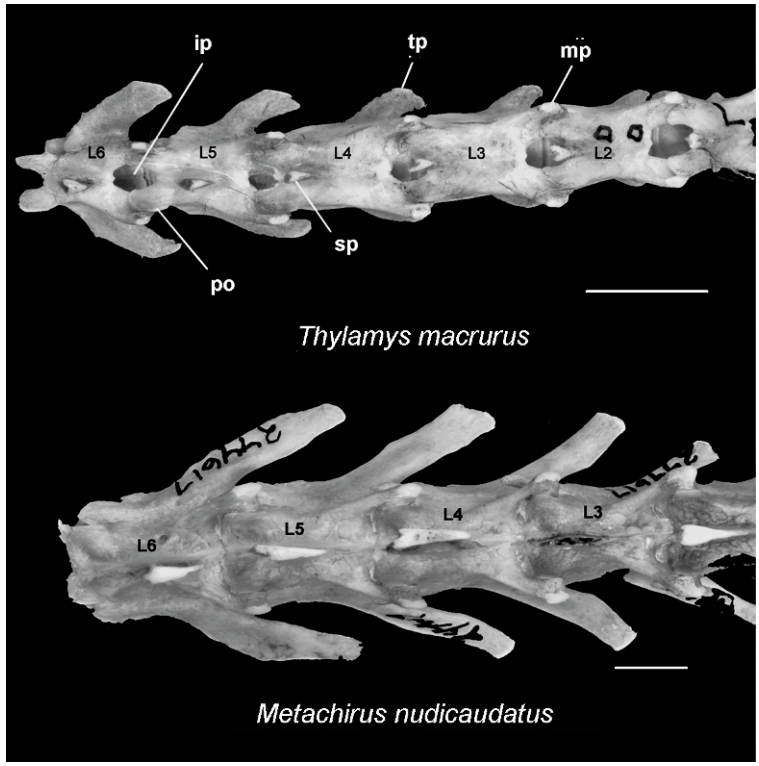

Fig. 7. *Thylamys macrurus* (MSB 70700) and *Metachirus nudicaudatus* (AMNH 244617), lumbar vertebrae in dorsal view. An intervertebral space (ip) is evident dorsally in *Thylamys* (ch. 36[0]), whereas in *Metachirus* this space is absent (ch. 36[1]). Other abbreviations: mp, mammillary process; po, postzygapophysis; sp, spinous process; tp, transverse process. Scale bar: 5 mm.

Caluromysiops, *Chironectes*, *Micoureus demerarae*, *Marmosa robinsoni*, *Marmosops noctivagus*, *M. incanus*, and *Cryptonanus unduaviensis*. Contrary to that, in *Metachirus*, *Lutreolina*, *Philander*, *Didelphis*, *Tlacuatzin*, *Thylamys*, *Monodelphis*, *Marmosa mexicana*, *M. murina*, *Marmosops impavidus*, *M. pinheiroi*, *M. parvidens*, and *Gracilinanus* the mammillary process does not extend beyond the anterior vertebra. Individual variation is observed just in *Micoureus regina* (coded {01}).

Character 35: Last lumbar vertebra, foramen on dorsal arch: (0) absent; (1) present. Although this character was described by Horovitz and Sánchez-Villagra (2003: ch. 29) only for the last lumbar vertebra, the foramen is present in all lumbar and most posterior thoracic vertebrae. I had seen evidence of individual variation and asymmetry in some didelphid taxa. Horovitz and Sánchez-Villagra (2003) coded *Didelphis* as 0, but I found notable asymmetry and individual variation in the sample analyzed (e.g., *D. albiventris* AMNH 205385; *D. marsupialis* AMNH 235003, 209164). Similarly, in most specimens of *Caluromys lanatus* the foramen is present, but in specimen AMNH 133199 it is absent. In the sample analyzed of *Chironectes* the asymmetry is the general condition. In the same way, some specimens of *Marmosa robinsoni* having no foramen are observed (AMNH 206596, 257210), and *M. murina* (AMNH 13659), *Marmosops impavidus* (AMNH 61382), and *M. noctivagus* (AMNH 136157) also exhibit asymmetry (coded {01}). Only *Marmosa mexicana* lacks the foramina.

Character 36: Intervertebral space in dorsal view: (0) intervertebral space evident; (1) intervertebral space reduced or absent (fig. 7). *Glironia* and the mouse opossums

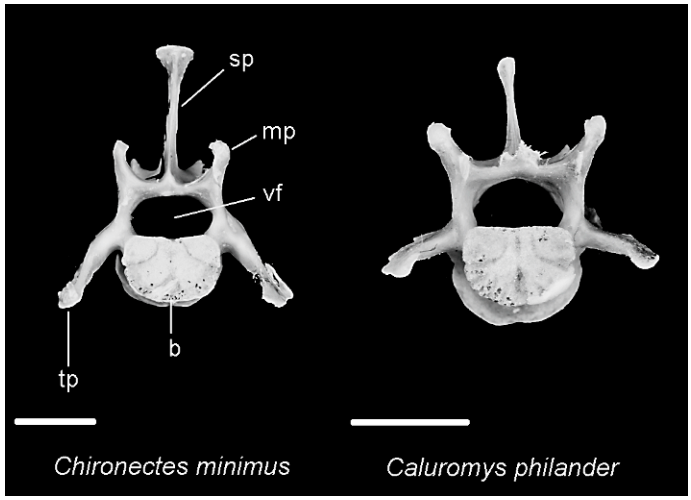

Fig. 8. *Chironectes minimus* (AMNH 264571) and *Caluromys philander* (AMNH 267001), fifth lumbar vertebra in anterior view. In *Chironectes*, the transverse process (tp) is ventrally extended beyond the vertebral body (b) (ch. 37[1]), whereas in *Caluromys* it is not extended beyond the vertebral body, being more laterally extended (ch. 37[0]). Other abbreviations: mp, mammillary process; sp, spinous process; vf, vertebral foramen. Scale bars: 5 mm.

have an evident intervertebral space in dorsal view, between the hemal arches of two contiguous vertebrae. In large opossums (including *Caluromys* and *Caluromysiops*) such space is absent.

Character 37: Ventral extension of L4–L6 transverse process: (0) not extended beyond the vertebral body; (1) extended beyond the vertebral body (fig. 8). The morphology of the lumbar transverse process has been related to the ventral flexion of the column (Shapiro, 1993, 1995; Johnson and Shapiro, 1998). In bounding-running forms, the ventral extension of the transverse process is related to an increased range of sagittal flexion (Shapiro, 1995, Sargis, 2001; Argot, 2003a) and creates a major space for epaxial musculature, particularly the lumbar division of m. longissimus dorsi (Sanders and Bodenbender, 1994; Shapiro, 1995, Sargis, 2001). The transverse process is ventrally extended beyond the vertebral body in some large opossums, except for *Glironia*, *Caluromys*, *Caluromysiops*, *Didelphis*, *Philander opossum*, and *P. mcilhennyi*, where the transverse process is not extended ventrally; a similar condition is also observed in mouse opossums. Instead, in *Metachirus*, *Lutreolina*, *Chironectes*, *P. frenatus*, and *Hyladelphys* the transverse process protrudes cranially and ventrally.

Sacrum and Caudal Vertebrae

Character 38: Number of vertebrae in contact with ilium: (0) one vertebra, (1) two vertebrae (fig. 9). This is a conservative character in the context of the taxonomic sample analyzed here, as most taxa analyzed here exhibit two vertebrae fused or in contact with ilium, except for *Glironia and Hyladelphys*, where only one vertebra (S1) is fused to ilium.

Character 39: Posterior process on the lateral sacral crest on S2: (0) absent; (1) present (figs. 9, 10). In general, didelphid taxa show a posterior process on S2, except for *Glironia*, *Marmosa rubra*, *Lestodelphys*, and *Hyladelphys*, where this process is clearly absent. No information is currently available about this character for *Gracilinanus microtarsus* (coded "?").

Character 40: Spinous process on sacrum: (0) spinous process just in S1; (1) spinous process present on S1 and S2 (fig. 11). Most of the didelphid group has a spinous process in both sacral vertebrae, except for *Glironia*, *Marmosops parvidens*, and *M. incanus*, where

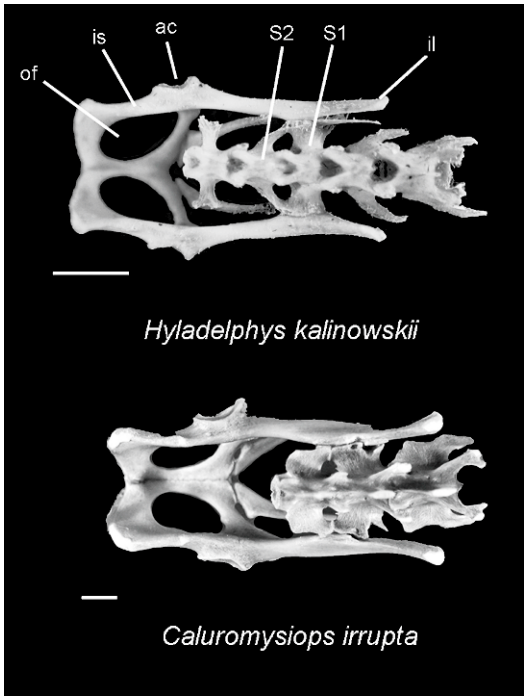

Fig. 9. *Hyladelphys kalinowskii* (RSV 1572) and *Caluromysiops irrupta* (AMNH 244364), pelvis, sacrum, and posterior lumbar vertebrae in dorsal view. In *Hyladelphys*, just the first sacral vertebra (S1) is contacting the illium (il) (ch. 38[0]), whereas in *Caluromysiops* both sacral elements (S1 and S2) are contacting the illium (ch. 38[1]). Note the absence of the posterior process on the lateral sacral crest of S2 in *Hyladelphys* (ch. 39[0]). Other abbreviations: ac, acetabulum; is, ischium; of, obturator foramen. Scale bars: 5 mm.

the process on S2 is absent. However, there is individual variation in the sample of *Thylamys venustus*, *Marmosops noctivagus*, and *M. pinheiroi* (coded {01}). No information is currently available about this character for *Gracilinanus microtarsus* (coded "?").

Character 41: Spinous process size on S1–S2: (0) S1 and S2 spinous processes of similar size; (1) S1 spinous process taller than S2 (fig. 11). In most didelphids, S1 and S2 have similar spinous process sizes. Only in some taxa, such as *Philander frenatus*, *P. mcilhennyi*, *Lutreolina*, *Chironectes*, *Metachirus*, *Marmosops pinheiroi*, *Thylamys macrurus*, and *Hyladelphys*, the S1 spinous process is taller than that of S2. The taxa coded 0 in character 40 are treated as inapplicable ("–") for this character. No information is currently available about this character for *Gracilinanus microtarsus* (coded "?").

Character 42: Ventral foramina on S1 body: (0) absent; (1) present (fig. 12). All taxa analyzed exhibit a ventral foramen on S1 body, except *Glironia*, *Caluromys*, *Caluromysiops*, and *Hyladelphys*.

Character 43: Caudal vertebra with transverse process length similar to vertebral body length: (0) absent; (1) present. In all taxa incuded in the analysis, the transverse process of the anterior caudal vertebrae forms a strong structure that protrudes laterally and expands craniocaudally. The muscles that insert in the apex of these processes are Mm. ischio-caudalis and abductor caudae dorsalis,

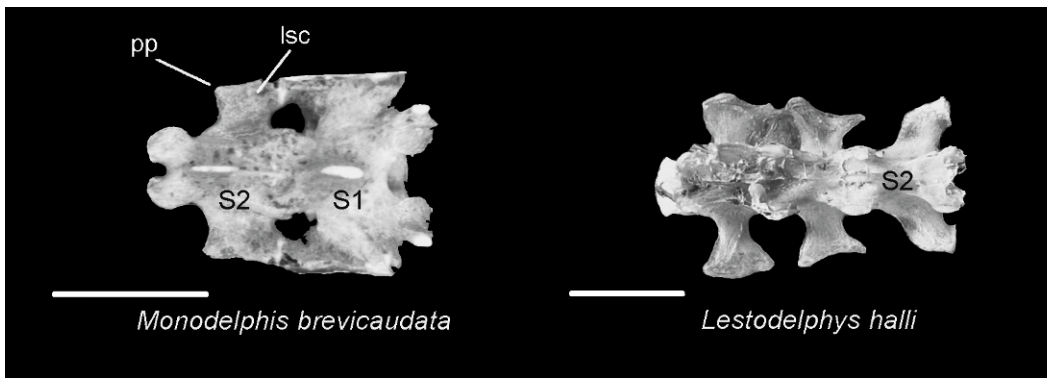

Fig. 10. *Monodelphis brevicaudata* (AMNH 257203) and *Lestodelphys halli* (UWZM 22422), sacral vertebrae in dorsal view. In *Monodelphis* there is a posterior process (pp) on the lateral sacral crest (lsc) on S2 (ch. 39[1]), whereas in *Lestodelphys* it is absent (ch. 39[0]). Scale bars: 5 mm.

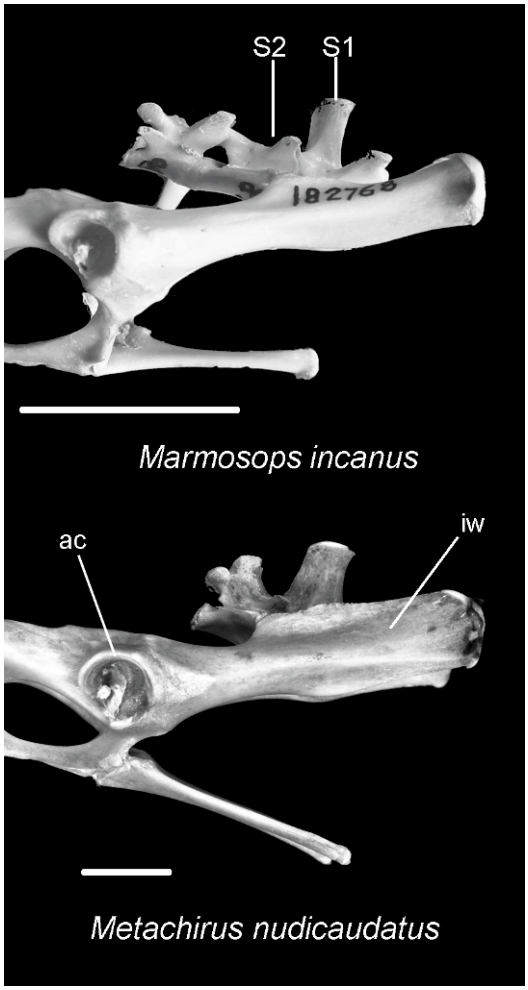

Fig. 11. *Marmosops incanus* (MVZ 182768) and *Metachirus nudicaudatus* (AMNH 267009), right os coxae with sacral vertebrae in lateral view. In the sacral vertebrae of *Marmosops incanus* the spinous process is present only in S1 (ch. 40[0]), whereas in *Metachirus* the process is present in both vertebrae (ch. 40[1]), and the S1 spinous process is taller than the S2 spinous process (ch. 41[1]). In *Metachirus*, the acetabulum (ac) is close, deep, and with the dorsal part laterally extended (ch. 83[1]), and the iliac wing (iw) forms a large blade (ch. 84[1]). Scale bars: 10 mm.

which move the tail in a transverse plane, in addition to muscles related to hindlimb movement (i.e. Mm. caudofemoralis, femoro-coccygeus, and semitendinosus caput dorsalis; Argot, 2002, 2003a). Most didelphid taxa treated herein show a caudal vertebra with the transverse process length similar to vertebral body craniocaudal length (see Argot, 2003a: fig. 10a), except for some taxa such as *Glironia*, *Caluromys*, *Monodelphis theresa*, *Marmosa rubra*, and *Cryptonanus unduaviensis*, where this kind of vertebra is absent. I only observed polymorphism in *Marmosa robinsoni* (coded {01}).

Character 44: Presence of spinous process in the first three caudal vertebrae: (0) spinous process absent; (1) spinous process only in first caudal vertebra; (2) spinous process in the first two caudal vertebrae; (3) spinous process present in the first three caudal vertebrae. The development of the spinous process on the anterior caudal vertebrae suggests development of the m. multifidus caudae, an important extensor muscle of the tail implied in vertical movements (Muizon and Argot, 2003). The spinous process is absent on the anterior caudal vertebrae in *Didelphis*, *Philander*, *Thylamys*, *Lestodelphys*, *Marmosops*, and *Cryptonanus*. Only *Lutreolina* and *Marmosa robinsoni* show the spinous process just in the first caudal vertebra, and *Monodelphis brevicaudata* and *Gracilinanus* exhibit the spinous process in the first two caudal vertebrae. The remaining taxa have the spinous process in the first three caudal vertebrae. Because I observed intermediate conditions in the presence of the spinous process in the caudal vertebrae, this character is treated as ordered ($0 \leftrightarrow 1 \leftrightarrow 2 \leftrightarrow 3$) in all analyses.

Character 45: Orientation of the spinous process in the three first caudal vertebrae: (0) spinous process in Ca1–Ca3 all vertical; (1) spinous process in Ca1–Ca2 vertical, and in Ca3 caudally oriented; (2) spinous process in Ca1 vertical, and in Ca2–Ca3 caudally oriented; (3) spinous process in Ca1–Ca3 caudally oriented. In those taxa with the spinous process present on the first three caudal vertebrae (i.e., state 3 in character 44), I observed variation related to the spinous process orientation. In some taxa, such as *Monodelphis adusta*, *M. theresa*, *Marmosa rubra*, *M. mexicana*, and *Micoureus*, the spinous processes are all vertical, but in *Caluromys* the two first are vertical, and the third one is caudally oriented. On the other hand, *Chironectes* and *Metachirus* have the second and third spinous process caudally

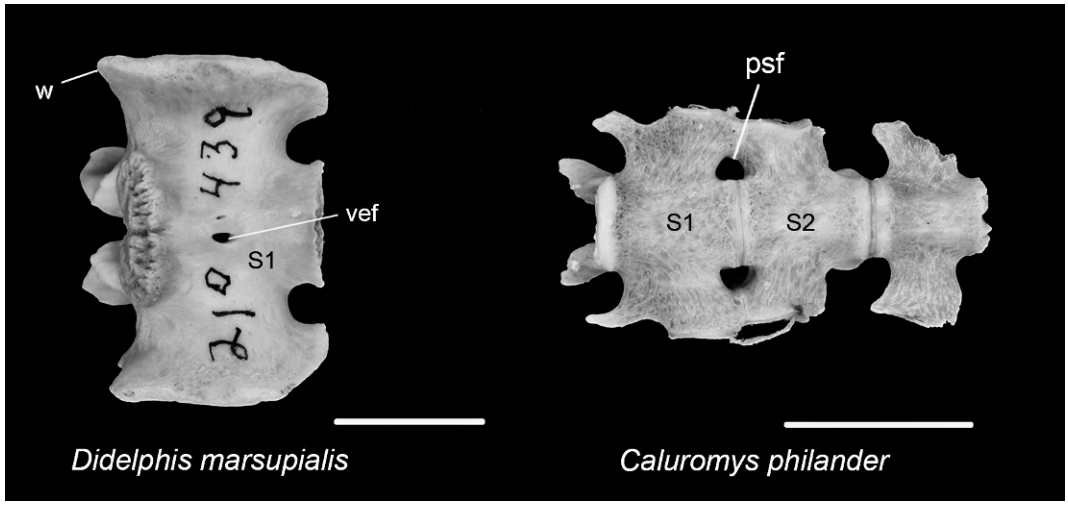

Fig. 12. *Didelphis marsupialis* (AMNH 210439 and *Caluromys philander* (AMNH 267001), sacral vertebrae in ventral view. A ventral foramen (vef) in the S1 body is present in *Didelphis* (ch. 42[1]), whereas in *Caluromys* it is absent (ch. 42[0]). Other abbreviations: psf, pelvic sacral foramen; w, wing. Scale bars: 10 mm.

oriented. Only in *Caluromysiops* and *Tlacuatzin* do the first three caudal vertebrae have the spinous process caudally oriented. In all taxa that do not have a spinous process on all first three caudal vertebrae, this character is treated as inapplicable (coded "–"). Because I observed intermediate conditions on the orientation of the spinous process, this character is treated as ordered (0 ↔ 1 ↔ 2 ↔ 3) in all analyses.

Character 46: Position of caudal vertebra with craniocaudal transverse process length similar to vertebral body length: (0) 3; (1) 4; (2) 5; (3) 6. On this character, I refer to the position of the vertebral element mentioned in character 43. The position of the first vertebra with this characteristic is variable in the didelphid crown group. In *Thylamys macrurus* and *Marmosops incanus*, this feature is placed in Ca3, whereas in *Lestodelphys* and *Monodelphis adusta* it is in Ca4. *Chironectes* and *Caluromysiops* have this morphology on Ca6. Lastly, the position in Ca5 is the most common condition in didelphids. It is interesting to note the posterior position of this element in the semiaquatic *Chironectes*, which is indicative of the posterior extension of the Mm. ischio-caudalis and abductor caudae dorsalis, both involved in lateral movements of the tail. All taxa that do not have this kind of vertebra (coding 0 in character 43) are treated as inapplicable (coded "–") for this character. No information is currently available about this character for *Gracilinanus microtarsus* (coded "?"). Because I observed intermediate conditions on the position of this element, this character is treated as ordered (0 ↔ 1 ↔ 2 ↔ 3) in all analyses.

Character 47: Foramen on the transverse process of the caudal vertebra referred in character 46: (0) absent; (1) present. The presence of a foramen in dorsal view on the transverse process of this particular vertebra is variable in didelphids. It is absent in *Caluromysiops*, *Thylamys*, *Gracilinanus*, and *Monodelphis*, but it is present in *Philander frenatus*, *P. mcilhennyi*, *Lestodelphys*, *Metachirus*, *Chironectes*, *Micoureus*, *Marmosa mexicana*, *Marmosops impavidus*, and *M. noctivagus*. In several taxa, such as *Philander opossum*, *Didelphis*, *Lutreolina*, *Tlacuatzin*, *Marmosa robinsoni*, *M. murina*, and *Marmosops incanus*, this character is treated as polymorphic (coded {01}) because of asymmetry. All taxa that do not have this kind of vertebra (coding 0 in character 43) are treated as inapplicable (coded "–") for this character.

Character 48: Position (from S1) of the first caudal vertebra with articulation through

vertebral body: (0) between 4 and 5; (1) between 5 and 6; (2) between 6 and 7. The caudal vertebrae exhibit two kinds of articulation: in the anterior portion of the tail, through pre- and postzygapophysis, similar to the sacral and lumbar vertebrae; and in the posterior portion, via the vertebral bodies and intervertebral discs. This joint configuration occurs with morphological modifications on the vertebral body (i.e., the vertebrae become longer, slender, and exhibit reduced apophyses). The articulation through intervertebral discs increases the flexibility of the posterior portion of the tail (Argot, 2003a). This simplified kind of articulation starts on different positions in the tail in different didelphids. The articulation between caudal vertebrae 4 and 5 occurs in *Glironia*, *Tlacuatzin*, *Thylamys macrurus*, *Monodelphis adusta*, *M. theresa*, and *Cryptonanus unduaviensis*. On the other hand, this articulation is placed between caudal vertebrae 5 and 6 in *Philander*, *Metachirus*, *Didelphis*, *Lutreolina*, *Thylamys venustus*, *T. pallidior*, *T. pusillus*, *Lestodelphys*, *Monodelphis brevicaudata*, *Micoureus*, *Marmosa*, *Marmosops* (except *incanus*), and *Gracilinanus agilis*. Lastly, in *Caluromys*, *Caluromysiops*, and *Chironectes*, the articulation is between caudal vertebrae 6 and 7. I found individual variation only in *Marmosops incanus* (coded {01}). No information is currently available about this character for *Gracilinanus microtarsus* (coded "?"). Because I observed the intermediate condition in the position of the articulation through the vertebral body, this character is treated as ordered ($0 \leftrightarrow 1 \leftrightarrow 2$) in all analyses.

Ribs and Sternum

Character 49: Ribs with anteroposterior extension: (0) present; (1) absent (fig. 5). Only in *Caluromys* and *Caluromysiops* do the ribs exhibit anteroposterior extension, which reduces the space filled by the intercostal muscles (Jenkins, 1970; Argot, 2003a). This morphology is also present in some primates, myrmecophagids, and dasypodids (Jenkins, 1970; MacPhee and Jacobs, 1986; Gebo, 1989). Rib morphology is indirectly related to the functionality of the vertebral column by altering mechanical properties of the thorax (Jenkins, 1970). The craniocaudal extension of the ribs increases the rigidity of the rib cage and reduces the flexibility provided by muscles and ligaments (Jenkins, 1970; Sargis, 2001; Argot, 2003a). Jenkins (1970) concluded that the expanded ribs increase the stability in the rib cage and the vertebral column as a whole. In arboreal forms such as *Caluromys* and *Caluromysiops*, this stability is necessary for locomotion during the bridging behavior (Jenkins, 1970; Sargis, 2001).

Character 50: Shape of the internal border of the first rib on distal half: (0) internal border notably curved; (1) internal border almost straight (fig. 13). In all didelphids, the first rib is short and robust since it is subject to tension forces, and it develops an especially strong connection with the manubrium (Klima, 1987). Some important muscles, such as Mm. pectoralis, scalenus, subclavius, and serratus ventralis thoracic, attach on the manubrium and the first pair of ribs (Jenkins and Weijs, 1979). Among other functions, these muscles support the head and forequarters and transmit forces between forelimb and trunk (Argot, 2003a, 2003b). In some taxa, such as *Caluromys*, *Caluromysiops*, *Thylamys*, *Marmosa murina*, *M. robinsoni*, *Marmosops*, *Monodelphis*, *Micoureus*, *Cryptonanus*, and *Lestodelphys*, the internal border at the distal half of the first pair of ribs is notably curved. In contrast, in *Didelphis*, *Metachirus*, *Philander*, *Lutreolina*, *Chironectes*, *Marmosa rubra*, *M. mexicana*, and *Gracilinanus agilis* this element is almost straight. No information is currently available about this character for *Gracilinanus microtarsus* (coded "?").

Character 51: Postmanubrium sternebrae morphology: (0) sternebrae not laterally compressed; (1) second sternebra laterally compressed; (2) second and third sternebrae laterally compressed. The body of the postmanubrium sternebrae appears laterally compressed in some taxa, which suggests an important function of the m. pectoralis. None of the sternebrae is laterally compressed in *Didelphis*, *Philander*, *Metachirus*, *Tlacuatzin*, *Marmosa mexicana*, *Marmosops incanus*, *M. noctivagus*, *M. impavidus*, *Monodelphis brevicaudata*, *M. adusta*, *Micoureus*, *Thylamys*, *Lestodelphys*, and *Gracilinanus*.

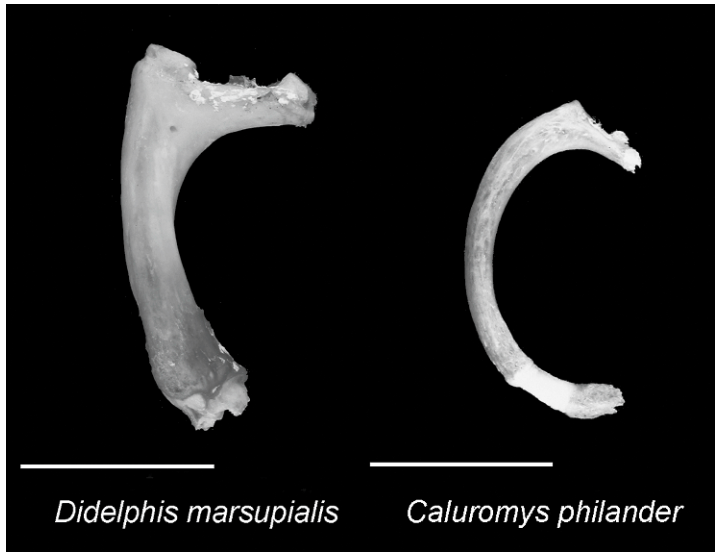

Fig. 13. *Didelphis marsupialis* (AMNH 23448) and *Caluromys philander* (AMNH 267001), first rib in anterior view. The internal border is notably curved in *Caluromys* (ch. 50[0]), whereas in *Didelphis* it is almost straight (ch. 50[1]). Scale bars: 5 mm.

On the other hand, *Lutreolina*, *Chironectes*, *Marmosa robinsoni*, *Marmosops pinheiroi*, *M. parvidens*, *Monodelphis theresa*, and *Cryptonanus* exhibit the second sternebra laterally compressed. Lastly, a third condition is evident in *Glironia*, *Caluromys*, and *Caluromysiops*, where the second and third sternebrae are laterally compressed. No information is currently available about this character for *Marmosa rubra* and *M. murina* (coded "?"). Because I observed the intermediate condition on the sternebrae morphology, this character is treated as ordered ($0 \leftrightarrow 1 \leftrightarrow 2$) in all analyses.

Character 52: Development of keel in the manubrium: (0) keel not very developed; (1) keel very developed (fig. 14). Similarly to the laterally compressed sternebrae, a keeled manubrium is indicative of important function of the m. pectoralis. The keel on the manubrium exhibits different levels of development in the taxa analyzed in this report. It is not very developed in *Lutreolina*, *Chironectes*, *Tlacuatzin*, *Marmosa mexicana*, *M. robinsoni*, *M. murina*, *Monodelphis*, *Thylamys*, *Micoureus*, *Gracilinanus*, and *Cryptonanus*. In contrast, the keel is notably developed in *Caluromys*, *Metachirus*, *Didelphis*, *Philander*, *Marmosops*, and *Lestodelpys*. A polymorphic condition is present in *Caluromysiops* (coded {01}). No information is currently available about this character for *Marmosa rubra* (coded "?").

Scapula

Character 53: Coracoid process shape: (0) hooklike process; (1) small process (fig. 15). This character is modified from Horovitz and Sánchez-Villagra (2003: ch. 36), as in this sample there are no taxa with the coracoid process absent. The development of the coracoid process is functionally important because this process is the point of origin of the Mm. coracobrachialis and biceps brachii, among other muscles. The first is involved in the extension and adduction of the shoulder joint (Taylor, 1974; Jenkins and Weijs, 1979; Evans, 1993; Sargis, 2002) and, according to Argot (2001), the morphology of this muscle depends on the species' habits. On the other hand, the m. biceps brachii is implied in the flexion of the elbow (Taylor, 1974; Argot, 2001). In this sense, a large coracoid process provides a longer lever arm for the m. biceps brachii, which is important during climbing in arboreal forms (Argot, 2001; Sargis, 2002). The coracoid process has a hooklike shape in

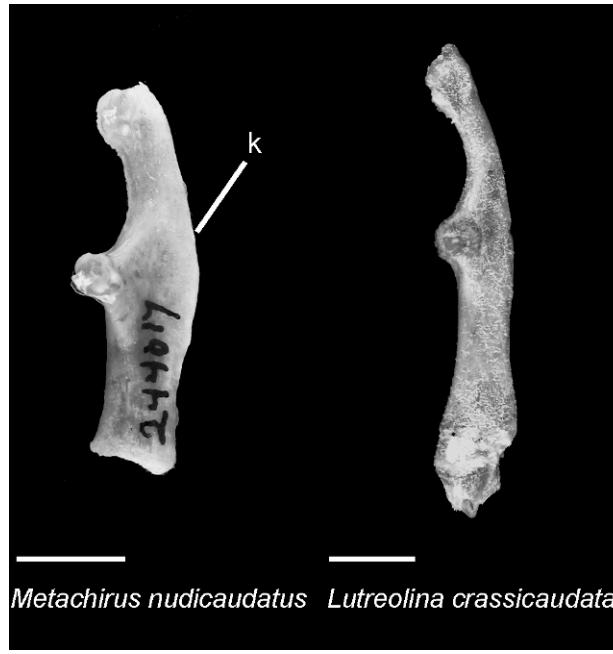

Fig. 14. *Metachirus nudicaudatus* (AMNH 244617) and *Lutreolina crassicaudata* (AMNH 33250), manubrium in lateral view. In *Metachirus* the keel (k) is well developed (ch. 52[1]), whereas in *Lutreolina* it is not prominent (ch. 52[0]). Scale bars: 5 mm.

Glironia, *Caluromys*, *Caluromysiops*, *Philander*, *Metachirus*, *Lutreolina*, *Chironectes*, *Marmosops parvidens*, *Marmosa rubra*, *M. robinsoni*, and *Tlacuatzin*. On the other hand, the process is small in *Lestodelphys*, *Didelphis*, *Thylamys*, *Micoureus*, *Monodelphis*, *Marmosa mexicana*, *M. murina*, *Marmosops* (except *M. parvidens*), *Cryptonanus*, and *Gracilinanus*.

Character 54: Supraspinous fossa width: (0) less than one-fourth its length; (1) between one-fourth and one-half its length (fig. 16). This character is modified from Horovitz and Sánchez-Villagra (2003: ch. 40), since in the sample there are not taxa with the infraspinous fossa width more than one-half its length, and the character is treated as binary. The supraspinous fossa contains the m. supraspinatus, which originates in the greater tubercle of the humerus (see Taylor, 1974: fig. 5; Evans, 1993: fig. 6–45; Argot, 2001: fig 3a). The function of this muscle is to extend the shoulder joint and advance the limb (Evans, 1993), and it is important to stabilize and prevent collapse in the shoulder joint (Goslow et al., 1981). An additional function is to absorb part of the kinetic energy generated when the forelimbs contact the substrate at the end of a leap (Maynard Smith and Savage, 1956; Roberts, 1974). This could explain the highly developed supraspinous fossa in *Metachirus*, a specialized leaper among didelphids (Argot, 2001). Most of the didelphids analyzed herein exhibit condition 1, except for some taxa such as *Lestodelphys*, *Chironectes*, *Monodelphis*, and *Hyladelphys*, where the spinous fossa width is less than one-fourth its length.

Character 55: Scapular spine width at neck level: (0) subequal to infraspinous fossa; (1) wider than infraspinous fossa. This character is modified from Horovitz and Sánchez-Villagra (2003: ch. 41) since in this sample there are no taxa with a scapular spine that is narrower than the infraspinous fossa at the neck level, so the character is treated as binary. This section of the scapular spine is the area of insertion of some muscles involved in limb flexion, such as the m. omotransversarius (Taylor, 1974) and the pars acromialis of m. trapezius (Mann-Fischer, 1953; Jenkins and Weijs, 1979),

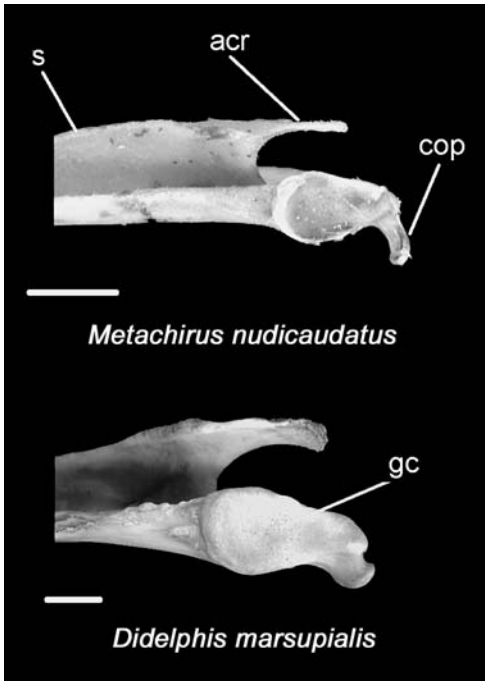

Fig. 15. *Metachirus nudicaudatus* (AMNH 244617) and *Didelphis marsupialis* (AMNH 210439), proximal area of scapula in ventrocaudal view. In *Metachirus*, the coracoid process (cop) shape is a hook-like process (ch. 53[0]), whereas in *Didelphis* this process is small (ch. 53[1]). Other abbreviations: acr, acromion; gc, glenoid cavity; s, spine. Scale bars: 5 mm.

which exert an anteriorly directed force to move this area craniodorsally, elevating the limb and moving it forward (Argot, 2003a, 2003b; Evans, 1993; Larson, 1993). Most of the didelphids show a scapular spine that is wider than the infraspinous fossa, except for *Caluromys*, *Didelphis*, and *Metachirus*, where both structures are subequal.

Character 56: Infraspinous/supraspinous fossa width at neck level: (0) infraspinous fossa narrower; (1) subequal; (2) supraspinous fossa narrower. This character was described by Horovitz and Sánchez-Villagra (2003: ch. 42), and it exhibits significant variation in the didelphid crown group analyzed here. Both fossae are subequal in *Philander*, *Didelphis*, *Metachirus*, *Monodelphis*, and *Gracilinanus agilis*. A supraspinous fossa narrower than the infraspinous fossa is present in *Glironia*, *Caluromys*, *Caluromysiops*, *Lestodelphys*, *Lutreolina*, *Chironectes*, *Tlacuatzin*, *Thylamys pallidior*, *T. pusilla*, *T. venustus*, *Micoureus*, *Marmosa*, *Marmosops*, *Cryptonanus unduaviensis*, and *Gracilinanus microtarsus*. Lastly, a narrower infraspinous fossa is present only in *Thylamys macrurus* and *Marmosa rubra*. Because I observed an intermediate condition in the relative width of the supra- and infraspinous fossae, this character is treated as ordered ($0 \leftrightarrow 1 \leftrightarrow 2$) in all analyses.

Character 57: Caudal angle: (0) acute; (1) rounded (fig. 16). The caudal angle shape of the scapula is related to the function of Mm. serratus and rhomboideus, which rotate the scapula in such a way that the vertebral border is pulled posteroventrally. The glenoid cavity is forced craniodorsally by the action of the m. omotransversarius (Maynard Smith and Savage, 1956; Taylor, 1974; Jenkins and Weijs, 1979; Larson, 1993; Argot, 2001; Muizon and Argot, 2003; see comments on character 55). The caudal angle is also the site for the attachment of m. teres major (Mann-Fischer, 1956; Jenkins, 1970; Taylor, 1974; Jenkins and Weijs, 1979), whose function is to flex the shoulder joint and move the humerus backwards (Maynard Smith and Savage, 1956; Taylor, 1974; Evans, 1993). The caudal angle of the scapula is acute in most taxa, such as *Glironia*, *Caluromys*, *Caluromysiops*, *Philander*, *Lutreolina*, *Chironectes*, *Tlacuatzin*, *Thylamys venustus*, *T. macrurus*, *Monodelphis*, *Micoureus*, *Marmosa*, *Marmosops*, *Lestodelphys*, *Cryptonanus*, and *Gracilinanus*. On the other hand, the caudal angle is rounded in *Didelphis*, *Metachirus*, and *Thylamys pallidior*. Individual variation is observed only in the samples of *Thylamys pusillus* and *Marmosops noctivagus* (coded {01}).

Character 58: Scapular notch extension: (0) extended less than half of the scapula; (1) extended to half of the scapula or beyond (fig. 16). An extended scapular notch determines the shape for the area of origin of the m. supraspinatus. The scapulae in living opossums exhibit two morphological types (Argot, 2001: fig 2), related to their rotational mode. These two types are conditioned by the development of the supraspinous and infraspinous fossae, as well as the scapular notch extension. The scapular notch is

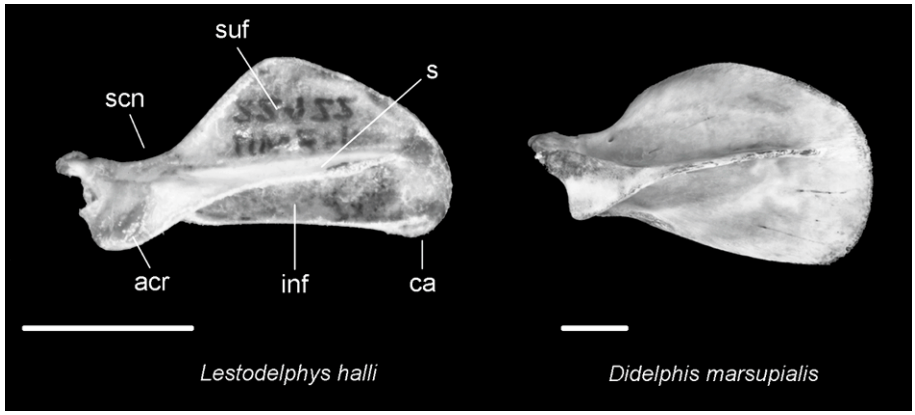

Fig. 16. *Lestodelphys halli* (UWZM 22422) and *Didelphis marsupialis* (AMNH 210439), left scapula in lateral view. In *Lestodelphys* the supraspinous fossa (suf) width is less than one-fourth its length (ch. 54[0]) and the caudal angle (ca) is acute (ch. 57[0]), whereas in *Didelphis* the supraspinous fossa width is between one-fourth and one-half its length (ch. 54[1]) and the caudal angle is rounded (ch. 57[2]). Note the scapular notch (scn) in *Didelphis*, extended to less than half of the scapula (ch. 58[0]), whereas in *Lestodelphys* it is extended to the middle of the scapula (ch. 58[1]). Other abbreviations: acr, acromion; inf, infraspinous fossa, s, spine. Scale bars: 10 mm.

extended less than half of the scapula in *Philander*, *Didelphis*, *Metachirus*, *Lutreolina*, *Chironectes*, and *Marmosops noctivagus*. Alternatively, the scapular notch is extended beyond half of the scapula in *Glironia*, *Caluromys*, *Caluromysiops*, *Lestodelphys*, *Tlacuatzin*, *Thylamys*, *Monodelphis*, *Marmosa*, *Marmosops impavidus*, *M. incanus*, *Cryptonanus*, and *Gracilinanus*.

Humerus

Character 59: Medial relief for m. teres major: (0) absent; (1) present. This character was defined by Horovitz and Sánchez-Villagra (2003: ch. 43). The relief for this muscle is absent in several species, such as *Hyladelphys*, *Didelphis albiventris*, *D. virginiana*, *Metachirus*, *Lutreolina*, *Chironectes*, *Thylamys venustus*, *T. macrurus*, *Monodelphis*, *Micoureus*, *Marmosops parvidens*, and *M. impavidus*. In contrast, the relief is apparent in *Glironia*, *Caluromys*, *Caluromysiops*, *Philander*, *Lestodelphys*, *Tlacuatzin*, *Thylamys pallidior*, *T. pusillus*, *Marmosa*, *Marmosops noctivagus*, *M. incanus*, *M. pinheiroi*, *Gracilinanus*, and *Cryptonanus*. I found a polymorphic condition in *Didelphis marsupialis*, *Philander opossum*, *Micoureus paraguayanus*, and *Marmosa robinsoni* (coded {01}).

Character 60: Capitulum shape: (0) spherical; (1) cylindrical (fig. 17). This character was defined by Horovitz and Sánchez-Villagra (2003: ch. 45). The capitulum articulates with the proximal radial head, and its shape is critical for arm movement. The spherical shape of the capitulum allows for a freer movement on the proximal radial head, during pronation-supination movements. The capitulum is spherical in several taxa, such as *Glironia*, *Caluromys*, *Caluromysiops*, *Philander mcilhennyi*, *Marmosa rubra*, *Tlacuatzin*, *Thylamys venustus*, *T. pallidior*, *T. pusillus*, *Monodelphis*, *Micoureus regina*, *Marmosa robinsoni*, *M. mexicana*, *Marmosops impavidus*, *Cryptonanus unduaviensis*, and *Gracilinanus microtarsus*. In contrast, it is cylindrical in *Philander franatus*, *P. opossum*, *Lestodelphys*, *Didelphis*, *Metachirus*, *Lutreolina*, *Chironectes*, *Thylamys macrurus*, *Marmosa murina*, *Marmosops noctivagus*, *M. incanus*, *M. parvidens*, and *Gracilinanus agilis*. Individual variation is observed in *Marmosops pinheiroi*, and *Micoureus demerarae* (coded {01}).

Character 61: Olecraneon fossa: (0) absent; (1) present; (2) present and large. This character is interpreted in the same way as by Horovitz and Sánchez-Villagra (2003: ch. 47), although the olecraneon foramen is not

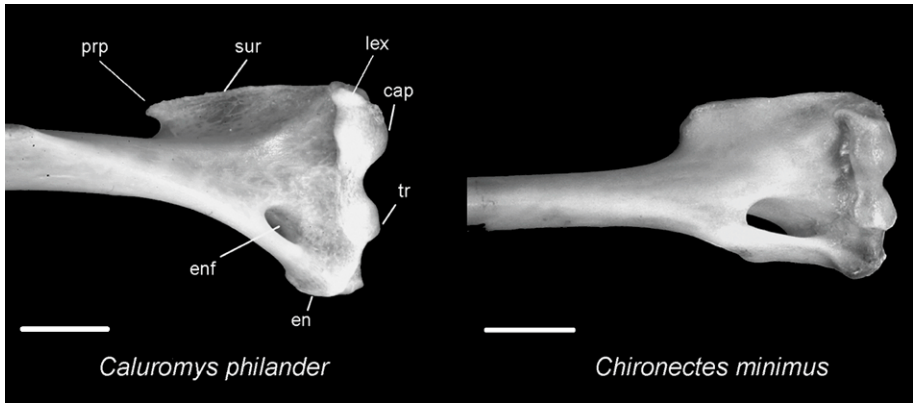

Fig. 17. *Caluromys philander* (AMNH 267001) and *Chironectes minimus* (AMNH 212909), distal portion of left humerus in anterior view. The capitulum (cap) in *Caluromys* is spherical in shape (ch. 60[0]), whereas in *Chironectes* it is cylindrical (ch. 60[1]). Note the more developed proximal extension of the capitulum in *Caluromys* relative to the proximal extension of the trochlea (tr) (ch. 63[1]). In both species there is a lateral extension (lex) of the capitulum (ch. (64[1]). In *Caluromys*, a proximal process (prp) in the supinator ridge (sur) is present (ch. 67[1]), whereas in *Chironectes* it is absent (ch. 67[0]). Other abbreviations: enf, entepicondylar foramen; en, entepicondyle. Scale bars: 5 mm.

observed in the sample. In the arm movement, the depth and size of the olecraneon fossa is important in the extension of the elbow joint. A deep olecraneon fossa allows for a maximum extension of the ulna, since the proximal part of the ulnar trochlear notch strikes the humeral olecraneon fossa during the maximum arm extension. An evident olecraneon fossa is absent only in *Caluromysiops* and *Marmosa mexicana*. In most didelphid groups a fossa is present, but only *Metachirus* exhibits a notably large fossa. Because I observed an intermediate condition in the development of the olecraneon fossa, this character is treated as ordered ($0 \leftrightarrow 1 \leftrightarrow 2$) in all analyses.

Character 62: Extension of the deltopectoral crest: (0) restricted to the proximal half; (1) reaching distal half. This character was described by Horovitz and Sánchez-Villagra (2003: ch. 50). Both parts of the m. deltoideus (i.e., pars clavicularis and pars acromialis) meet along the deltopectoral crest (Argot, 2001). A distal extension of the deltoid crest increases the length of the muscular fibers, emphasizing the function of flexion of the shoulder joint. Most didelphid taxa analyzed herein exhibit the deltoid crest restricted to the proximal half of the humerus. Nonetheless, in some terrestrial and generalist forms, such as *Philander*, *Didelphis*, *Metachirus*, *Lutreolina*, and *Monodelphis*, the deltoid crest reaches the distal half. Individual variation is observed in *Gracilinanus agilis* and *Micoureus paraguayanus* (coded {01}).

Character 63: Proximal extension of capitulum and trochlea: (0) equal extension; (1) longer proximal extension of capitulum (fig. 17). This character was modified from Horovitz and Sánchez-Villagra (2003: ch. 52), since in the sample there are no taxa with a longer extension of the trochlea, and the character is treated as binary. The humeral trochlea, capitulum, proximal radial head, and the trochlear notch of the ulna are involved in flexion/extension movements in the elbow joint (Taylor, 1974; Gebo, 1989; Argot, 2001; Szalay and Sargis, 2001; Muizon and Argot, 2003). A proximal extension of the capitulum allows for a close angle of flexion in the elbow joint. Most didelphid groups exhibit equal proximal extension of the capitulum and trochlea, except for *Glironia*, *Caluromys*, and *Caluromysiops*, where there is a longer proximal extension of the capitulum. Individual variation is present in *Chironectes* and *Gracilinanus agilis* (coded {01}).

Character 64: Capitulum lateral extension: (0) absent; (1) present (fig. 17). The character is interpreted in the same way as in Horovitz and Sánchez-Villagra (2003: ch. 56). Accord-

ing to Argot (2001: figs. 4a, 13d), the m. supinator brevis originates in this area, inserting in the proximal portion in the anterior side of the radius. This muscle is involved in the supination of the paw, so the palmar surface faces medially (Evans, 1993). All large opossums show a lateral extension of the capitulum, which is absent in mouse opossums.

Character 65: Shaft curvature: (0) straight; (1) curved. This character is interpreted in the same way as in Horovitz and Sánchez-Villagra (2003: ch. 57). Among the didelphid groups, just *Glironia*, *Caluromys*, and *Caluromysiops* display an almost straight humerus.

Character 66: Olecraneon fossa depth: (0) shallow; (1) deep. This character is independent from character 61, since here I specifically evaluate the variation existing in the olecraneon fossa depth in the taxa where it is present (coded as 1 and 2 in character 61). As mentioned above, the depth and enlargement of the olecraneon fossa are important in the extension of the elbow joint, because a deep fossa allows a major angle of extension in the joint. In this sense, the olecraneon fossa exhibits different depth in the didelphid group. It is not very deep in *Glironia*, *Caluromys*, *Lestodelphys*, *Tlacuatzin*, *Thylamys pallidior*, *T. venustus*, *T. macrurus*, *Micoureus*, *Marmosops impavidus*, *M. noctivagus*, *Cryptonanus unduaviensis*, and *Gracilinanus*. On the other hand, some taxa such as *Philander*, *Didelphis virginiana*, *Metachirus*, *Lutreolina*, *Chironectes*, *Monodelphis*, *Marmosops pinheiroi*, *M. parvidens*, and *M. incanus* exhibit a deep fossa. Individual variation is common in several taxa such as *Didelphis albiventris*, *D. marsupialis*, *Marmosa robinsoni*, *M. murina*, and *Thylamys pusillus* (coded {01}). *Caluromysiops* and *Marmosa mexicana* are inapplicable in this character (coded ''–''), because the olecraneon fossa is absent (coding 0 in character 61).

Character 67: Proximal process on the supinator ridge: (0) absent; (1) present (fig. 17). Some muscles involved in the flexion and extension of the elbow joint originate on the supinator ridge. The presence of a posterior process on the supinator ridge increases the area for the Mm. triceps brachii caput laterale and the m. brachioradialis. The former inserts on the olecraneon of the ulna and produces the extension of elbow joint, and the m. brachioradialis inserts on the distal portion of the medial side of radius, and it is involved in the rotation of the radius dorsolaterally (Jenkins and Weijs, 1979; Evans, 1993). A small proximal process on the supinator ridge is present in *Glironia*, *Caluromys*, *Caluromysiops*, *Marmosa rubra*, *Marmosops parvidens*, and *Lestodelphys*. Individual variation is observed in *Marmosa robinsoni* (coded {01}).

Character 68: Deltopectoral crest notably developed: (0) absent; (1) present. As mentioned above, this crest is important for the insertion of the m. deltoideus. This character is independent of character 62, because here I focus on the variation existing on the development but not on the extension of the deltopectoral crest. The crest is notably developed in *Glironia*, *Caluromys*, *Caluromysiops*, *Didelphis*, *Metachirus*, *Chironectes*, *Monodelphis*, *Micoureus demerarae*, *Marmosa murina*, *M. rubra*, and *Marmosops*. On the other hand, the crest is not well developed in *Philander*, *Lestodelphys*, *Lutreolina*, *Tlacuatzin*, *Thylamys*, *Micoureus regina*, *Marmosa mexicana*, *Cryptonanus unduaviensis*, and *Gracilinanus microtarsus*. Individual variation is observed in *Marmosa robinsoni* and *Gracilinanus agilis* (coded {01}).

Character 69: Entepicondyle mesial expansion: (0) absent; (1) barely expanded, approximately the same width as the trochlea; (2) notably expanded, wider than the trochlea (fig. 17). Most muscles moving the wrist and the hand originate on the humeral epicondyles (Taylor, 1974; Argot, 2001). The entepicondyle, also called the medial epicondyle, is the area where the Mm. flexor carpi radialis and the flexor digitorum profundus and superficialis originate. The former inserts on the palmar side of metacarpals II and III through two tendons. The flexor profundus and superficialis are involved in digit flexion (Abdala et al., 2006). The development of the entepicondyle is associated with powerful flexors, which are necessary for climbing habits (Taylor, 1974). However, the entepicondyle is a particularly expanded process only in some taxa, which are not always associated with arboreal locomotion, such as *Lestodelphys*, *Micoureus demerarae*, *Mar-*

mosa murina, *Marmosops impavidus*, and *Gracilinanus agilis*. Since I observed an intermediate condition in the development of the entepicondyle, this character is treated as ordered (0 ↔ 1 ↔ 2) in all analyses.

Character 70: Depth of bicipital groove: (0) absent; (1) present but shallow; (2) very deep. The bicipital groove is filled by the m. biceps brachii, originating from the coracoid process in the scapula. In arboreal taxa this muscle is well developed, having an important role in pulling the body up when climbing (Taylor, 1974; Argot, 2001). The bicipital groove is absent in *Metachirus*, *Philander*, *Didelphis*, *Lutreolina*, *Chironectes*, and *Marmosa mexicana*. This groove is very deep in *Glironia*, *Caluromys*, *Caluromysiops*, and *Marmosa rubra*. Polymorphism is evidenced in *Micoureus demerarae* and *M. paraguayanus*, as in those taxa some specimens show a very deep bicipital groove (coded {12}). Because I observed an intermediate condition in the depth of the bicipital groove, this character is treated as ordered (0 ↔ 1 ↔ 2) in all analyses.

Radius and Ulnae

Character 71: Ulna, shape of the proximal posterior border: (0) curved; (1) straight (fig. 18). In some taxa the posterior border of the ulna presents a proximal curvature, a product of the combinations of tractions, produced by flexors and extensors of the elbow joint (Argot, 2001). In this particular area is inserted the m. triceps brachii, whose function is to extend the elbow joint (Evans, 1993). Some authors linked this curvature to arboreal habits (Walker, 1974; Argot, 2001). Although most taxa have the ulnar proximal posterior border curved, in *Metachirus*, *Didelphis*, and *Lutreolina*, this section of the ulna is almost straight.

Character 72: Ulna, olecraneon shape: (0) olecraneon strong, short, and wide; (1) olecraneon slender (fig. 19). The short olecraneon would not only be related to the reduction of power, but also to the increment of the speed of movement. This was reasonably interpreted as an adaptation for arboreal habits, since the extension of the elbow does not require power but rapidity to grasp a support in arboreal locomotion (Muizon and Argot, 2003). However, although continuous variation in the development of the olecraneon is observed, it is possible to identify a different condition in the short and wide olecraneon exhibited by *Metachirus*, *Hyladelphys*, and *Marmosops parvidens*.

Fig. 18. *Didelphis marsupialis* (AMNH 210427) and *Micoureus regina* (AMNH 48757), proximal portion of ulna in lateral view. The caudal border is straight in *Didelphis* (ch. 71[1]), whereas it is strongly curved in *Micoureus* (ch. 71[0]). Scale bars: 10 mm.

Character 73: Ulna, crest on the anterior side, for the origin of Mm. pronator quadratus and flexor digitorum profundus: (0) absent; (1) present. Except for *Metachirus* and *Didelphis*, all groups analyzed herein present an evident crest on the anterior side of the ulna for the origin of Mm. flexor digitorum profundus and pronator quadratus. These muscles are involved in the prehensility of the manus and in maintaining the integrity of the antebrachium near the carpus (Argot, 2001).

Character 74: Ulna, extension of the fossa for the exterior ligament: (0) absent; (1) restricted to olecraneon; (2) extended to the trochlear notch; (3) extended beyond the

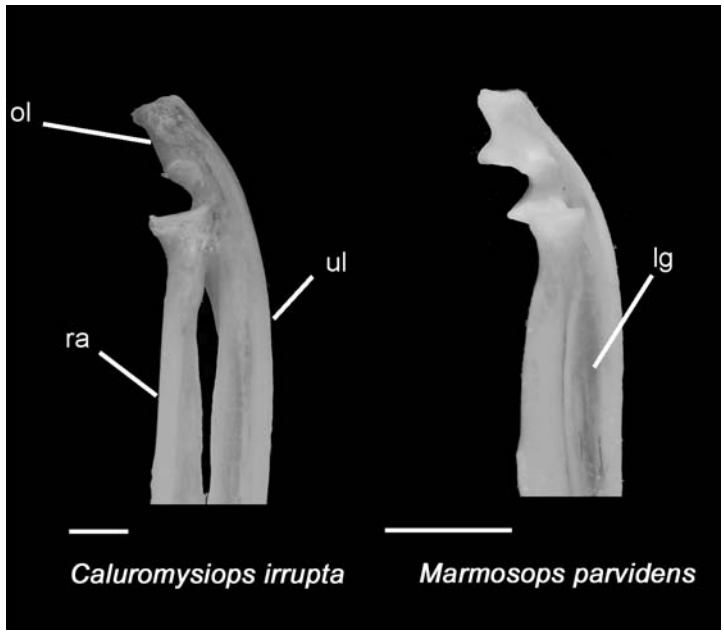

Fig. 19. *Caluromysiops irrupta* (AMNH 244364) and *Marmosops parvidens* (AMNH 267348), proximal portion of ulna (ul) and radius (ra) in lateral view. The olecraneon (ol) is short and wide in *Marmosops* (ch. 72[0]), whereas it is proportionally longer and more slender in *Caluromysiops* (ch. 72[1]). In both species, the longitudinal groove (lg) for Mm. anconeus and abductor pollicis longus (ch. 77[2]) is well developed. Scale bars: 5 mm.

trochlear notch (fig. 20). This fossa can be deep in some taxa, and it is part of the extensive surface for the origin of m. flexor digitorum profundus (Muizon and Argot, 2003). It has also been associated with arboreal habits, because of the importance of this muscle for grasping during locomotion (Muizon and Argot, 2003) and food manipulation. In didelphids, the fossa for the exterior ligament is evident in mesial view, and it shows different levels of distal extension. It is restricted to the olecraneon only in *Metachirus*, whereas it is extended to the trochlear notch in *Caluromysiops*, *Philander mcilhennyi*, *Didelphis*, *Lutreolina*, *Chironectes*, *Marmosa*, *Thylamys*, *Monodelphis brevicaudata*, *M. adusta*, *Micoureus regina*, *Lestodelphys*, and *Marmosops* (except *M. parvidens*, where it is absent). The fossa is extended beyond the trochlear notch in *Glironia*, *Caluromys*, *Philander opossum*, *P. frenatus*, *Tlacuatzin*, *Monodelphis theresa*, *Micoureus demerarae*, *M. paraguayanus*, and *Gracilinanus*. Since I observed an intermediate condition in the extension of the fossa for the exterior ligament, this character is treated as ordered ($0 \leftrightarrow 1 \leftrightarrow 2$) in all analyses.

Character 75: Ulna, mesial extension of the greater sigmoid cavity: (0) not extended; (1) notably extended, beyond the level of the anconeal process (fig. 21). The humeral trochlea rests in the greater sigmoid cavity and serves like a pivot during the elbow joint movement. Functionally, a mesial extension of the greater sigmoid cavity contributes to the safety of the elbow joint. In general, didelphids have the greater sigmoid cavity notably extended to the mesial side. However, in some taxa such as *Metachirus*, *Philander mcilhennyi*, *Marmosops parvidens*, and *Lestodelphys*, the cavity does not have a particular mesial extension.

Character 76: Ulna, development of the anconeal process: (0) present but not very developed; (1) well developed (fig. 21). The anconeal process is part of the insertion of m. anconeus, which is involved, together with m. triceps brachii, in the extension of the elbow joint (Jenkins and Weijs, 1979; Evans, 1993). The process is well developed in *Metachirus*,

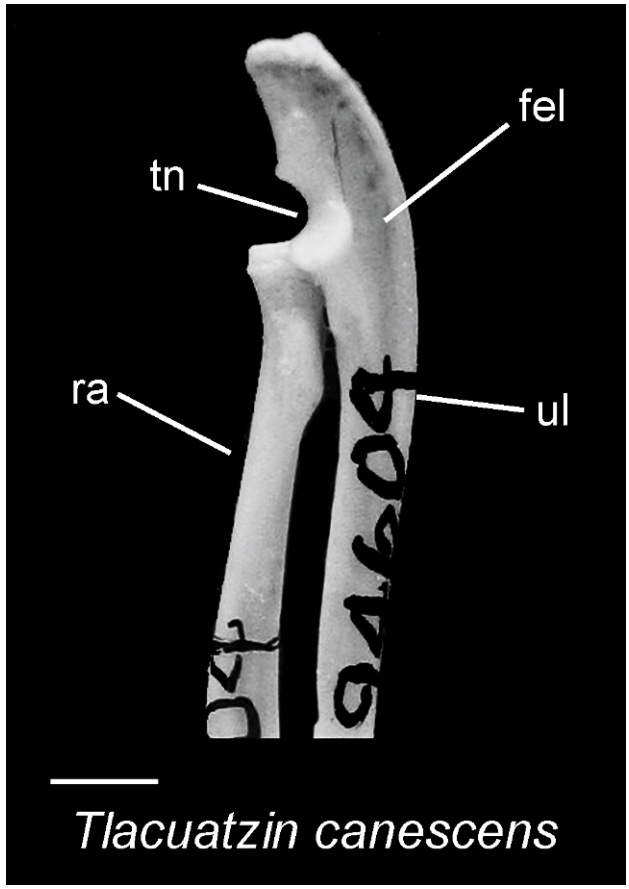

Fig. 20. *Tlacualtzin canescens* (UMMZ 94604), proximal portion of ulna (ul) and radius (ra) showing the fossa for exterior ligament (fel) extended beyond the trochlear notch (tn) (ch. 74[3]). Scale bar: 5 mm.

Philander opossum, *Didelphis*, *Lutreolina*, *Chironectes*, *Thylamys*, *Monodelphis adusta*, *Lestodelphys*, *Marmosops incanus*, *M. parvidens*, and *Gracilinanus agilis*.

Character 77: Ulna, longitudinal groove in lateral surface for the insertion of Mm. abductor pollicis longus and anconeus: (0) absent; (1) present and shallow; (2) present and notably deep (fig. 19). In the lateral surface of the ulna there is an area for the insertion of m. anconeus and origin of the m. abductor pollicis longus, both related to the extension of the elbow joint (Evans, 1993). According to Argot (2001), those muscles are well developed in arboreal forms. However, some arboreal forms, such as *Caluromys*, do not have a well-developed groove when it is compared to *Caluromysiops*. The groove in the lateral surface is absent in *Thylamys*, *Monodelphis brevicaudata*, *M. adusta*, and *Marmosa mexicana*. It is present though not very deep in *Glironia*, *Metachirus*, *Caluromys*, *Philander*, *Didelphis*, *Lutreolina*, *Chironectes*, *Tlacuatzin*, *Marmosa rubra*, *Monodelphis theresa*, *Micoureus*, *Lestodelphys*, *Marmosops* (except *M. parvidens*), *Cryptonanus*, and *Gracilinanus microtarsus*. This groove is very deep only in *Caluromysiops* and *Marmosops parvidens*, indicating a very developed m. anconeus. Polymorphism is observed in *Marmosa murina*, *Micoureus paraguayanus*, and *Gracilinanus agilis* (coded {01}). Because I observed an intermediate condition in the development of the longitudinal groove in the lateral surface, this character is treated as ordered ($0 \leftrightarrow 1 \leftrightarrow 2$) in all analyses.

Character 78: Ulna, lateral extension of the coronoid process: (0) absent; (1) notably

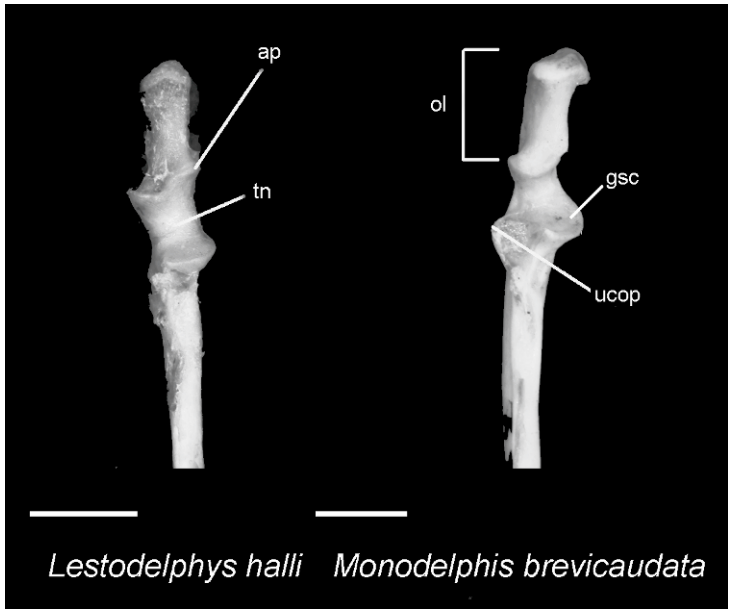

Fig. 21. *Lestodelphys halli* (UWZM 22422) and *Monodelphis brevicaudata* (AMNH 257203), proximal part of right ulna, anterior surface. In *Monodelphis*, the anconeal process (ap) is poorly developed (ch. 76[0]) and the ulnar coronoid process (ucop) is well developed in the lateral side (ch. 78[1]). In contrast, in *Lestodelphys* the anconeal process is well developed (ch. 76[1]) and the ulnar coronoid process is not very developed on the lateral side (ch. 78[0]). The greater sigmoid cavity (gsc) is mesially extended in *Monodelphis* (ch. 75[1]), whereas in *Lestodelphys* it is not mesially extended (ch. 75[0]). Other abbreviations: ol, olecraneon; tn, trochlear notch. Scale bars: 5 mm.

extended, beyond the level of the trochlear notch (fig. 21). The coronoid process on the lateral side appears notably developed only in *Monodelphis*, *Marmosops parvidens*, and *M. incanus*.

Character 79: Radius, lateral compression: (0) radius little or not laterally compressed; (1) radius notably laterally compressed. A laterally compressed radius has been functionally associated to a major flexibility during pronation-supination movements (Oxnard, 1963; Walker, 1974). The radius is notoriously compressed in some species such as *Glironia*, *Caluromysiops*, *Caluromys lanatus*, *Lutreolina*, *Monodelphis*, *Marmosa rubra*, *Micoureus demerarae*, *Marmosops parvidens*, and *Lestodelphys*.

Character 80: Radius, shape of articular facet for humerus: (0) circular; (1) anteroposteriorly compressed. This character was defined by Horovitz and Sánchez-Villagra (2003: ch. 61). The radial head has some functional implications in pronation-supination movements (Argot, 2001). In arboreal forms, the circular radial head allows a wide potential range of pronation-supination movement. A radial head craniocaudally compressed is indicative of a more stable radio-capitullum joint, which is observed in scansorial forms, different from the circular shape observed in arboreal forms (MacLeod and Rose, 1993). The articular facet is anteroposteriorly compressed only in *Philander*, *Marmosa rubra*, and *Chironectes*.

Character 81: Radius, development of the bicipital tuberosity: (0) scarcely marked; (1) very developed (fig. 22). The bicipital tuberosity of the radius is the site of insertion of m. biceps brachii. According to Argot (2001), the bicipital tuberosity is more developed in arboreal forms. I found a well-developed bicipital tuberosity in *Glironia*, *Caluromys*, *Caluromysiops*, *Didelphis*, *Lutreolina*, *Marmosops*, *Lestodelphys*, *Cryptonanus*, and *Gracilinanus agilis*. On the other hand, the tuberosity is scarcely marked in *Metachirus*, *Philander*, *Chironectes*, *Tlacuatzin*, *Marmosa*, *Monodelphis*, *Thylamys*, *Micoureus*, and *Gracilinanus microtarsus*.

Fig. 22. *Caluromys philander* (AMNH 267337) and *Chironectes minimus* (AMNH 148720), radius in lateral view showing the well-developed bicipital tuberosity (bt) (ch. 81[1]) and the bony plate (bp) on the caudal portion (ch. 82[1]) in *Caluromys*, whereas in *Chironectes* the bicipital tuberosity is small (ch. 81[0]) and the bony plate is absent (ch. 82[0]). Scale bar: 10 mm.

Character 82: Radius, presence of a thin bony plate extended posterolaterally along the diaphysis: (0) absent; (1) present (fig. 22). Only in *Caluromys*, *Caluromysiops*, and *Lestodelphys* is there a thin bony plate on the diaphysis of the radius. According to Argot (2001), this structure reinforces the origin for the Mm. flexor digitorum profundus and pollicis longus, both important in the prehensility of the manus. Although this bony plate and a prounced curvature of radius have been associated to arboreal habits (Argot, 2001; Lanyon, 1980), the morphology of the radius in the terrestrial *Lestodelphys* suggests an important capacity for manipulating prey.

Pelvis and Epipubic Bones

Character 83: Acetabulum morphology: (0) shallow, dorsal part of acetabular fossa not laterally expanded; (1) deep, with the dorsal part extended laterally (fig. 11). The acetabulum morphology is critical in femur flexion (Elftman, 1929). A shallow acetabular fossa allows a wide range of movements of the femur (Jenkins and Camazine, 1977; Argot, 2002), especially in abduction, which is related to arboreal habits (Elftman, 1929; Muizon and Argot, 2003). However, this morphology implies a reduced stability of the joint, because of as it was established for *Caluromys* (Muizon and Argot, 2003), arboreal didelphids pressumably have slow climbing habits. In this context, *Metachirus* is autapomorphic for this character since it exhibits a deep acetabular fossa, with the dorsal portion laterally extended, which is a specialized morphology for its cursosaltatorial mode of locomotion.

Character 84: Iliac wing forming a large blade: (0) absent; (1) present (fig. 11). The

Fig. 23. *Marmosops parvidens* (AMNH 267348), os coxae in lateral view showing the posteroventral extension (pex) on the pubis (ch. 86[1]). Scale bar: 5 mm.

iliac wing, which forms a large blade, is an autapomorphy only present in *Metachirus*, which shows a reduced iliac fossa as well. This extension is occupied by a well-developed m. gluteus medius (Argot, 2002; Taylor, 1974) and is indicative of high activity of this muscle as well as the development of the epaxial musculature (Maynard Smith and Savage, 1955; Grand, 1983). The morphology exhibited by *Metachirus* is consistent with the results of Grand (1983) as well, because the lower back musculature of this taxon represents more than 55% of the total epaxial musculature, different from the 25–35% in other didelphid taxa. Although the iliac fossa is also reduced in *Metachirus* due to the blade shape of the iliac wing, the m. iliacus is well developed (Argot, 2002; Elftman, 1929).

Character 85: Angle formed by the two posterior rami of ischium in caudal view: (0) 90° or scarcely more; (1) less than 90°. In caudal view, the angle formed by the two rami of ischium can accentuate the extroversion of the ischiatic spine, which is important in the origin of abductors and gracilis muscles (Elftman, 1929; Argot, 2002). Additionally, the angle has been related to the range of abduction (Jenkins and Camazine, 1977). As it was stated by Argot (2002), a sharp angle (or an oblique orientation of the ischium) emphasizes the degree of abduction. In the sample analyzed, the two rami of the ischium form an angle of 90° in *Metachirus*, *Chironectes*, *Philander*, *Didelphis*, *Lestodelphys*, *Hyladelphys*, and *Gracilinanus*. In the remaining taxa, the angle is less than 90°.

Character 86: Presence of an osseous posteroventral extension on the ischium: (0) absent; (1) present (fig. 23). The posteroventral extension on the ischium is a synapomorphy observed only in the species of *Marmosops*. This extension seems to increase the area for origin of the hamstring muscles complex (i.e., Mm. biceps femoris, semimembranosus, and semitendinosus), which inserts on the tibia and fibula and contributes to the knee flexion.

Character 87: Development of iliopubic process: (0) absent; (1) present (fig. 24). This character was described by Horovitz and Sánchez-Villagra (2003: ch. 73). In this area the m. psoas minor is inserted, which originates in the last thoracic and the first lumbar vertebrae, and whose action is to flex the lumbar part of the vertebral column (Elftman, 1929; Evans, 1993). Although in some specimens it was not be very conspicuous, the process is present in both terrestrial as well as arboreal forms, such as *Caluromysiops*, *Metachirus*, *Lutreolina*, and *Thylamys pusillus*. Polymorphism is evidenced in *Philander frenatus* and *Chironectes* (coded {01}).

Character 88: Epipubic bones, proximal size: (0) short; (1) long. In the same way as in Horovitz and Sánchez-Villagra (2003: ch. 77), I coded short proximal size of epipubic bones when the contact is equal to or less than half of the distance between the pubic symphysis and the point at the anterior edge of the pelvis, whose level is coincident with the middle of the acetabulum. The proximal size of the epipubic bones is long in *Caluromysiops*, *Caluromys*, *Philander*, *Didelphius*, *Lutreolina*, *Chironectes*, *Thylamys*, *Monodelphis*, *Micoureus demerarae*, *Lestodelphys*, *Marmosa* (except *M. rubra*), and *Marmosops*.

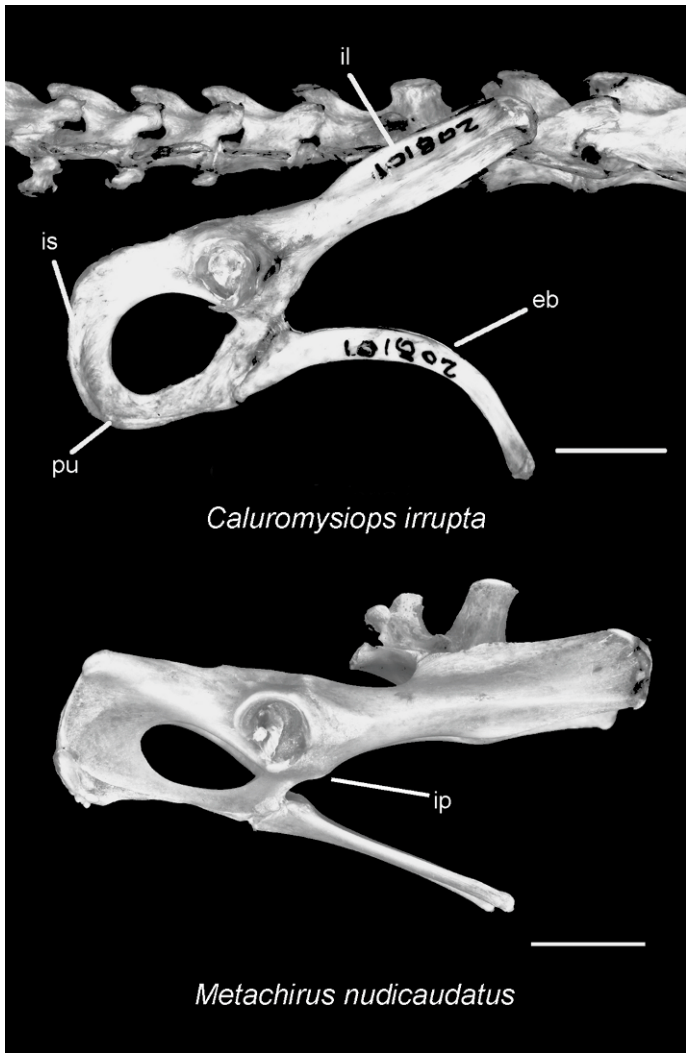

Fig. 24. *Caluromysiops irrupta* (AMNH 208101) and *Metachirus nudicaudatus* (AMNH 267009), right os coxae with epipubic bones (eb) in lateral view. The epipubic bones are notably curved (ch. 89[1]) in *Caluromysiops*, whereas in *Metachirus* the bones are straight (ch. 89[0]). Note the iliopubic (ip) process well developed in *Metachirus* (ch. 87[1]). Other abbreviations: il, ilium; is, ischium; pu, pubis. Scale bars: 10 mm.

Polymorphism is exhibited only in *Micoureus regina*. No information about this character is currently available for *Thylamys venustus* and *Philander mcilhennyi* (coded "?").

Character 89: Epipubic bones distal shape: (0) straight; (1) curved (fig. 24). In general terms I founded evidence of sexual dimorphism in the development of epipubic bones (at least those taxa in which a good series was analyzed, see appendix 1), being larger in females of pouchless taxa (as observed by White, 1989). Its shape shows two apparently defined morphotypes across the taxa analyzed. The condition of straight epipubic bones is the most common morphology exhibited in the sample. On the contrary, the epipubic bones are clearly curved in the distal portion in some taxa, such as *Caluromysiops*, *Caluromys*, *Marmosops parvidens*, *Chironectes*, and *Marmosa rubra*. No information is currently available about this character for *Philander mcilhennyi* (coded "?").

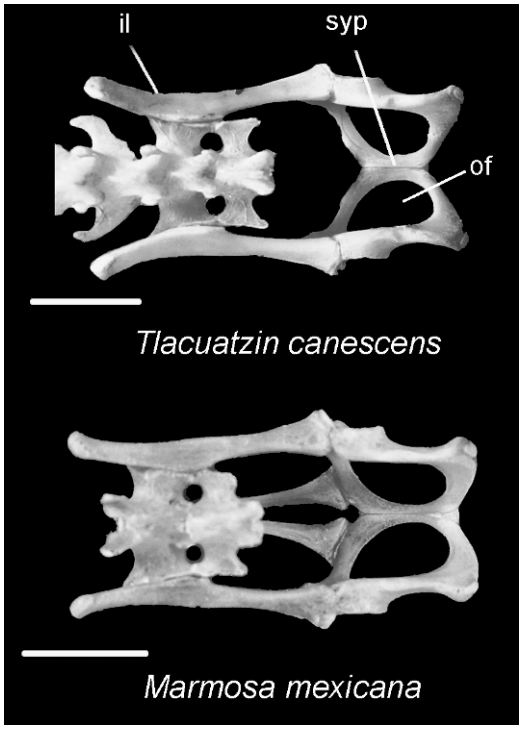

Fig. 25. *Tlacuatzin canescens* (UMMZ 94604) and *Marmosa mexicana* (ROM 99604), pelvis in dorsal view. In *Tlacuatzin* the symphysis pubis (syp) is shorter than the obturator foramen (of) (ch. 91[0]), whereas the symphysis size is similar to the obturator foramen in *Marmosa mexicana* (ch. 91[1]). Note the anterior portion of the ilium (il) curved laterally in *Tlacuatzin* (ch. 90[1]), and in *Marmosa* it is almost straight (ch. 90[0]). Scale bars: 5 mm.

Character 90: Ilium shape: (0) straight; (1) with the distal portion barely curved laterally (fig. 25). In character 84, I considered the general development of the iliac wing. Here, I focused on the direction of the distal portion of the ilium. As mentioned above, the shape of the ilium is important in the movements of the hip, since this is the area of origin of some muscles involved in the extension-flexion of the hip joint such as the Mm. glutei, iliacus, and sartorius. The distal portion slightly curved laterally probably increased the development of the m. glutei, as well as the epaxial musculature (Maynard Smith and Savage, 1956; Grand, 1983). Even though in the study of Argot (2002) the terrestrial *Metachirus* is the only didelphid species analyzed with this particular morphology of the ilium (see Argot, 2002: fig 7b), I found the same pattern in other didelphid species as well, such as *Glironia*, *Chironectes*, and *Tlacuatzin*, which are not always directly associated with terrestrial habits.

Character 91: Pubic symphysis size in relation to the craniocaudal size of the obturator foramen: (0) shorter; (1) equal or longer (fig. 25). Although the obturator foramen is well developed in all didelphid species analyzed herein, I detected a remarkable variation in pubic symphysis pubis size. Variation in this character could be linked with the area of origin of m. gracilis, implied in the flexion of the tibia (Elftman, 1929), and assisting the hamstring muscles in the extension of the femur (Argot, 2002; Maynard Smith and Savage, 1955). In most didelphid species, the symphysis is equal to or longer than the obturator foramen. However, in *Glironia*, *Tlacuatzin*, and *Thylamys macrurus*, the symphysis is shorther than the obturator foramen.

Character 92: Caudal portion of ischium body curved laterally (other than the ischiatic tuberosity): (0) absent; (1) present (fig. 26). This is the region of the ischium where important muscles involved in the flexion of the tibia and tail movements originate, such as Mm. biceps femori and semitendinosus. The curved shape of the ischium probably increases the function of those muscles. Both muscles (i.e., Mm. biceps femoris and semitendinosus) are well developed in *Metachirus*, probably due to the typical cursosaltatorial locomotion (Maynard Smith and Savage, 1956). Besides *Metachirus*, I found the posterior part of ischium body to be laterally curved also in *Philander*, *Didelphis*, *Lutreolina*, and *Chironectes*.

Femur

Character 93: Development of lesser trochanter: (0) not very developed; (1) well developed, surpassing the half of the mesial extension of the femoral head (fig. 27). Although the lesser trochanter is present in all didelphids, I detected two character states for its development. In this structure the Mm. iliacus and psoas major insert, which is implied in the flexion of the hip joint, as well

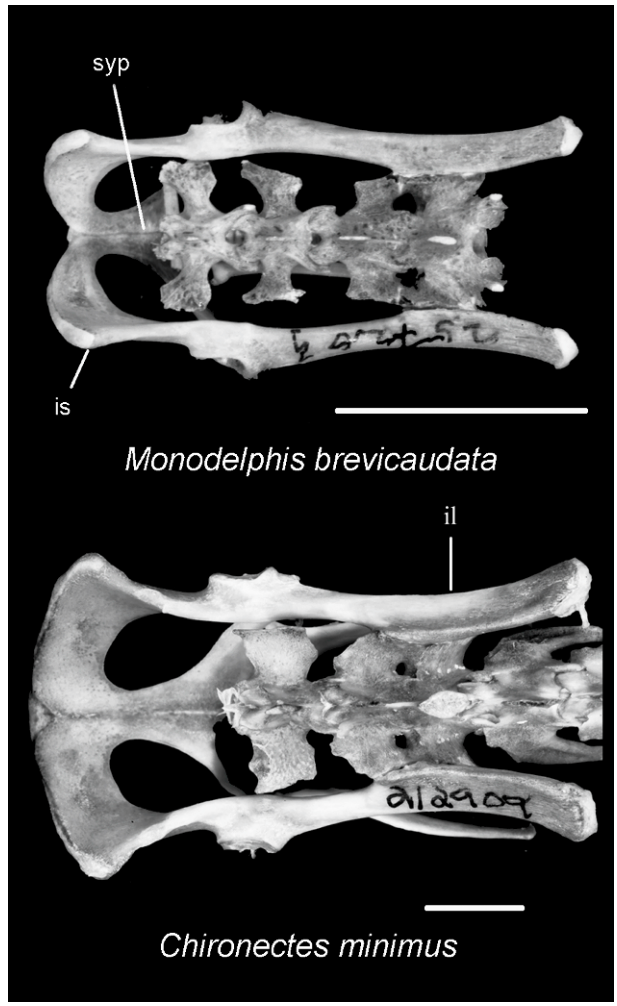

Fig. 26. *Monodelphis brevicaudata* (AMNH 257203) and *Chironectes minimus* (AMNH 212909), pelvis in dorsal view. In *Chironectes* the posterior part of the ischium (is) body is laterally deflected (ch. 92[1]), whereas in *Monodelphis* it is almost straight (ch. 92[0]). Other abbreviations: il, illium; syp, symphysis pubis. Scale bars: 10 mm.

as the flexion and fixation of the vertebral column (Evans, 1993). In arboreal forms, such as *Caluromys* or *Micoureus*, the iliacus and psoas major act as flexors and as external rotators and adductor of the leg (Muizon and Argot, 2003). Argot (2002) reported differences on the development of the lesser trochanter of *Caluromys*, *Metachirus*, *Monodelphis*, and *Micoureus*. In the sample analyzed, the lesser trochanter is notably developed in *Glironia*, *Caluromys*, *Caluromysiops*, *Thylamys pusillus*, *T. macrurus*, *Micoureus*, *Marmosa* (except *M. rubra*), *Marmosops*, *Cryptonanus*, and *Gracilinanus*. No information is currently available about this character for *Thylamys venustus* (coded "?").

Character 94: Protuberance between trochanteric fossa and head: (0) absent; (1) present (fig. 27). This protuberance seems to be an impression of the insertion of obturatores and gemelli muscles. It is present in most species analyzed herein, except for *T. pallidior*, which is autapomorphic in this character, as this structure is absent. No information is currently available about this character for *Thylamys venustus* (coded "?").

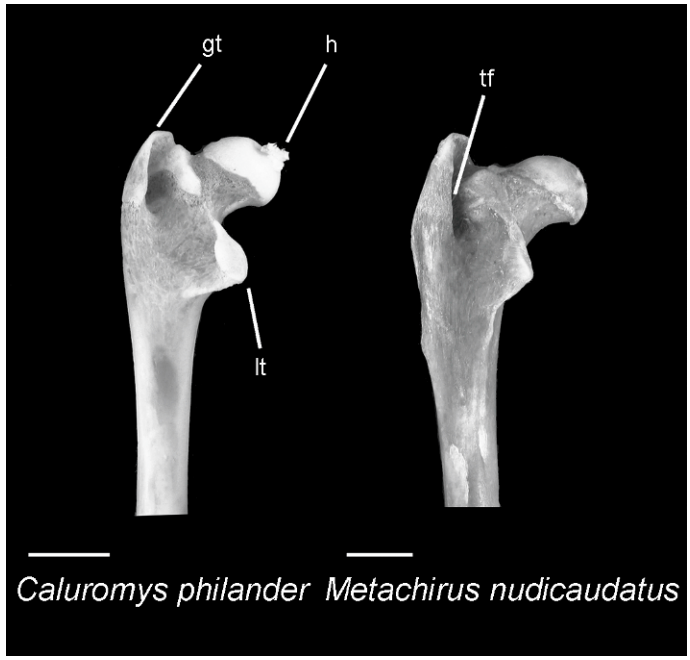

Fig. 27. *Caluromys philander* (AMNH 267001) and *Metachirus nudicaudatus* (AMNH 244617), proximal portion of right femur. In *Metachirus*, the greater trochanter (gt) is well developed (ch. 95[1]), whereas in *Caluromys* it is not very developed (ch. 95[0]). The lesser trochanter (lt) is more developed in *Caluromys* (ch. 93[1]) than in *Metachirus* (ch. 93[0]). Note in both species the protuberance between the trochanteric fossa (tf) and femoral head (h) (ch. 94[1]). Scale bars: 5 mm.

Character 95: Development of greater trochanter: (0) not surpassing the level of the head; (1) surpassing the level of the head (fig. 27). According to Argot (2002), didelphids usually exhibit a greater trochanter not higher than the femoral head. However, besides *Metachirus*, I judged greater trochanter notably developed in *Didelphis*, *Philander*, *Lutreolina*, *Chironectes*, *Tlacuatzin*, *Marmosa robinsoni*, *M. mexicana*, *Marmosops impavidus*, *M. parvidens*, and *M. pinheiroi*.

Character 96: Distal epiphysis anteroposteriorly compressed: (0) absent; (1) present. The anteroposterior compression of the distal femoral epiphysis is probably related to the intercondyloid fossa being delimited by low crests (Argot, 2002). Some didelphids with well-developed arboreal habits (*Caluromys*, *Micoureus*) show this morphology (Muizon and Argot, 2003), and the same relationship was evidenced in viverrids (Taylor, 1976) and primates (Tardieu, 1983). In the sample, the distal epiphysis is anteroposteriorly compressed in *Caluromys*, *Caluromysiops*, *Philander*, *Marmosa mexicana*, *M. murina*, *M. rubra*, and *Micoureus*.

Tibia and Fibula

Character 97: Sesamoids in the articular area between tibia, fibula, and astragalus: (0) absent; (1) one sesamoid present. This character is modified from Horovitz and Sánchez-Villagra (2003: ch. 86), since in the sample there are no taxa with two sesamoids. One sesamoid in the area between tibia, fibula, and astragalus is present in *Glironia*, *Metachirus*, *Philander*, *Didelphis virginiana*, *Tlacuatzin*, *Thylamys*, *Monodelphis*, *Marmosops incanus*, *M. parvidens*, *M. pinheiroi*, and *Cryptonanus unduaviensis*. Polymorphism is exhibited only in *Chironectes* (coded {01}). No information is currently available about this character for *Philander mcilhennyi*, *Marmosa rubra*, *Lutreolina*, *Thylamys pusillus*, *Lestodelphys*, and *Gracilinanus microtarsus* (coded "?").

Character 98: Tibia length relative to femur length: (0) tibia shorter than femur;

Fig. 28. *Chironectes minimus* (AMNH 212909) and *Didelphis marsupialis* (AMNH 210439), right tibia in anterior view. In *Chironectes* the tibia has a sigmoid shape (ch. 99[0]), whereas in *Didelphis* it is almost straight (ch. 99[1]). Scale bars: 5 mm.

(1) tibia longer than or equal to femur. This character was described by Horovitz and Sánchez-Villagra (2003: ch. 89). *Glironia* is autapomorphic in this character, as the femur is longer than the tibia. Maynard Smith and Savage (1955) found similar proportions only in large mammals, such as *Rhinoceros*, *Mastodon*, and horses. In marsupials, this characteristic was also evidenced in some Australasian taxa with a diversity of habits, such as *Phalanger*, *Pseudochirops*, *Phascolarctos*, and *Vombatus* (Horovitz and Sánchez-Villagra, 2003), as well as the fossil *Mayulestes* (Muizon, 1998). In the remaining American marsupials, the tibia is longer than the femur (see table 3 in Hershkovitz, 1999).

Character 99: Tibia shape: (0) sigmoid-shaped; (1) sigmoid shape present but not so marked (fig. 28). Although the sigmoid shape of the tibia is the most common condition in didelphids, some taxa exhibit a notable sigmoid shape. This morphology was interpreted as plesiomorphic and is not restricted to didelphids (Szalay and Sargis, 2001). The diaphysis starts in a sigmoid curvature at the level of the insertion of hamstring muscles, which suggests the possibility that this shape appears due to the pull of these extensors of the leg (Argot, 2002). On the other hand, Lanyon (1980) demonstrated the biomechanical advantages of the curved shape on load transmission. The sigmoid shape of the tibia

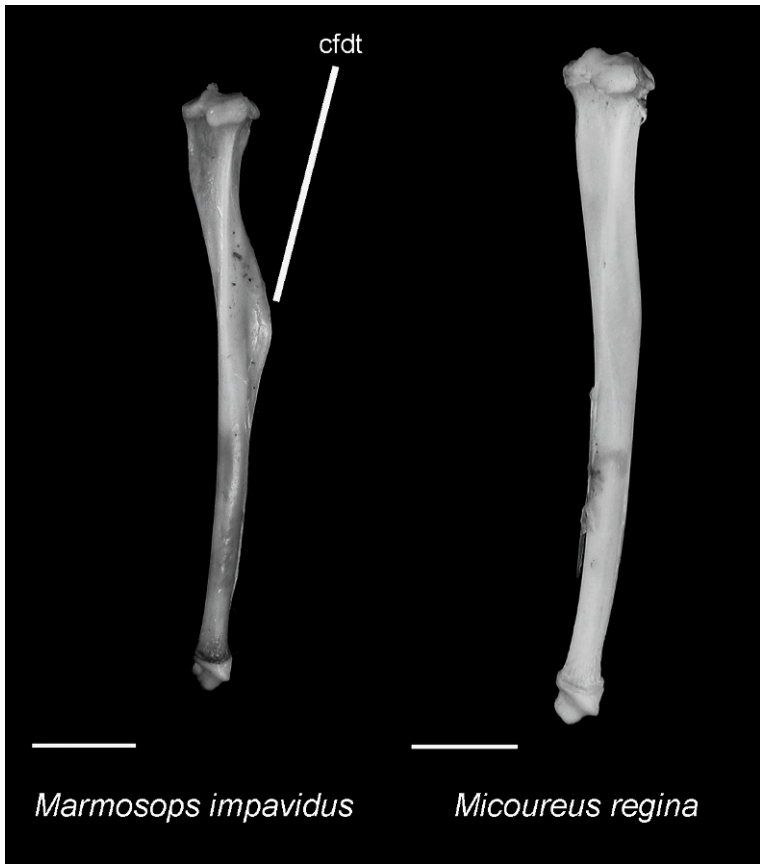

Fig. 29. *Marmosops impavidus* (AMNH 139226) and *Micoureus regina* (AMNH 148757), right tibia in mesial view. In *Marmosops* there is a notable crest for insertion of m. flexor digitorum tibialis (cfdt) (ch. 101[1]), which is absent in *Micoureus* (ch. 101[0]). Scale bars: 5 mm.

is also related to the asymmetrical condition of the femoral condyles in the knee joint. The lateral displacement of the load line is linked to the tibia shape and its function on load transmission (Szalay and Sargis, 2001). In the sample, *Chironectes*, *Tlacuatzin*, and *Gracilinanus microtarsus* exhibit a remarkably sigmoid-shaped tibia.

Character 100: Tibial tuberosity developed: (0) absent; (1) present. The tendon of the m. quadriceps, a powerful extensor of the knee, inserts directly on the tibial tuberosity, as the patella is absent in didelphids. In some taxa with well-developed arboreal habits (e.g., *Caluromys*, *Caluromysiops*, *Micoureus*), the tibial tuberosity is neither very evident or anteriorly expanded (personal obs.; Muizon and Argot, 2003). Only the terrestrial *Metachirus* exhibits this structure as notably developed, which is coherent with a more stabilized knee joint, useful for the saltatorial mode of locomotion. In slow-climbing didelphids, a more mobile and less stabilized knee joint is necessary, because of the range of hindlimb movements during arboreal displacement.

Character 101: Tibia, development of the posterior crest for the insertion of m. flexor digitorum tibialis: (0) absent; (1) present (fig. 29). The crest is present in *Hyladelphys*, *Marmosa mexicana*, *Marmosops noctivagus*, *M. impavidus*, *M. incanus*, *Lestodelphys*, *Gracilinanus*, and *Cryptonanus*.

Character 102: Head of fibula notably developed craniocaudally: (0) absent; (1) present. An anteroposteriorly expanded head of the fibula is associated with the development of the area of insertion of the m.

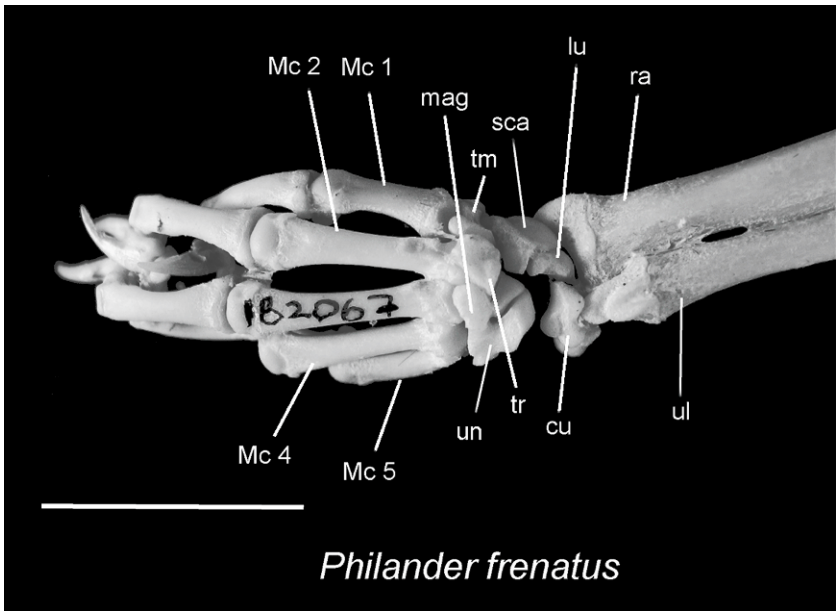

Fig. 30. *Philander frenatus* (MVZ 182067), dorsal aspect of distal ulna (ul), radius (ra), carpal, and metacarpal (Mc) bones. Note the lunate (lu) relatively large and in contact with other elements (ch. 103[1]). A distolateral process of the scaphoid (sca) separates the lunate and magnum (mag) (ch. 105[1]). Other abbreviations: un, unciform; cu, cuneiform; tm, trapezium; tr, trapezoid. Scale bar: 5 mm.

peroneus longus, which is involved in flexion of the tarsus (Evans, 1993). Consequently, this is linked to arboreal habits, as the mentioned muscle inserts on the proximal portion of the first metatarsal (Muizon and Argot, 2003; Argot, 2003a) and is associated with the opposability of the hallux. The head of the fibula is notably developed anteroposteriorly in *Caluromys*, *Caluromysiops*, *Chironectes*, *Tlacuatzin*, *Marmosa*, *Marmosops*, *Thylamys* (except *T. macrurus*), *Lestodelphys*, *Micoureus*,, *Gracilinanus*, and *Cryptonanus*.

Carpus and Metacarpus

Character 103: Lunate: (0) small (contacting only with scaphoid and cuneiform); (1) relatively large (contacting with scaphoid, cuneiform, magnum, and unciform) (fig. 30). This character is modified from Horovitz and Sánchez-Villagra (2003: ch. 62) since in this sample there are no taxa with the lunate absent or fused with other elements. In most didelphids, the lunate is relatively large and in contact with other elements. However, this bone is notably smaller in *Philander mcilhenyi*, *Tlacuatzin*, *Thylamys pusillus*, *Marmosa murina*, *Marmosops*, *Cryptonanus unduaviensis*, and *Gracilinanus agilis*. No information is currently available about this character for *Micoureus regina*, *M. paraguayanus*, *Lestodelphys*, and *Gracilinanus microtarsus* (coded "?").

Character 104: Prepollex: (0) absent; (1) present. This character was described by Horovitz and Sánchez-Villagra (2003: ch. 63). Because the prepollex is the smallest element on the wrist, its loss is common during the cleaning process. The prepollex is present in most groups analyzed herein, except for *Metachirus*, *Chironectes*, and *Thylamys pusillus*, where this element seems to be absent. No information is currently available about this character for *Lutreolina*, *Tlacuatzin*, *Micoureus paraguayanus*, *Lestodelphys*, *Marmosops impavidus*, *M. noctivagus*, *Cryptonanus unduaviensis*, and *Gracilinanus microtarsus* (coded "?").

Character 105: Distolateral process of scaphoid separating lunate from magnum dorsally: (0) absent; (1) present (fig. 30). This character was described by Horovitz and

Sánchez-Villagra (2003: ch. 64). This process of the scaphoid is present in most groups analyzed, except for *Glironia* and *Cryptonanus unduaviensis*. No information is currently available about this character for *Lutreolina*, *Tlacuatzin*, *Monodelphis brevicaudata*, *M. adusta*, *Micoureus paraguayanus*, *Lestodelphys*, and *Gracilinanus microtarsus* (coded "?").

Tarsus

Character 106: Astragalus, angle between medial and lateral facets for tibia: (0) intermediate, between 90° and 180°; (1) 180°. This character is modified from Horovitz and Sánchez-Villagra (2003: ch. 94), since in the current sample there are no taxa with a 90° angle, and the character is treated as binary. According to Jenkins and McClearn (1984) and Szalay (1982, 1994), the medial and lateral astragalotibial facets form a broad and almost flat plane in didelphids. However, I observed a continuous variation in the angle formed by the facets, and all conditions were met in a single interval (90°–180°). In terrestrial forms, as *Metachirus* or *Monodelphis*, the facets are better delimited, forming a sharper angle (personal obs.; Szalay, 1994). On the other hand, the angle between medial and lateral facets for the tibia was 180° only in some large opossums such as *Philander*, *Lutreolina*, *Didelphis*, and *Chironectes*. No information is currently available about this character for *Monodelphis adusta*, *Micoureus paraguayanus*, and *Lestodelphys* (coded "?").

Character 107: Astragalus, dimensions of astragalonavicular facet in distal view: (0) transversely wider; (1) dorsoventrally wider. This character was described by Horovitz and Sánchez-Villagra (2003: ch. 97). In the taxa analyzed here, only *Metachirus* exhibits the astragalonavicular facet dorsoventrally wider. No information is currently available about this character for *Monodelphis adusta*, *Micoureus paraguayanus*, and *Lestodelphys* (coded "?").

Character 108: Astragalus, ridge between medial and lateral astragalotibial facets: (0) absent; (1) present (fig. 31). This character was described by Horovitz and Sánchez-Villagra (2003: ch. 107). The ridge between medial and lateral astragalotibial facets is present in large opossums, such as *Glironia*, *Caluromys*, *Caluromysiops*, *Didelphis*, *Metachirus*, *Lutreolina*, and *Chironectes*. Contrary to Horovitz and Sánchez-Villagra (2003), I coded 0 for *Monodelphis*, since I did not observe a ridge in this area of the astragalus. No information is currently available about this character for *Monodelphis adusta*, *Micoureus paraguayanus*, and *Lestodelphys* (coded "?").

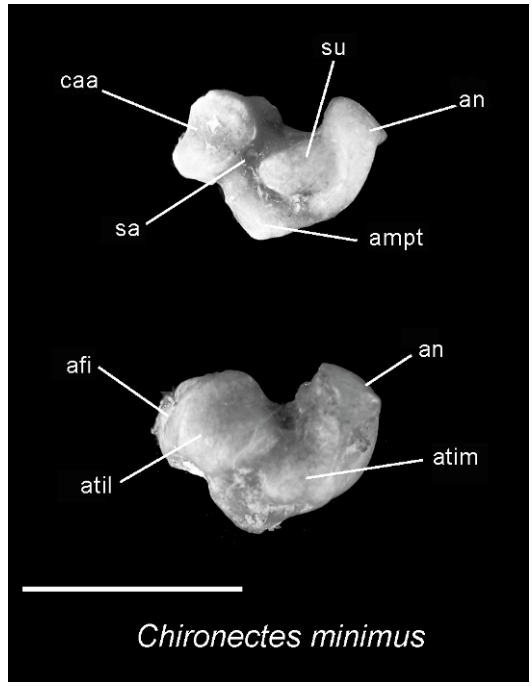

Fig. 31. *Chironectes minimus* (AMNH 148720), plantar and dorsal views of left astragalus. The ridge between the medial (atim) and lateral (atil) astragalotibial facets is present (ch. 108[1]), as well as being between the lateral atragalotibial and astragalofibular (afi) facets (ch. 109[1]). There is no contact between the astragalonavicular (an) and sustentacular (su) facets (ch. 110[0]), and the sustentacular facet is separated from the calcaneoastragalar (caa) facet by the well-developed sulcus astragali (sa) (ch. 111[0]). Other abbreviation: ampt, astragalar medial plantar tuberosity. Scale bar: 5 mm.

Character 109: Astragalus, ridge between lateral astragalotibial facet and astragalofibular facet: (0) absent; (1) present (fig. 31). This character was described by Horovitz and Sánchez-Villagra (2003: ch. 108). Similar

to the anterior character, the ridge is present only in large opossums. No information is currently available about this character for *Monodelphis adusta*, *Micoureus paraguayanus*, and *Lestodelphys* (coded "?").

Character 110: Astragalus, contact between astragalonavicular and sustentacular facets: (0) absent; (1) present. This character was described by Horovitz and Sánchez-Villagra (2003: ch. 110). I found evidence of contact between both facets in most taxa, except *Glironia*, *Caluromysiops*, *Metachirus*, *Chironectes* (fig. 31), and *Thylamys pallidior*. Individual variation is observed in *Didelphis virginiana* and *D. marsupialis* (coded {01}). No information is currently available about this character for *Monodelphis adusta*, *Micoureus paraguayanus*, and *Lestodelphys* (coded "?").

Character 111: Astragalus, continuous lower ankle joint pattern: (0) absent (fig. 31); (1) present. This pattern results from the contact between posterior calcaneoastragalar and sustentacular facets, which is in relation to the absence of the sulcus astragali. I found evidence of the absence of this pattern in most didelphid groups analyzed here, except for *Gracilinanus microtarsus* and *Hyladelphys*, where a continuous lower ankle joint pattern is observed. Opposite to this, individual variation is observed in *Marmosa mexicana*. No information is currently available about this character for *Monodelphis adusta*, *Micoureus paraguayanus*, and *Lestodelphys* (coded "?").

Character 112: Astragalus, astragalonavicular facet vertically oriented and distal calcaneocuboid facet deep: (0) absent; (1) present. Most didelphid groups analyzed herein exhibit the astragalonavicular facet transversely oriented, except for the terrestrial *Metachirus*, where the astragalonavicular facet is almost vertically oriented, which is accompanied by an increase in depth of the distal calcaneocuboid facet of the calcaneus. Although the orientation of the astragalonavicular facet of *Monodelphis* seems to be somewhat vertical (as was also observed by Szalay, 1994: 191), its position reflects the condition exhibited by most of didelphids groups (i.e., condition 0). The particular vertical orientation of the astragalonavicular facet showed by *Metachirus* (and partially by *Monodelphis*) suggests the increased functional importance of flexion-extension rather pronation-supination of the hindfoot. Polymorphism is evidenced in *Philander opossum* (coded {01}). No information is currently available about this character for *Monodelphis adusta*, *Micoureus paraguayanus*, and *Lestodelphys* (coded "?").

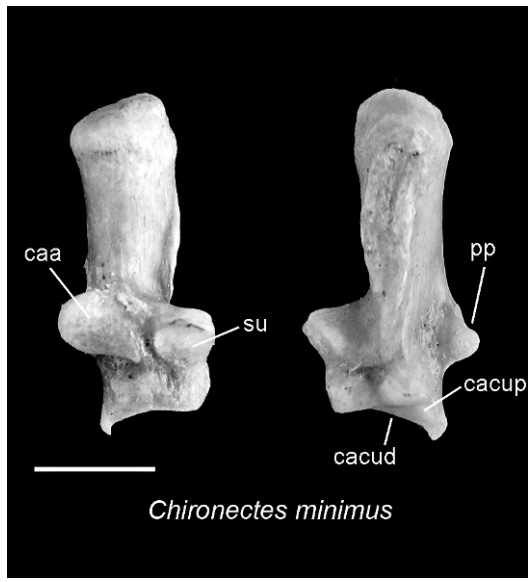

Fig. 32. *Chironectes minimus* (AMNH 148720), dorsal and plantar views of right calcaneus. The peroneal process (pp) is well developed (ch. 113[1]), and the calcaneal sustentaculum (su) is placed on the anterior tip (ch. 114[1]). Other abbreviations: caa, calcaneoastragalar facet; cacud, distal calcaneocuboid facet; cacup, proximal calcaneocuboid facet; sc, sulcus calcanei. Scale bar: 5 mm.

Character 113: Calcaneus, development of peroneal process of calcaneus: (0) small; (1) well developed (fig. 32). Most of the didelphid group analyzed herein exhibits the peroneal process well developed, except for *Metachirus* and *Monodelphis*, where this process is smaller (see Szalay, 1994: figs. 8–12). No information is currently available about this character for *Monodelphis adusta*, *Micoureus paraguayanus*, and *Lestodelphys* (coded "?").

Character 114: Calacaneus, calcaneal sustentaculum position: (0) subterminal; (1) on anterior tip (fig. 32). The calcaneal sustentaculum is placed on the anterior tip of the calcaneum only in *Chironectes*. No informa-

TABLE 5
Tree Statistics from Parsimony Analyses of Different Didelphid Data Sets, Considering Polymorphism as Composite Entries (CO) and Transformation Series (TS)

	Morphology (Jansa and Voss, 2005)[a]		Postcranial		Nonmolecular data set combined[b]		Total evidence[c]		Total evidence[d]	
	CO	TS	CO	TS	CO	TS	CO	TS	CO	TS
No. MPTs[e]	76	1098	3	7	120	6	2	4	6	4
Consistency index (CI)[f]	0.50	0.50	0.27	0.25	0.33	0.29	0.61	0.59	0.46	0.43
Retention index (RI)	0.84	0.84	0.62	0.59	0.68	0.65	0.80	0.79	0.75	0.72
Tree length[g]	178	177	502	540	723	926	6203	6464	1938	2192
Resolved ingroup nodes	20	28	31	18	29	27	38	31	36	37
Nodes with ≥4 absolute Bremer support	5 (25%)	7 (25%)	4 (13%)	6 (33%)	9 (31%)	10 (37%)	26 (68%)	20 (64%)	23 (64%)	20 (54%)

[a]Nonmolecular data set including craniodental, external morphology, and karyotype; defined by Voss and Jansa (2003).
[b]Morphological data set combining 71 nonmolecular characters defined by Voss and Jansa (2003), and 114 postcranial characters described in this report.
[c]All combined evidence including IRBP, DMP-1, RAG-1, and morphology.
[d]Partitioned combined evidence including IRBP, DMP-1, and morphology (RAG-1 eliminated).
[e]Equally most parsimonious trees recovered by heuristic searches as described in "Materials and Methods".
[f]Excluding autapomorphies.
[g]Including autapomorphies.

tion is currently available about this character for *Monodelphis adusta*, *Micoureus paraguayanus*, and *Lestodelphys* (coded "?").

Postcranial Data Set Summary

The data set described above includes 114 postcranial characters, of which 106 (93%) are parsimony informative and 8 (7%) are autapomorphic. Sixty-six characters (58%) are binary, 47 (41%) describe ordered multistate (additive) transformations, and only 1 character (0.9%) describes unordered multistate (nonadditive) transformations (table 3). The data matrix (appendix 2) has $114 \times 38 = 4332$ cells, of which only 79 (2%) are scored as missing ("?") and 44 (1%) are scored as inapplicable ("–"). The remaining 4209 matrix cells (97%) record organismal traits, with data completeness for individual terminal taxa ranging from 88 to 100% (table 4). Polymorphism was detected for 30 characters (2% of the total matrix cells), which showed intraspecific variation in the sample analyzed (table 2).

Analytic Results of Postcranial Characters

A heuristic analysis of the postcranial data analyzed with CO polymorphic entries resulted in three equally most parsimonious trees (502 steps, CI = 0.27, RI = 0.62; table 5) whose highly resolved strict consensus is shown in figure 33. The three caluromyines included (except the root) form a single clade in which *Caluromys* is recovered as a monophyletic group. Unlike results from the previous analysis of a different nonmolecular data set analyzed by Jansa and Voss (2005: fig. 1C), the deep branch topology in the didelphine group is well resolved in the consensus topology, and some already recognized groups are recovered. *Hyladelphys* appears in basal and intermediate positions between caluromyines and didelphines, which is consistent with hypotheses attained by previous nonmolecular data, IRBP sequences, and combined analyses (table 6). Successively, *Marmosa robinsoni* and *Cryptonanus unduaviensis* appear as sister taxa of the remaining didelphines, which form a well-resolved topology. As in previous morphological and molecular analyses, *Thylamys* is recovered as a monophyletic group, arranged in the sequence (*T. pallidior*-*T. venustus* (*T. macrurus* (*T. pusillus*))). On the other hand, all species of *Marmosops* included in this analysis (*pinheiroi*, *parvidens*, *noctivagus*, *impavidus*, and *incanus*) form a monophyletic group (node M), which have been recovered

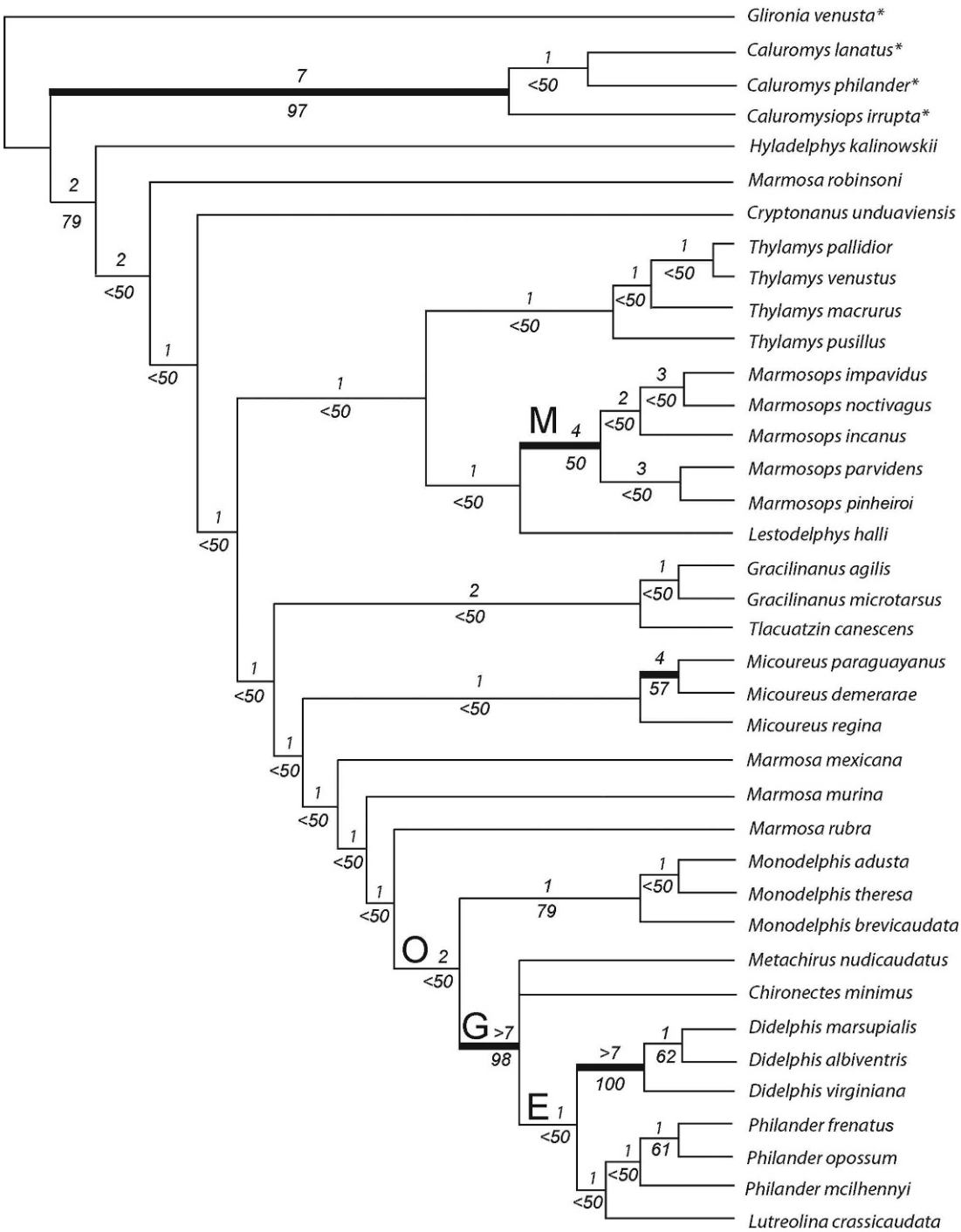

Fig. 33. Strict consensus of three equally most parsimonious trees resulting from cladistic parsimony analysis of 114 postcranial characters for 38 taxa described in this report, where polymorphic data were treated as composite entries (CO) (see tables 2–4 for summary data set characteristics and tree statistics). Numbers above branches refer to absolute Bremer support values (≥1). Numbers below branches refer to

TABLE 6
Different Data Sets Supporting an Intermediate Position of *Hyladephys* between Caluromyinae and Didelphinae.

	Postcranial
Morphology (Jansa and Voss, 2005)	
All morphology[a]	
IRBP	
DMP-1	
RAG-1	
Jansa and Voss, 2005 (combined)[b]	
Gruber et al., 2007 (combined)[c]	
Gruber et al., 2007 (combined partitioned)[d]	
Total evidence[e]	
Total evidence (partitioned)[f]	

[a]Morphological data set including postcranial evidence described here, and the nonmolecular characters defined by Voss and Jansa (2003).

[b]Data set combining nonmolecular characters, IRBP, and DMP-1 sequences (postcranial excluded).

[c]Data set combining nonmolecular characters, IRBP, DMP-1, and RAG-1 sequences (postcranial excluded).

[d]Data set combining nonmolecular characters, IRBP, DMP-1, and RAG-1 sequences (postcranial excluded, RAG-1 third position eliminated).

[e]Data set combining nonmolecular characters, IRBP, DMP-1, and RAG-1 sequences (postcranial included).

[f]Data set combining nonmolecular characters, IRBP, and DMP-1 (postcranial included, RAG-1 excluded).

in previous results with other kinds of evidence. In this group, *Marmosops impavidus* and *M. noctivagus* are sister species, as well as *M. parvidens* and *M. pinheiroi*. Lastly, *Lestodelphys* is placed as sister of *Marmosops*. Up in the tree, *Tlacuatzin* appears as sister of the group *Gracilinanus agilis-G. microtarsus*, and *Micoureus* is recovered as a monophyletic group in the sequence (*M. demerarae-M. paraguayanus*) *M. regina*)). The three remaining species of marmosa (*M. mexicana*, *M. murina*, and *M. rubra*) are successively arranged. Finally, the species of *Monodelphis*, resolved in the sequence (*M. brevicaudata* (*M. adusta* + *M. theresa*)) are recovered as sister group of the large opossums (node O). Although in general the large opossums (*Didelphis*, *Philander*, *Metachirus*, *Chironectes*, and *Lutreolina*; node G) form an unresolved clade, *Didelphis* is recovered as a monophyletic group in the sequence (*Didelphis virginiana* (*D. marsupialis* + *D. albiventris*), as well as *Philander* in the sequence (*P. mcilhennyi* (*P. opossum-P. fre-natus*)). Both genera form a monophyletic group with *Lutreolina* (node E).

The heuristic search of the postcranial data set with polymorphic entries analyzed with TS resulted in seven most parsimonious trees of 540 steps (CI = 0.25, RI = 0.59). The strict consensus (fig. 34) resulted in a less resolved topology than CO analysis, where *Hyladelphys* appears again in an intermediate position. Under this criterion, the species of *Marmosa*, *Gracilinanus*, *Cryptonanus unduaviensis*, and *Tlacuatzin* are arranged in a basal polytomy. The monophyletic *Monodelphis* is resolved in the sequence (*M. adusta* (*M. brevicaudata-M. theresa*), with *Thylamys macrurus* in basal position, forming a trichotomy with *T. pusillus* and the *T. pallidior-T. venustus* group. The last clade is the more speciose one and includes the monophyletic *Marmosops* (node M; arranged in the same sequence as in the CO analysis), *Lestodelphys*, and the large opossums (node G). Unexpectedly, the position of the Patagonian *Lestodelphys* is not close to some group of

←

jackknife frequencies (cutoff value = 50%). Heavy lines denote branches with a decay index of ≥4. Outgroup taxa are indicated with asterisks, and alphabetic labels indicate didelphine clades discussed in the text.

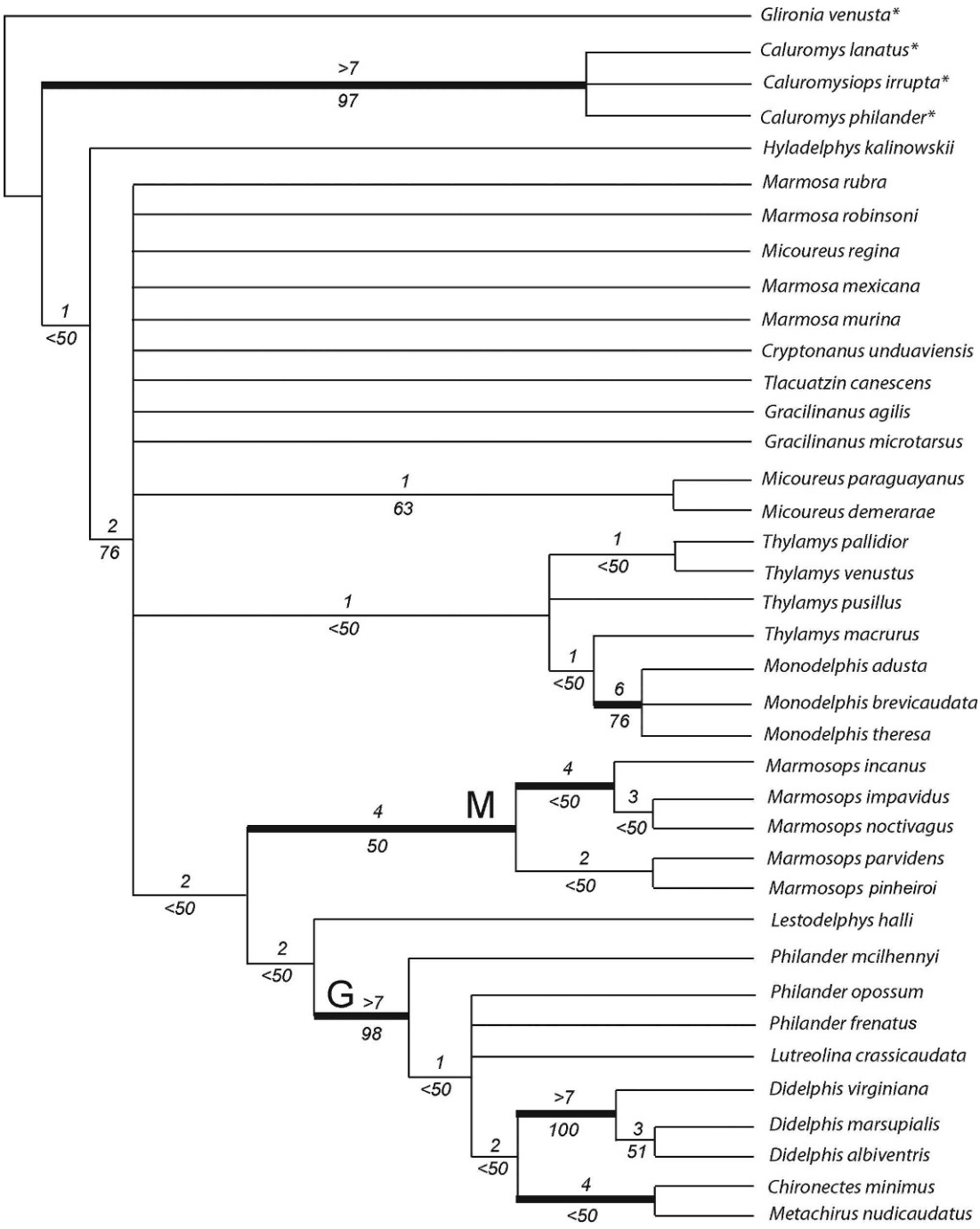

Fig. 34. Strict consensus of seven equally most parsimonious trees resulting from cladistic parsimony analysis of 114 postcranial characters for 38 taxa described in this report, where polymorphic data were treated as transformation series (TS) (see tables 2 and 4 for summary data set characteristics and tree statistics). Numbers above branches refer to absolute Bremer support values (≥1). Numbers below branches refer to jackknife frequencies (cutoff value = 50%). Heavy lines denote branches with a decay index of ≥4. Outgroup taxa are indicated with asterisks. Alphabetic labels indicate didelphine clades discussed in the text.

mouse opossums, but as sister of large opossums. In the last group, the topology is almost similar to the one obtained in CO analysis, but *Philander* is paraphyletic and *Metachirus* and *Chironectes* are sister groups.

Nonmolecular Evidence on Didelphid Phylogeny: The Inclusion of Postcranial Characters

In table 3 are summarized and compared basic statistics for the nonomolecular data set published by Jansa and Voss (2005), the postcranial data presented herein, and the combination of both morphological data sets. Note that both nonmolecular data sets are proportionally similar regarding some basic statistics, that is, as percentages of missing and inapplicable data, parsimony informative characters, and autapomorphies. However, the percentage of ordered multistate characters is higher in the postcranial data set presented here. Combining both nonmolecular data sets analyzed with CO polymorphic entries, I recovered 120 most parsimonious trees (723 steps, CI = 0.33, RI = 0.68) whose strict consensus is shown in figure 35. In this topology, the caluromyines (*Caluromys* + *Caluromysiops*) form a monophyletic group, with both species of *Caluromys* as sister taxa. The intermediate position of *Hyladelphys* between caluromyines and didelphines appears here again (table 6). Up in the tree, the topology appears as a deep dichotomy, which includes the remaining didelphids arranged basically in two monophyletic clades. In the first group, *Tlacuatzin* is sister taxon of the group *Gracilinanus-Cryptonanus-Chacodelphys-Thylamys-Lestodelphys* (node B). In this clade, *Gracilinanus* and *Cryptonanus* are respectively recovered as monphyletic groups, and *Lestodelphys* is nested in the paraphyletic *Thylamys* (node A) in an unresolved trichotomy with *T. venustus* and *T. pallidior*. *T. pusillus* and *T. macrurus* are successively basal to this group. The second clade is formed by a basal polytomy including *Micoureus regina*, *Marmosa murina*, *M. lepida*, *M. mexicana*, and *M. robinsoni*; the group resolved as the sequence *Marmosa rubra* (*Micoureus paraguayanus-M. demerarae*)); and the group conformed by the monophyletic *Marmosops* (node M) and the clade formed by the monophyletic *Monodelphis* and the large opossums as sister groups (node O). The species of *Marmosops* are split in two sister clades, one formed by (*Marmosops incanus* (*M. impavidus-M. noctivagus*)), and another including *M. parvidens-M. pinheiroi*. The four species of *Monodelphis* considered in the morphological analysis are clustered in a well-supported monophyletic clade where *M. brevicaudata* and *M. emiliae* form a pair and *M. adusta* and *M. theresa* complete a trichotomy. The clade formed by the large opossums (node G) includes the monophyletic *Didelphis*, *Philander* (sister of the monotypic *Lutreolina*, node E), and *Chironectes* and *Metachirus* successively arranged in increasingly basal positions (nodes F and G, respectively). The three species of *Didelphis* form an unresolved polytomy, and the species of *Philander* are resolved as (*P. mcilhennyi* (*P. opossum-P. frenatus*)).

A heuristic search of all morphological data sets with polymorphic entries analyzed as TS resulted in six most parsimonious trees of 926 steps (CI = 0.29, RI = 0.65). The strict consensus (fig. 36) results in a barely less resolved topology than the CO analysis (table 5). Deep in the tree, *Hyladelphys* is placed in its typical intermediate position, and *Marmosa lepida*, *M. rubra*, and *M. robinsoni* are successively arranged basal to the remaining didelphids, which are split in two groups: the clade conformed by the sister species *Micoureus paraguayanus-M. demerarae*, and a polytomy including the remaining didelphine species. Seven natural groups can be recognized in this unresolved polytomy. Three out of seven monophyletic groups consist of pairs of species: *Gracilinanus agilis-G. microtarsus*, *G. aceramarcae-G. emiliae*, and *Cryptonanus unduaviensis-C. chacoensis*. The four remaining natural groups include the complex *Thylamys-Lestodelphys* (node A), the monophyletic *Marmosops* (node M) and *Monodelphis*, and the large opossums (node G) in the same topology as in the CO analysis. However, in the TS analysis *Monodelphis adusta* and *M. theresa* are sister species, *Philander* is recovered as an unresolved trichotomy, and *Didelphis* is recovered in the arrangenment (*Didelphis virginiana* (*D. albiventris-D. marsupialis*).

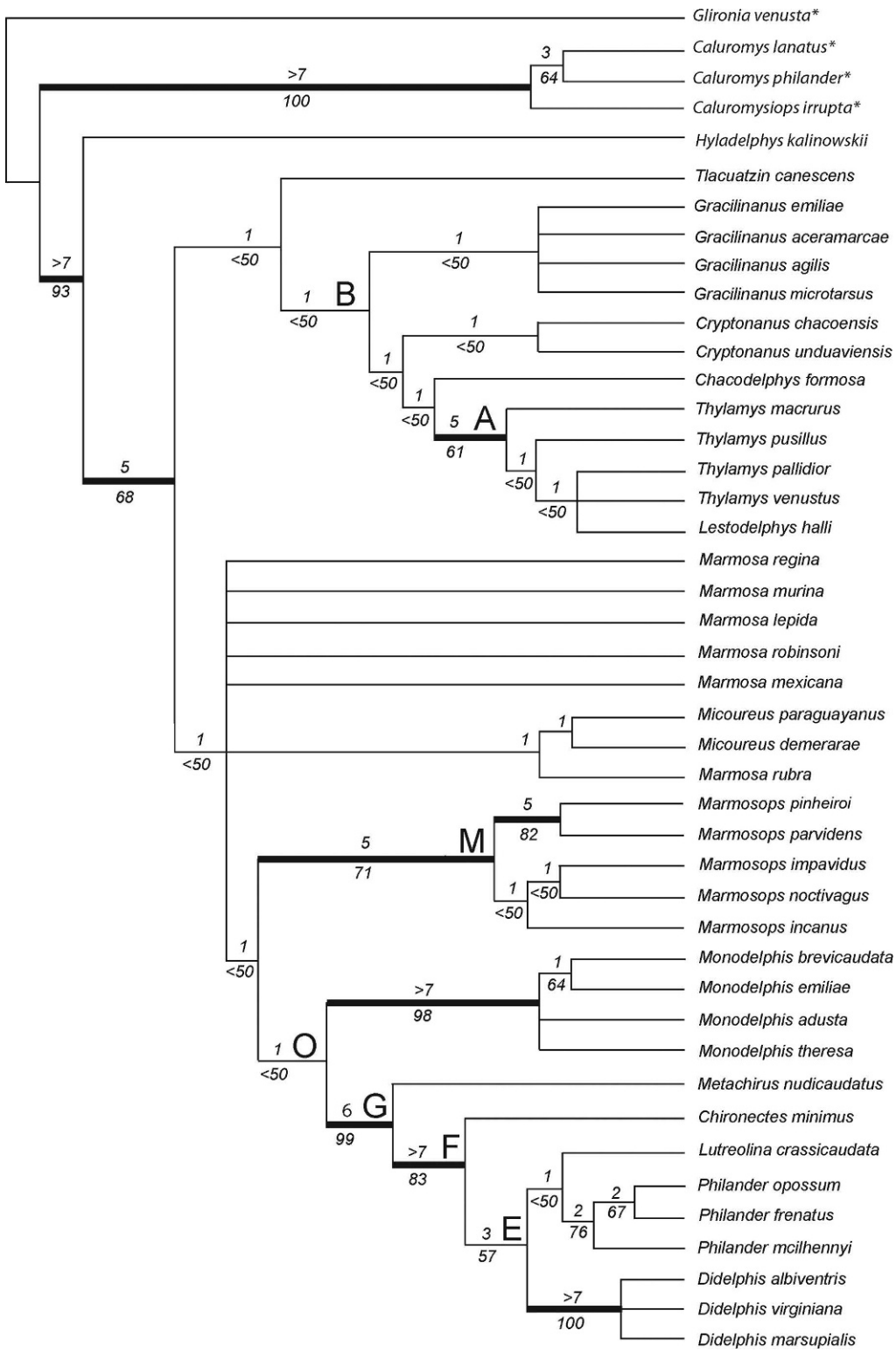

Combined Analysis

Parsimony analysis combining the new postcranial evidence with the nonmolecular characters previously defined, plus IRBP, DMP-1, and RAG-1 sequences analyzed with CO polymorphic entries, resulted in two most parsimonious trees (6203 steps, CI = 0.61, RI = 0.80). The strict consensus topology (fig. 37) resembles, in some positions, the didelphid relationships obtained in the combined evidence by Jansa and Voss (2005: fig. 1D) and Gruber et al. (2007: fig. 2), although the deep branch topology differs remarkably. The relationships within the outgroup are similar to the one obtained with nonmolecular evidence (i.e., *Caluromys and Caluromysiops* forming a monophyletic group, and both species of *Caluromys* as sister taxa). *Hyladelphys* kept its intermediate position between caluromyines and didelphines. From this point of the tree, two traditionally recognized groups in the didelphine subfamily are recovered as monophyletic groups: the 2n = 22 large opossums (node F), and the mouse opossums (node L, although including *Metachirus*). Among the large opossums, the two polytypic living genera (*Didelphis* and *Philander*) are recovered as monophyletic and sister groups (node D). *Lutreolina* and *Chironectes* are successively arranged in increasingly basal positions (nodes E and F, respectively). The remaining taxa are split into three diverse clades. The first one contains the monophyletic *Monodelphis*, resolved in the sequence (*M. emiliae* (*Monodelphis theresa* (*M. adusta-M. brevicaudata*))), and *Chacodelphys* as sister taxa. More nested in the tree, the complex *Micoureus-Marmosa* (node I) is resolved on the monophyletic *Micoureus* in the sequence (*Micoureus regina* (*M. demerarae-M. paraguayanus*)), and *Marmosa* as paraphyletic. *Marmosa lepida* and *M. murina* are successively basal to *Micoureus*. On the other hand, this group is sister of the group (*Marmosa rubra* (*M. mexicana-M. robinsoni*)). The last clade (node C) includes the paraphyletic *Marmosops*, *Metachirus*, and the complex *Thylamys-Lestodelphys* (node A), sister of *Gracilinanus-Cryptonanus* group (node B). Although *Marmosops* is recovered as monophyletic in other analyses (e.g., nonmolecular and previous combined analyses), the complete evidence presented here recovered the species in two different clades. Three species are resolved in the grouping (*Marmosops incanus* (*M. impavidus-M. noctivagus*), and the sister taxa *M. parvidens* and *M. pinheiroi* are clustered with *Metachirus*. The species of *Thylamys* are clustered in a monophyletic group as an unresolved polytomy, although *T. venustus* is placed basal in relation to the remaining species of the genus. As in other results, *Lestodelphys* is sister of *Thylamys*. Both species of *Cryptonanus* (*chacoensis* and *unduaviensis*) are recovered as sister taxa, clustered with the monophyletic *Gracilinanus* (node N), which shows the sequence (*Gracilinanus emiliae* (*G. aceramarcae* (*G. agilis-G. microtarsus*))).

A heuristic search of combined data sets with polymorphic entries analyzed as TS resulted in four most parsimonious trees (6464 steps, CI = 0.59, RI = 0.79). The strict consensus (fig. 38) under this parameter is notably less resolved than the topology obtained in CO analysis (table 5), and some differences can be detected. In this scheme, the position of the 2n = 22 large opossums (node F), which under CO treatment is a sister group of the mouse opossums (fig. 37), is clustered with most of the mouse opossums in a polytomy where the nodes B and C (observed in CO analysis) are not recovered (figs. 37, 38). Another minor difference with CO analysis is the inverted position of *Monodelphis theresa* and *M. emiliae*.

←

Fig. 35. Strict consensus of 120 equally most parsimonious trees resulting from cladistic parsimony analysis of 185 morphological characters for 44 didelphid taxa, where polymorphic data were treated as composite entries (CO) (see tables 2–4 for summary data set characteristics and tree statistics). Numbers above branches refer to absolute Bremer support values (≥1). Numbers below branches refer to jackknife frequencies (cutoff value = 50%). Heavy lines denote branches with a decay index of ≥4. Outgroup taxa are indicated with asterisks. Alphabetic labels indicate didelphine clades discussed in the text.

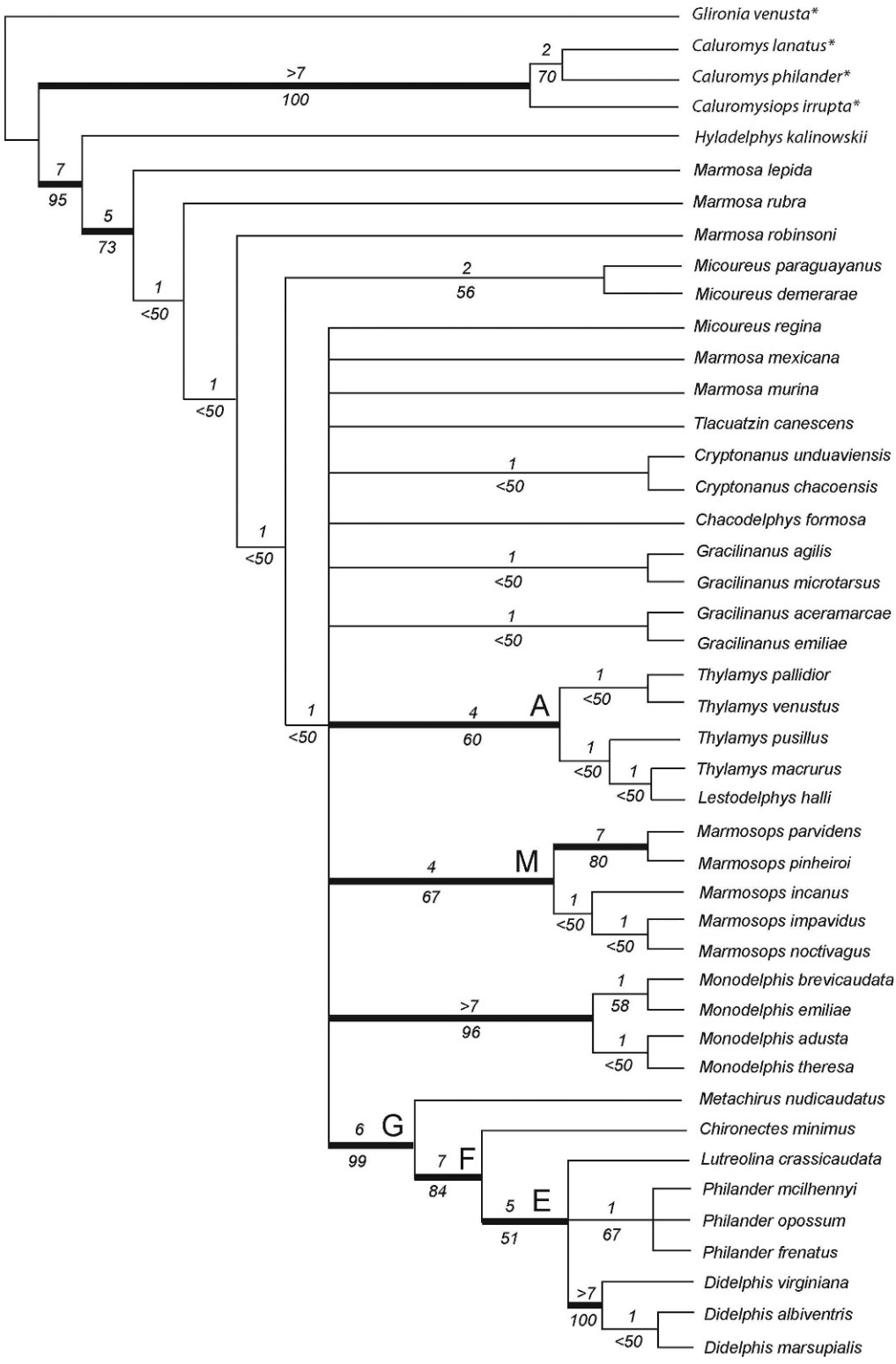

Nodal Support

Bremer support values obtained from the postcranial evidence are, in general terms, low. For instance, in the CO analysis (fig. 33), 21 nodes (68% of resolved nodes) collapse in trees that are one step longer, 4 additional nodes (13%) collapse in trees that are two steps longer, whereas 2 more nodes (6%) collapse in trees that are three steps longer. Only four nodes (13% of the total) have a decay index ≥4 (table 5). Although the TS analysis has less resolved ingroup nodes in the consensus tree (fig. 34; table 5), the amount of well-supported nodes is higher (table 5). Five nodes (28%) collapse in trees that are one step longer, five additional nodes (28%) collapse in trees two steps longer, and two nodes (11%) collapse in trees three steps longer. Lastly, the remaining six nodes (14%) have a decay index ≥4 (table 5). Resampling values were also low: in CO analysis 22 nodes (71%) have jackknife values below 50%, and 6 nodes (19%) have jackknife values between 50% and 85%, while the remaining 3 nodes (9%) have jackknife values higher than 85%. In the TS postcranial analysis 11 nodes (61%) have jackknife values below 50%, 4 nodes (22%) have jackknife values between 50% and 85%, while only 2 nodes (11%) have jackknife values higher than 85%.

Nodal support values for morphology of the total tree are slightly higher. In the CO analysis (fig. 35), 17 nodes (59%) collapse in trees that are one step longer, 2 additional nodes (7%) collapse in trees two steps longer, 1 node (3%) collapses in trees that are three steps longer, and 9 nodes (31%) have a decay index ≥4 (table 5). The consensus tree of the TS analysis (fig. 36) is less resolved than the CO analysis, although in the TS analysis there is one more well-supported node than for the CO results. Twelve nodes (44%) collapse in trees that are one step longer, four additional nodes (15%) collapse in trees two steps longer, and only one node (4%) collapses in trees three steps longer. The remaining 10 nodes (37%) have a decay index ≥4 (table 5). Similarly, resampling values are slightly higher in morphology of the total tree: in the CO analysis 16 nodes (55%) have jackknife values below 50%, 8 nodes (27%) have jackknife values between 50% and 85%, while the remaining 4 nodes (14%) have jackknife values higher than 85%. In the TS morphology/total analysis, 15 nodes (55%) have jackknife values below 50%, 8 nodes (29%) have jackknife values between 50% and 85%, and the remaining 4 nodes (15%) have jackknife values higher than 85%.

Nodal support values for the combined CO analysis indicate that most of 38 resolved ingroup nodes in the consensus tree (fig. 37) are moderately well supported. Only eight nodes (21%) collapse in trees one step longer, one additional node (3%) collapses in trees two steps longer, and three more nodes (8%) collapse in trees three steps longer. The remaining 26 nodes (57%) have a decay index ≥4 (table 5). The consensus tree of the TS analysis (fig. 38) shows less resolved ingroup nodes than for the CO analysis. Only three nodes (10%) collapse in trees one step longer, two additional nodes (6%) collapse in trees two steps longer, and six more nodes (19%) collapse in trees three steps longer. The remaining 20 nodes (64%) have a decay index ≥4 (Table 5). Similarly, resampling values were relatively high both in the CO and TS combined analyses. In the CO analysis 10 nodes (26%) have jackknife values below 50%, 6 nodes (16%) have jackknife values between 50% and 85%, and the remaining 22 nodes (58%) have jackknife values higher than 85%. On the other hand, in the TS combined analysis 16 nodes (52%) have jackknife values below 50%, 8 nodes (26%) have jackknife values between 50% and 85%,

←

Fig. 36. Strict consensus of six equally most parsimonious trees resulting from cladistic parsimony analysis of 185 morphological characters for 44 didelphid taxa, where polymorphic data were treated as transformation series (TS) (see tables 2 and 4 for summary data set characteristics and tree statistics). Numbers above branches refer to absolute Bremer support values (≥1). Numbers below branches refer to jackknife frequencies (cutoff value = 50%). Heavy lines denote branches with a decay index of ≥4. Outgroup taxa are indicated with asterisks. Alphabetic labels indicate didelphine clades discussed in the text.

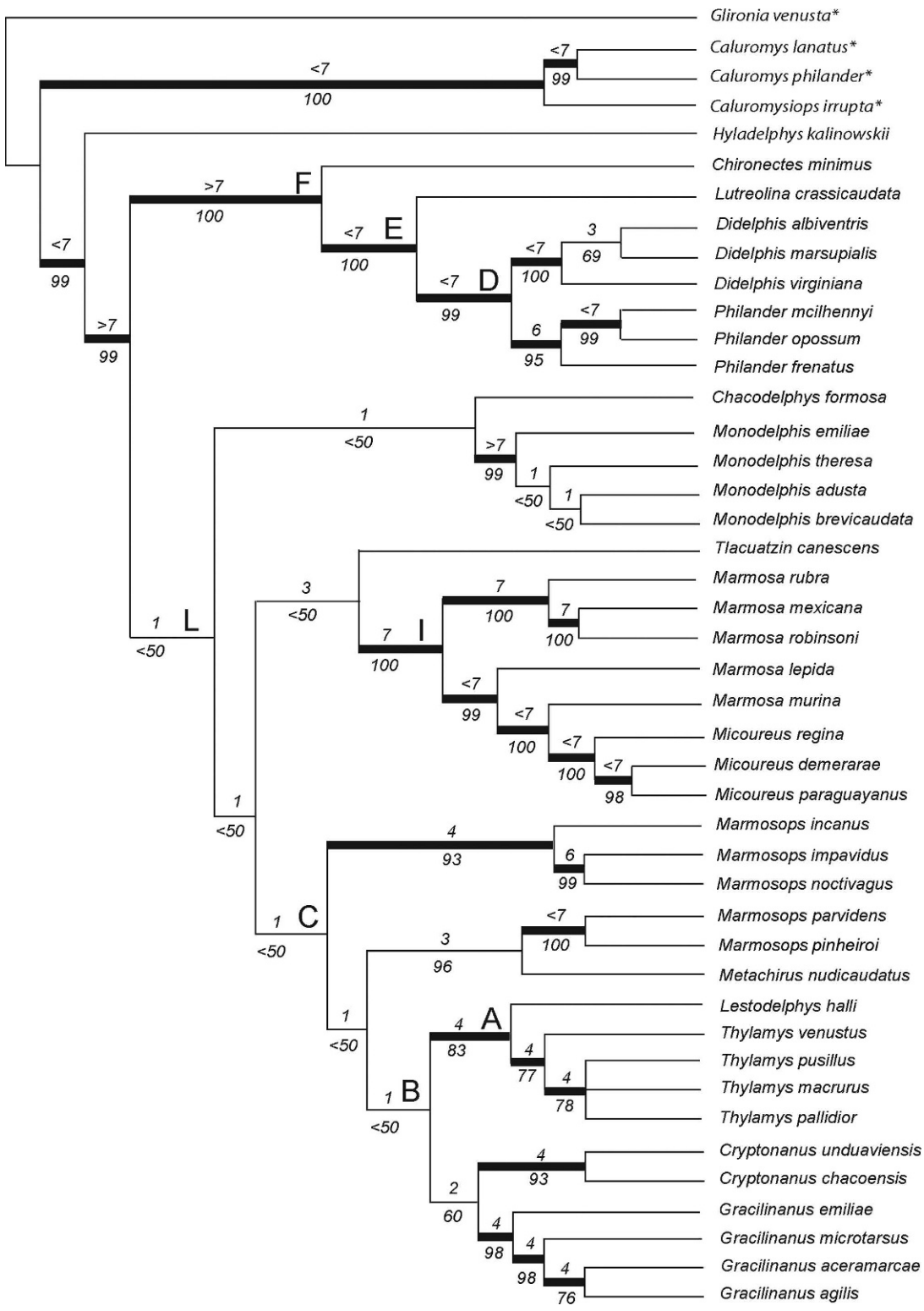

and the remaining 7 nodes (23%) have jackknife values higher than 85%.

DISCUSSION

Effects of Different Codings of Polymorphic Data

The kind of treatment of polymorphic characters may have a significant impact on phylogenetic analyses. Different methods for dealing with polymorphism may lead to very different estimations of phylogeny, even when relationships are strongly supported by one or more methods (Wiens, 1999). The abundance and impact of polymorphic characters are especially clear for closely related species, but the application of different criteria for analyzing polymorphic data may affect higher level relationships as well. In this sense, although different codings of polymorphic postcranial characters in didelphids produced topologies in general not contradictory, some discrepancies were evident. The principal difference was the loss of resolution of the TS analysis compared to the CO analysis, with the consistency index and retention index being slightly higher in the CO analysis (table 5). In the postcranial results, the nodes weakly supported in the CO analysis collapsed in the TS topology (figs. 33, 34). However, more resolution is expected for the additional phylogenetic information with TS coding (Mabee and Humpries, 1993). Different codings caused little impact on the nodal support, since in both topologies the number of nodes with high decay index (≥4) was similar in all analyses, except in the combined analysis considering RAG-1 (table 5), where the CO coding had more well-supported nodes. An inverted bias on nodal support and resolution was observed in a combined analysis in Oryzomyini rodents performed by Weksler (2006). In the case of didelphids, despite the differences in resolution in the combined total evidence, most relationships obtained in the TS analysis are not contradicted by the CO analysis, except for two punctual cases: the inverted position of *Monodelphis emiliae* and *M. adusta*, and the basal position of the *Marmosa-Micoureus* group (node I) in TS analysis (being instead sister of node C in the CO analysis, figs. 37, 38).

In the total morphology analysis, the effects of different codings on polymorphic data were similar with respect to the postcranial-only data set: the topology obtained with the CO coding analysis is notably better resolved than the TS coding analysis (figs. 35, 36), although the values of Bremer support are in general rather similar (table 5). Contrary to the congruence observed in the topology obtained by both kinds of coding in the potscranial-only analysis, the low resolved topology observed with the TS coding in the total morphology analysis differs considerably in some positions with regard to the CO coding analysis. In the TS coding total morphology analysis, the change of position of *Marmosa lepida* and *M. rubra* is unexpected for different reasons. In the first case, all postcranial characters are missing, and the remaining morphological characters do not show polymorphic entries (see Voss and Jansa, 2003: appendix 5). In *Marmosa rubra*, although 95% of the postcranial characters were scored (table 4), there were no polymorphisms since the sample consisted of only one specimen (see appendix 1), and the remaining morphological characters do not show any polymorphic entries (see Voss and Jansa, 2003: appendix 5). Lastly, the change observed in *Marmosa robinsoni* is perhaps a consequence of the high polymorphism present in postcranial morphology (table 2; appendix 2). Other

←

Fig. 37. Strict consensus of two equally most parsimonious trees resulting from cladistic parsimony analysis of combined morphological and genetic data (i.e., all morphology, IRBP, DMP-1, and RAG-1 sequences) for 44 didelphid taxa, where polymorphic data were treated as composite entries (CO) (see tables 3 and 4 for summary data set characteristics and tree statistics). Numbers above branches refer to absolute Bremer support values (≥1). Numbers below branches refer to jackknife frequencies (cutoff value = 50%). Heavy lines denote branches with a decay index of ≥4. Outgroup taxa are indicated with asterisks. Alphabetic labels indicate didelphine clades discussed in the text.

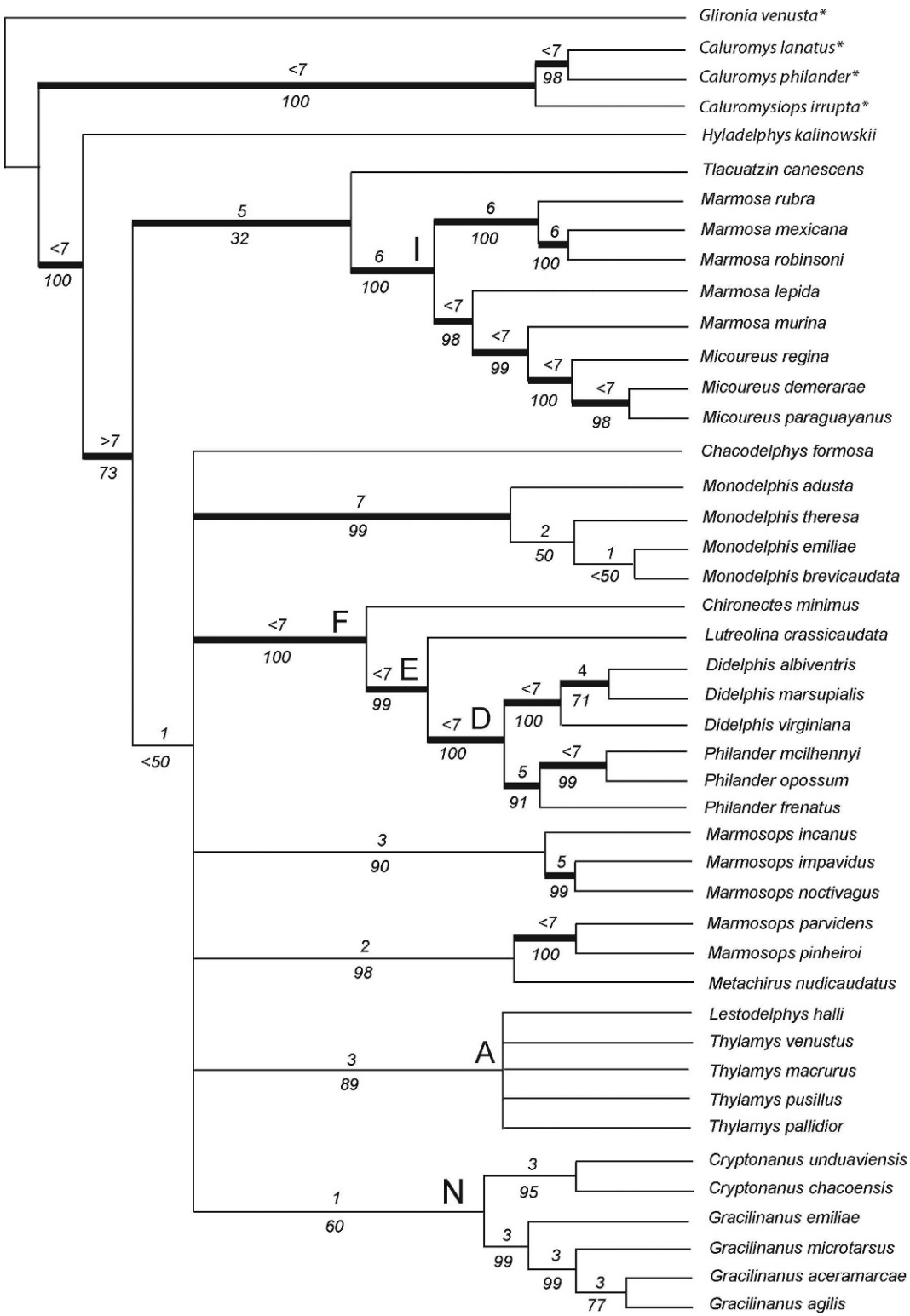

differences can be noted between both kinds of coding, such as the monophyletic condition of *Gracilinanus* in CO coding total morphology analysis, the changing position of *Thylamys macrurus* and *T. pusillus*, and the relationship among the species of the monophyletic *Didelphis* and *Philander*. Despite the differences in deep branch topology, the well-supported clades in CO coding total morphology analysis were all recovered in TS coding morphology-total analysis as well (i.e., the monophyly of *Monodelphis*, *Philander*, *Marmosops*, and *Didelphis*, the relationship of large opossums [nodes E, F, and G], and the relationship of *Thylamys-Lestodelphys* [node A]). Similarly to postcranial-only analysis, in the case of total morphology, the TS coding analysis seems not to contribute to the retention of more phylogenetic information.

As described in the results, the topologies obtained including the genetic evidence (i.e., combined analysis) are in general highly resolved and better supported than the morphology-only analyses. Despite the fact that the topologies from both kind of codings of polymorphic data are significantly congruent in some aspects, the clustering of the mouse opossums and the better resolution applying CO coding analysis (fig. 37) are interesting. The mouse opossums are the most speciose group in the didelphid living radiation, and the genera currently recognized (sensu Gardner, 2005) are not always recovered as natural groups in the cladistic context. Contrasting with the large opossums, which were considered as a monophyletic group based in a diverse array of previous evidence, the mouse opossums were partially supported only in a morphological framework (e.g. Creighton, 1984; Reig. et al., 1987; Goin, 1995; Flores, 2003). Here, the addition of postcranial evidence to the previous nonmolecular and genetic evidence causes the moderately supported clustering of the mouse opossums in a group just in CO coding analysis (although *Metachirus* is nested in the group when RAG-1 is included; fig. 37; appendix 3). However, the group is paraphyletic in all previous nonmolecular and molecular (IRBP, DMP-1, RAG-1) analyses (Kirsch and Palma, 1995; Patton et al., 1996; Jansa and Voss, 2000, 2005; Voss and Jansa, 2003; Voss et al., 2005; Jansa et al., 2006; Gruber et al., 2007), and even in all remaining analyses of this report. In this sense, applying different criteria for the treatment of morphological polymorphic data, the relationships and monophyly of the mouse opossums are strongly affected.

Effect of the Inclusion of Postcranial Characters in Previous Nonmolecular and Combined Hypotheses

Nonmolecular Hypotheses: Comparing the topology of nonmolecular evidence illustrated by Jansa and Voss (2005: fig. 1C), the inclusion of the postcranial data set causes considerable changes and better resolution in topology and support values (figs. 35, 36; tables 5–7). As mentioned above, the intermediate position of *Hyladelphys* is consistent in postcranial-only and combined analyses (table 6). The trichotomy conformed by the monophyletic *Didelphis* and *Philander*, as well as the monotypic *Lutreolina* (node E), is kept both in CO and TS analyses of total morphology evidence, as well as the monophyly of *Monodelphis* and its sister relationship with large opossums (node O in the CO analysis, fig. 35), the relationship of *Lestodelphys-Thylamys* (node A), and the monophyly of *Marmosops* (node M), *Gracilinanus*, and *Cryptonanus* (although the TS coding analysis produces the rupture of

←

Fig. 38. Strict consensus of four equally most parsimonious trees resulting from cladistic parsimony analysis of morphological and genetic data (i.e., all morphology, IRBP, DMP-1, and RAG-1 sequences) for 44 didelphid taxa, where polymorphic data were treated as transformation series (TS) (see tables 3 and 4 for summary data set characteristics and tree statistics). Numbers above branches refer to absolute Bremer support values (≥1). Numbers below branches refer to jackknife frequencies (cutoff value = 50%). Heavy lines denote branches with a decay index of ≥4. Outgroup taxa are indicated with asterisks. Alphabetic labels indicate didelphine clades discussed in the text.

TABLE 7
Nodes Recovered under Different Analyses and Values of Absolute Bremer Support and Jackknife Frequencies[a]

Node	1	2	3	4	5	6	7	8
A			5/61	4/60	4/83	3/89	4/83	5/86
B			1/<50		1/<50		1/<50	2/<50
C					1/<50[b]		1/<50	2/<50
D					>7/99	>7/100	4/73	4/78
E	1/<50		3/<50	6/<50	>7/100	>7/99	>7/97	>7/99
F			>7/66	6/84	>7/100	>7/100	>7/100	>7/100
G	>7/98	>7/98	6/83	7/99			5/99	7/99
H								2/<50
I					7/100	6/100	7/99	>7/94
J							1/<50	2/<50
L					1/<50[b]		4/75[c]	
M	4/50	4/50	5/71	5/67			5/97	6/98
N					2/60	1/50	1/<50	2/<50
O	1/<50		1/<50					

[a]Letters indicate the nodes labeled as in figures 33–40. Each column corresponds to different analyses described and compared in the text. 1, Postcranial data, CO coding for polymorphic entries; 2, postcranial data, TS coding; 3, all nonmolecular data set (including postcranium), CO coding; 4, all nonmolecular dataset (including postcranium), TS coding; 5, combined data (including postcranium), CO coding; 6, combined data (including postcranium), TS coding; 7, combined data (including postcranium), RAG-1 eliminated, CO coding; 8, combined data (including postcranium), RAG-1 eliminated, TS coding.

[b]Including *Metachirus*.

[c]Excluding *Metachirus*.

the monophyly of *Gracilinanus*, fig. 36). However, some alterations in the topology can be detected by including the postcranial characters. In the CO coding analysis (fig. 35), both species of *Cryptonanus* (*chacoensis* and *unduaviensis*) appear as a monophyletic group sister to the clade *Chacodelphys*-node A (*Thylamys-Lestodelphys*), and the species of *Gracilinanus* are also clustered as monophyletic basal in node B. The monophyly of node B in the CO coding analysis (fig. 35) is recovered by including the postcranial evidence. In this sense, consideration of the postcranial characters on the morphological evidence previously defined (Jansa and Voss, 2005) is consistent with the genetic evidence, since clustering of the monophyletic genera *Gracilinanus* and *Cryptonanus* with node A was obtained using only genetic and combined evidence (Jansa and Voss, 2005; Gruber et al., 2007). The position of *Metachirus* is also altered when the postcranial evidence is included, since this monotypic taxon is basal to the large 2n = 22 opossums in the total morphology analysis (node G in figs. 35, 36), whereas it is located as the sister taxon of the group consisting of 2n = 22 opossums-*Monodelphis* in the morphological analysis excluding the postcranial characters (see Jansa and Voss, 2005: fig. 1C; table 7). Although *Metachirus* shows a particular mode of locomotion and some postcranial autapomorphies (see the character descriptions and appendix 2), its close relationship with the 2n = 22 large opossums (node G in figs. 35, 36) is well supported by postcranial morphology (table 7). Similarly, the inclusion of postcranial evidence notably affects the position of the recently redescribed *Tlacuatzin canescens*. This taxon appears in a basal polytomy together with some species of *Marmosa* and *Micoureus* in the morphological evidence of Jansa and Voss (2005: fig. 1C). A similar position is obtained when the TS coding criterion is applied for polymorphic characters in the total morphology analysis (fig. 36), but when the postcranial data set is included in the CO coding analysis, this taxon is placed as sister to node B, although with low support (fig. 35).

The relationship *Thylamys-Lestodelphys* (node A) and the paraphyly of *Thylamys* are also kept when postcranial evidence is considered (table 7), but the position of this

clade in the total morphology consensus tree is remarkably different. In the topology obtained by Jansa and Voss (2005: fig. 1C) this clade is located as sister of the *Monodelphis*-large opossums group (node O), whereas when including the postcranial evidence this group appears as forming part of node B in the CO coding analysis (fig. 35). The monophyly of *Marmosops* (node M) is also kept, but its position is different when the postcranial characters are considered. When omitting postcranial evidence, its position is basal in the clade that includes the large opossums, *Monodelphis* (node O), and the complex *Thylamys-Lestodelphys-Chacodelphys* (Jansa and Voss, 2005: fig. 1C). Nonetheless, in the CO coding total morphology analysis this monophyletic genus appears as sister to node O (node G and *Monodelphis*, fig. 35).

Although the parsimony analysis considering only the postcranial data set resulted in a well-resolved strict consensus but with lower consistency and retention indices compared to the total morphology analysis (i.e., the postcranial characters defined here and the 71 nonmolecular characters defined by Voss and Jansa, 2003; see tables 5, 7; figs. 33, 35), several relationships (which are recovered in both analyses separately) are kept with the inclusion of postcranial evidence (tables 6, 7): the intermediate position of *Hyladelphys* between caluromyines and didelphines is recovered in all morphological analyses, as is the monophyly of *Monodelphis*, *Marmosops* (node M), and the large opossums (*Didelphis*, *Philander*, *Lutreolina*, *Chironectes*, and *Metachirus* [node G]). Several nodes recovered by including genetic evidence (Jansa and Voss, 2005; Jansa et al., 2006; Gruber et al., 2007) were not found based on morphological evidence omitting postcranial characters. As mentioned above, the inclusion of postcranial evidence also produces better resolution. Nodes B and G (fig. 35) specifically are also recognized in a more inclusive morphological data set, with the postcranial characters concatenated to the previously defined nonmolecular evidence (table 7).

HYPOTHESES BASED ON COMBINED EVIDENCE: The inclusion of postcranial characters in the combined data set performed by Jansa and Voss (2005), Jansa et al. (2006), and Gruber et al. (2007) causes some interesting alterations in the resulting hypotheses (table 7). The general topology (figs. 37, 38) shows several congruences with diverse aspects of molecular (IRBP, DMP-1) and nonmolecular evidence (table 8). The recent inclusion of RAG-1 sequences (Gruber et al., 2007: figs. 1, 2) resulted in the well-supported clustering of distantly related clades based on profuse evidence: clade B (*Thylamys-Cryptonanus-Gracilinanus*) as sister of clade I (*Marmosa-Micoureus* complex). However, the addition of postcranial evidence to the supermatrix analyzed by Gruber et al. (2007) did not recover this apparently spurious clade (figs. 37, 38). The homoplasy caused by the convergence in CG content on the third position in RAG-1 sequences (Gruber et al., 2007) is hidden by the effect of the phylogenetic information coming from the postcranial evidence, independent of the treatment applied to polymorphic characters.

Another example of the influence of postcranial data on previously combined data sets is the position of *Hyladelphys* (table 6). As mentioned before, this monotypic and recently recognized genus was located in a basal position, intermediate to didelphines and caluromyines, based on profuse molecular and morphological support (Jansa and Voss, 2005). The recent inclusion of RAG-1 sequences alters the typical phylogenetic position of this taxon, being sister to the already mentioned and apparently spurious clade (B + I in Gruber et al., 2007: fig. 2), although with low support values. The inclusion of postcranial characters in the combined data set (even including the RAG-1 sequences and its third positions) replaces the typical intermediate position of *Hyladephys* (figs. 37, 38) between caluromyines and didelphines.

Although the combined evidence incorporating the postcranial characters shows some relationships congruent with earlier evidence (tables 7, 8), the position of the cursosaltatorial *Metachirus* and the recently described *Tlacuatzin* are highly affected, as was also demonstrated in total morphology analyses. In previous molecular and combined analyses (table 8), *Metachirus* was within the clade conformed by the large opossums (*Didelphis*, *Philander*, *Lutreolina*, and *Chironectes*; node G), usually in a basal position (see Gruber et

TABLE 8
Nodes Recovered in Previous Molecular and Combined Evidence
(All combined analyses excluding postcranial evidence. Letters indicate the nodes labeled as in figures 33–40.)

Node	IRBP (Jansa and Voss, 2005)	DMP-1 (Jansa et al., 2006)	RAG-1 (Gruber et al., 2007)	Combined (Jansa and Voss, 2005)[a]	Combined (Gruber et al. 2007)[b]	Combined (Gruber et al., 2007)[c]
A[d]	■	■		■		■
B	■	■	■	■	■	■
C	■	■	■	■	■	■
D	■	■	■	■	■	■
E	■	■	■	■	■	■
F	■	■	■	■	■	■
G	■	■	■	■	■	■
H	■	■		■		■
I	■	■	■	■	■	■
J		■		■		■
L						
M	■	■	■	■	■	■
N		■	■	■	■	■
O						

[a]RAG-1 not included.
[b]RAG-1 included.
[c]Third position of RAG-1 eliminated.
[d]Node A (*Lestodelphys-Thylamys*) is not documented in Gruber et al. (2007) because the RAG-1 sequence data for *Lestodelphys* is unavailable.

al., 2007; Jansa and Voss, 2005; Jansa et al., 2006). Nonetheless, the addition of postcranial characters to the combined evidence relates *Metachirus* with *Marmosops parvidens-M. pinheiroi*, nested in the speciose clade labeled C in figures 37 and 38 (table 7). The inclusion of *Metachirus* in that group is unlikely in view of the huge amount of phylogenetic information (even postcranial) relating this species to other large opossums. The inclusion of postcranial characters in previously combined evidence (considering also RAG-1 sequences, see appendix 3) apparently affects the presumably true phylogenetic position of *Metachirus*.

Similarly, consideration of postcranial morphology in combined analyses notably alters the position of *Tlacuatzin canescens*, which is sister of *Monodelphis* in all recent combined evidence (see Jansa and Voss, 2005: fig. 1D; Jansa et al., 2006: fig. 5; Gruber et al., 2007: fig. 2). By adding the new data set, *Tlacuatzin* became sister to the *Marmosa-Micoureus* complex (node I), a relationship not found in previous analyses. This topology is highly interesting because *T. canescens* was traditionally included in the nonmonophyletic genus *Marmosa*. However, even when the decay index of this clade is high in the TS and CO coding combined analyses, the jackknife values in both analyses are notably lower (figs. 37, 38).

As described in the results, the topology obtained by including genetic evidence in the CO coding analysis is highly resolved and better supported than the morphology-only analyses (tables 7, 8). However, even if the topologies from both kinds of coding of polymorphic characters are considerably congruent in some aspects (figs. 37, 38; table 7), the clustering of the mouse opossums recovered with the CO coding analysis is remarkable (node L; table 7; although *Metachirus* is nested in this clade). Here, the addition of postcranial evidence to previous nonmolecular and genetic evidence causes the clustering of the mouse opossums only in the CO coding analysis, although with most of the support values being low (fig. 37; table 7), which were also paraphyletic in all previous nonmolecular and molecular (table 8) analyses (e.g. Voss and Jansa, 2003; Jansa and Voss, 2000, 2005; Voss et al., 2005; Jansa et al., 2006; Kirsch and Palma, 1995; Patton et al., 1996), and even in all remaining analyses in this report (table 7).

As discussed above, the addition of postcranial characters recovered some relationships already supported by previous combined analyses (tables 7, 8), but the resulting topologies are contradictory in some positions. Despite the mentioned incongruences in the positions of *Metachirus* and *Tlacuatzin*, the node labeled O, which includes *Monodelphis* as sister to the large 2n = 22 opossums, is recovered when considering the postcranial evidence, but it has not been obseved before in any previous molecular or combined analyses (table 8), except in two analyses in this report (table 7), and in the partial morphological evidence from Jansa and Voss (2005: fig 1C). However, this node is recovered with low support (fig. 38; table 7). Another clear difference concerns the already recognized nodes J and H (Voss and Jansa, 2005: fig. 1D; Gruber et al., 2007: fig. 6A–C; Jansa et al., 2006: fig. 4B; table 8), which are well-supported sister groups in previous combined evidence, although this relationship is broken by inclusion of the RAG-1 sequence (figs. 37, 38; see Gruber et al., 2007: fig. 2).

In view of the high convergence of CG content on the third positions, a more congruent topology was obtained when the third positions of RAG-1 were experimentally eliminated (table 8: Gruber et al., 2007). When omitting the RAG-1 sequence from the combined data set presented here, the relationships obtained are highly congruent with previous evidence recently published, recovering almost all nodes already recognized, even in the TS coding analysis (figs. 39, 40; tables 7, 8). Independent of deep branch differences of the partitioned evidence (depending on the CO or TS treatment of polymorphic characters), *Metachirus* recovers its traditional position as sister of the remaining 2n = 22 large opossums (node G), and *Tlacuatzin* is relocated as sister to *Monodelphis*. The topology obtained with the TS partitioned analysis (fig. 40) is basically similar to the one obtained in the combined analysis by Jansa and Voss (2005: fig. 1D) and some combined topologies obtained by Gruber et al. (2007: fig. 6A–C) and Jansa et al. (2006: fig. 5). Most nodes already documented are recovered: nodes H, J, C, G, B, and I (table 7). However, as in the complete combined data set, the application of different criteria for treatment of polymorphic data in the partitioned analysis strongly affects the relationships and phyletic condition of the mouse opossums, since in the CO coding analysis node H is not recovered, and the mouse opossums (node L) are monophyletic although moderately supported (fig. 39; table 7). In this sense, the inclusion of postcranial evidence concatenated to the previous combined data set has notable influence on deep branch topology, depending of the mode of coding polymorphic characters. The partitioned TS combined analysis (excluding RAG-1; fig. 40) recovers all of the topologies already observed (table 7), which indicates that the inclusion of postcranial characters does not contradict the relationships obtained with profuse previous combined evidence (table 8).

The Postcranial Anatomy as Evidence of Didelphid Relationships and Postcranial Synapomorphies in Didelphinae

The study of diversity of the cranioskeletal system is one of the most critical areas of research for the understanding of various aspects of behavior and ecological morphology, particularly locomotion and feeding habits in marsupials (Szalay, 1994). Even if the most common conception points toward the close evolutionary relationship between craniodental anatomy and feeding demands, the movements linked to locomotion, posture, and other behavioral patterns are particularly dependent on the musculoskeletal system. Moreover, the skeletal morphology of the most abundantly represented Neogene forms, or extant marsupials, has not been adequately studied from the perspective of evolutionary morphology (Szalay, 1994). Because the skeletal structure is highly correlated with posture, habits, and locomotion, several patterns (both in the axial and appendicular skeleton) have been associated with an apparent functionality. Several recent papers (e.g. Argot 2001, 2002, 2003a, 2003b, 2004a, 2004b; Szalay, 1994; Sears, 2004; Szalay and Sargis, 2001; Weisbecker and Sánchez-Villagra, 2006) have revised the postcranial morphological patterns in mar-

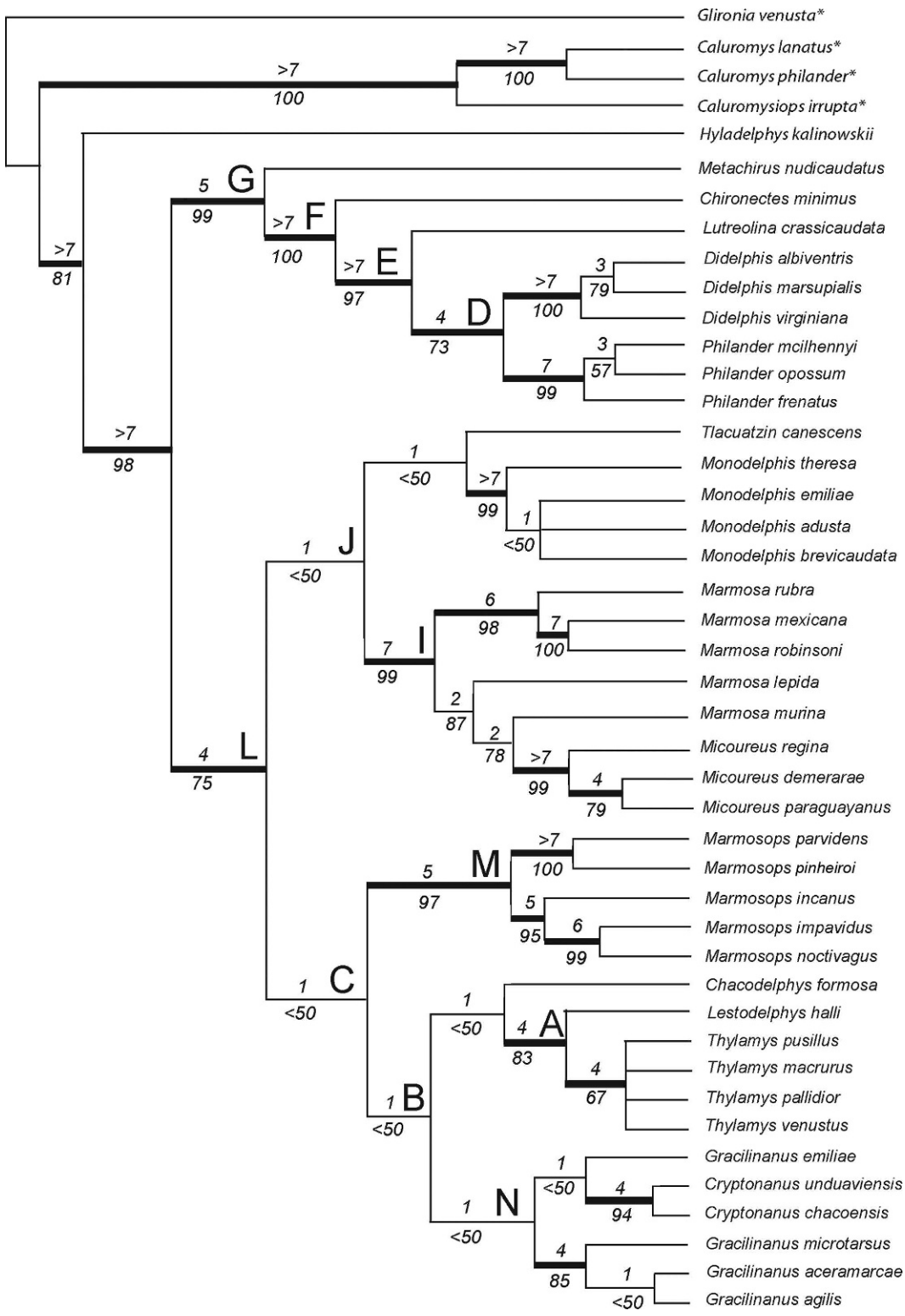

supials and their associated forms-functions on the metatherian postcranium.

The didelphid relationships have been examined with different kinds of data (molecular and morphological), but the application of postcranial characters has never been considered as evidence of didelphid phylogeny in a cladistic frame on a denser taxon sampling. Several postcranial characters defined by Horovitz and Sánchez-Villagra (2003) are highly variable within the didelphid taxa included in this report, although the postcranial unambiguous synapomorphies proposed for Didelphidae in the cited work are also evidenced in all didelphid taxonomic samples considered herein.

Some postcranial topologies recovered in this study (figs. 33, 34) are clearly congruent and noncontroversial with clades already recognized based on other evidence (morphological and molecular; tables 6–8). The postcranial morphology has showed inherent phylogenetic information in recovering some traditionally recognized relationships and monophyletic groups (tables 7, 8; appendix 3). However, the postcranial evidence in didelphids also produces some unusual relationships, a product of the convergence of characters strongly associated with form-function patterns. In other words, several postcranial characters exhibited the same condition in taxa with analogous locomotion and/or posture patterns, which are clearly linked to specific form-function. For instance, the particular vertical orientation of the astragalonavicular facet of the astragalus (ch. 112[1]) and the depth of the distal calcaneocuboid facet of the calcaneus showed by *Metachirus* and *Monodelphis* suggest an increased functional importance of flexion-extension of the hindfoot in both terrestrials but not closely related taxa (Szalay, 1994). This is a hint that some atypical relationships obtained are possibly caused by morphological constraints of form-function in some structures, which can hide the true relationships obtained from other kinds of evidence when the postcranial data set is analyzed separately. This homoplasy is presumably the cause of the low values of consistency index and the poor resolution of the strict consensus (mainly in the TS coding postcranial-only topology, fig. 34) compared to the more resolved trees obtained from the total morphology (fig. 35) and combined evidence (figs. 37–40; table 5).

In the topologies based on the postcranial-only data set, the monophyly of several traditionally recognized polytypic genera (sensu Gardner, 2005), such as *Gracilinanus*, *Marmosa*, and *Cryptonanus*, are not recovered, and some relationships had not been recovered in previous analyses (figs. 33, 34). For instance, the monophyly between the partially terrestrial *Thylamys* and the highly terrestrial *Monodelphis* is recovered in the strict consensus of the TS coding postcranial analysis (fig. 34), which is supported by an array of characters clearly related to specific capacities of movements: position of the vertebra where the accessory process is differentiated from the transverse process on T7 (implying an anterior point restricting lateral flexibility; ch. 30[1]), or absence of a longitudinal groove on the lateral surface of the ulna for insertion of Mm. abductor pollicis longus and anconeus (muscles well developed in arboreal forms [Argot, 2001]; ch. 77[0]). In all other topologies obtained here (i.e., total morphology and combined, figs. 35–40), as well as in previous hypotheses (Jansa and Voss, 2000, 2005; Gruber et al., 2007; Voss and Jansa, 2003; Jansa et al., 2006; Reig et al., 1987; Kirsch and Palma, 1995), *Monodelphis* and *Thylamys* are clustered in clearly distant clades. Only in the pioneer nonmolecular analysis of Creighton (1984) are both taxa clustered in a mono-

←

Fig. 39. Strict consensus of six equally most parsimonious trees resulting from cladistic parsimony analysis of morphological and genetic data combined, excluding RAG-1 sequences, for 44 didelphid taxa where polymorphic data were treated as composite entries (CO). Numbers above branches refer to absolute Bremer support values (≥1). Numbers below branches refer to jackknife frequencies (cutoff value = 50%). Heavy lines denote branches with a decay index of ≥4. Outgroup taxa are indicated with asterisks. Alphabetic labels indicate didelphine clades discussed in the text.

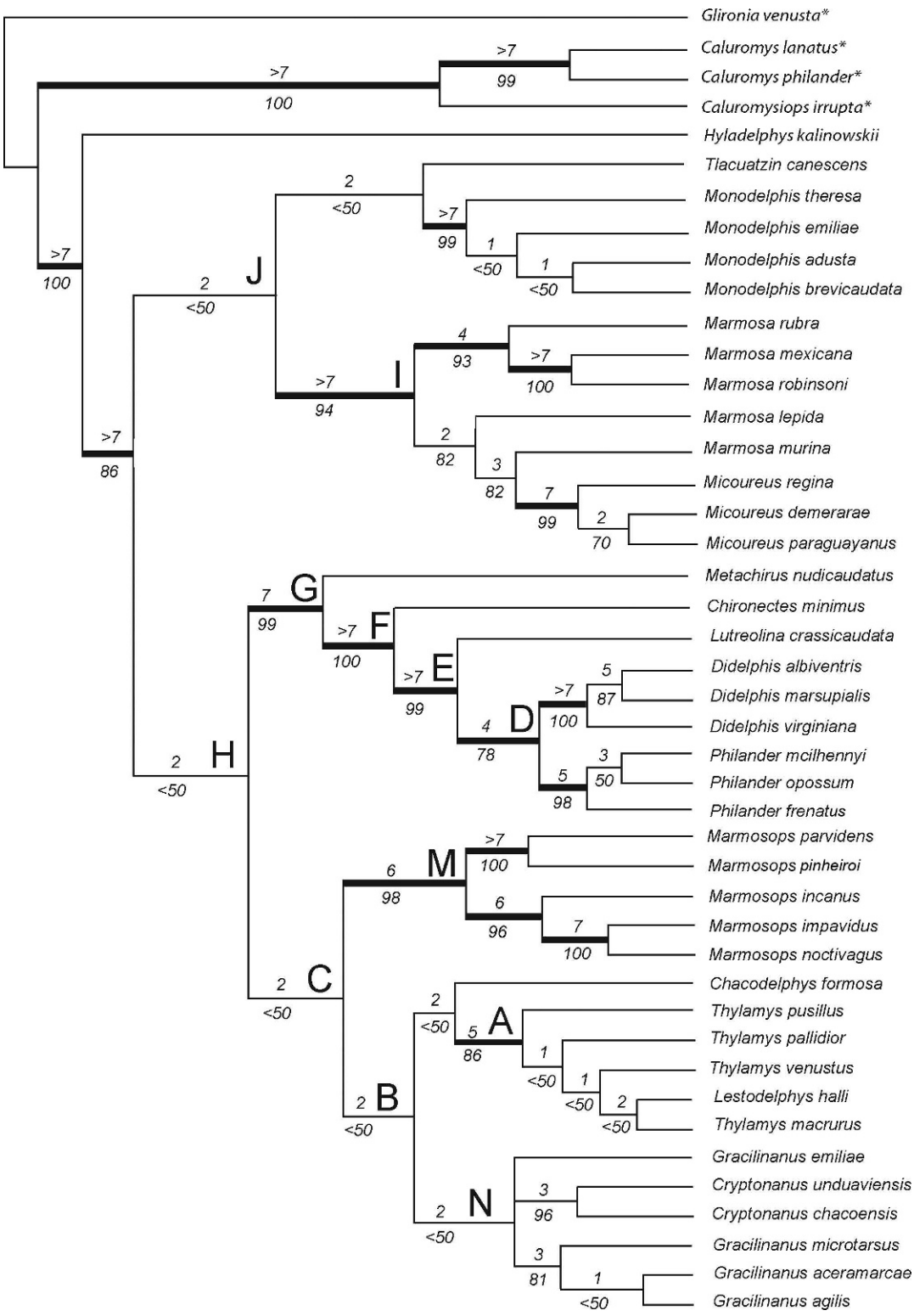

phyletic clade. Another interesting example of a functional component in postcranial characters is the unusual basal position of *Lestodelphys* on the large opossum clade (node G) in the TS coding postcranial evidence (fig. 34). The typical position of this terrestrial mouse opossum is close to *Thylamys* (node A), based on profuse previous evidence (Jansa and Voss, 2000, 2005; Voss and Jansa, 2003; Jansa et al., 2006; Flores, 2003; Creighton, 1984; Reig et al., 1987; Kirsch and Palma, 1995; tables 7, 8). However, *Lestodelphys* and most of the large opossums shared some character states linked to functional implications on posture and locomotion. In both *Lestodelphys* and most of large opossums, the spinous process on C6 is laminar (ch. 17[2]) and the femoral lesser trochanter is scarcely developed (ch. 93[0], see *Metachirus* in fig. 27).

An additional example of an unusual relationship possibly caused by constraints from functional demands is the sister relationship between the terrestrial *Metachirus* and the specialized swimmer *Chironectes* in the TS coding postcranial analysis, being closely related to the long recognized monophyletic *Didelphis*. The previous phylogenetic evidence does not recover *Metachirus-Chironectes* as sister taxa, with both being successively arranged in the clade containing the large opossums (Reig et al., 1987; Kirsch and Palma, 1995; Jansa and Voss, 2000, 2005; Voss and Jansa, 2003; Gruber et al., 2007). In the scheme obtained from postcranial evidence (fig. 34), both monotypic taxa are clustered as a monophyletic group sharing some synapomorphies associated with specific locomotion or postural patterns: ventral tubercle of atlas of triangular shape (ch. 5[3]), cranial notch of neural arch of axis wide (ch. 15[1], fig. 1), ilium with the distal portion barely curved laterally (ch. 90[1], fig. 26), prepollex absent (ch. 104[0]), and astragalus with well-developed astragalonavicular facet not contacting the sustentacular one (ch. 110[0], fig. 31), although in AMNH 148720 both facets are slightly in contact (see Szalay, 1994: fig. 7.12).

Alternatively, as stated above, the postcranial evidence supports the monophyly of some traditionally already recognized groups (tables 6–8; fig. 33), such as *Thylamys*, *Micoureus*, *Monodelphis*, *Marmosops* (node M), *Didelphis*, *Philander*, and the large opossums (node G), which are currently recognized by other kinds of evidence (e.g., Reig et al., 1987; Kirsch et al, 1995; Kirsch and Palma, 1995; Jansa and Voss, 2000, 2005; Jansa et al., 2006; Voss and Jansa, 2003; Gruber et al., 2007; table 8). Similarly, the intermediate position of *Hyladelphys* among caluromyines and didelphines is also recovered here based on postcranial evidence (figs. 33, 34; table 6), proving its basal position in the didelphid crown group and reinforcing its intermediate phylogenetic position between caluromyines and didelphines already obtained from other sorts of evidence (table 6).

Although not strongly supported, the species of *Monodelphis* included in this analysis are clustered in a monophyletic group supported by an array of postcranial traits coming from caudal vertebrae morphology, scapula, and some characters from the forelimb and hindlimb. In the same way, *Marmosops* (node M) is also recovered as monophyletic based on postcranial morphology, although the support values are not high in both TS and CO coding (table 7). This group was already recovered as monophyletic by different kinds of evidence (tables 7, 8); in this report, I add two postcranial characters (deltopectoral crest notably developed, ch. 68[1], and osseous posteroventral extension of the ischium, ch. 86[1]; fig. 23) that reinforce the monophyletic nature of this genus (appendix 3). Other groups of mouse

←

Fig. 40. Strict consensus of four equally most parsimonious trees resulting from cladistic parsimony analysis of morphological and genetic data combined, excluding RAG-1 sequences, for 44 didelphid taxa where polymorphic data were treated as transformation series (TS). Numbers above branches refer to absolute Bremer support values (≥1). Numbers below branches refer to jackknife frequencies (cutoff value = 50%). Heavy lines denote branches with a decay index of ≥4. Outgroup taxa are indicated with asterisks. Alphabetic labels indicate didelphine clades discussed in the text.

opossums previously recognized, such as *Thylamys* and *Micoureus*, are also recovered under CO coding postcranial morphology alone (fig. 33). However, even if both genera where recovered as well-supported natural groups in some published analyses (e.g., Jansa and Voss, 2005; Gruber et al. 2007), their monophyletic condition was proved only in a molecular or combined frame. Here, both groups are slightly supported in a morphological context (appendix 3): in *Thylamys* the diaphragmatic element is placed on T10 (ch. 27[0]), the longitudinal groove in the lateral surface of the ulna is absent (ch. 77[0]), and the bicipital tuberosity of the radius is scarcely marked (ch. 81[0]), whereas in *Micoureus* the medial relief for m. teres major on the humerus is absent (59[0]).

As mentioned above, the large opossums (*Didelphis*, *Lutreolina*, *Chironectes*, *Philander*, and *Metachirus*; node G) were widely recognized in previous papers (table 8). Some postcranial characters, principally traits coming from vertebrae, ribs, and humerus morphology, also add synapomorphies that support the monophyletic condition of this group (appendix 3). A last noncontroversial outcome is the monophyly of *Didelphis* and *Philander*, since those genera were largely recovered as natural groups based on several kinds of characters (e.g., Patton et al., 1996; Kirsch et al., 1995; Jansa and Voss, 2003; Flores, 2003; Jansa et al., 2006; Jansa and Voss, 2005; Gruber et al., 2007). The three species of *Didelphis* included in this report shared the especially strong and scarcely mobile articulation of cervical and thoracic vertebrae (appendix 3), which was illustrated by Coues (1869), whereas the three species of *Philander* included in this study are clustered by the morphology of the axis, as well as by some special patterns of the forelimb and femur (appendix 3).

CONCLUSIONS

The recent impulse and increase of knowledge on didelphid phylogeny is the result of the contribution of the inclusion of a denser taxon sampling and the consideration of varied evidence coming from both nuclear sequences (IRBP, DMP-1, and RAG-1) and morphology. Although the nonmolecular aspects frequently have resulted in low resolved topologies compared with hypotheses based on genetic evidence, they are in general agreement with genetic and combined data sets. Topologies coming from postcranial characters only are in general well resolved (mainly in CO coding analysis) and do not conflict with well-supported groups and relationships (e.g., *Hyladelphys* as intermediate between didelphines and caluromyines; the monophyly of large opossums; and *Didelphis*, *Philander*, *Monodelphis*, *Thylamys*, *Micoureus*, and *Marmosops* as natural genera), although some unusual clusterings are observed that result from convergences possibly caused by functional demands. However, the contribution of phylogenetic information from postcranial morpohology substantially improves the resolution of previous morphological hypotheses. Some relationships, formerly evidenced only with nuclear sequences, are now recovered with the addition of postcranial characters as well in a morphological framework. Even with the recent consideration of RAG-1 sequences, which reveals some unusual relationships, the phylogenetic information coming from postcranial morphology produces topologies in better agreement with earlier combined hypotheses. However, combined evidence considering postcranial evidence (including and excluding RAG-1 sequences) recovered the clustering of the mouse opossums in the CO polymorphic character coding. In this sense, the phylogenetic condition of the mouse opossums is still problematic when postcranial characters are considered in a combined data set, although this diverse group is not recovered in other partitioned analyses performed in this report.

The inclusion of new informative sequences and other kinds of morphological characters could provide additional support to groups recognized before or to new topologies. In this sense, the anatomical comparisons on forearm muscles in didelphids and some Australasian taxa performed by Abdala et al. (2006) added some potential new morphological synapomorphies to clades already recognized (i.e., nodes C, G, I, and D). Including a denser taxon sample in such alternative anatomical systems is an important priority in future research on didelphid

phylogeny for the sake of completeness. Finally, the pending postcranial observations in taxa still not analyzed, as well as the exact condition of missing data of some skeletal traits, could also reinforce several phylogenetic topologies that are slightly supported.

ACKNOWLEDGMENTS

The financial support for this investigation was provided by a Kalbfleisch Postdoctoral Fellowship of the American Museum of Natural History and partially by CONICET (Consejo de Nacional de Investigaciones Cientificas y Tecnicas, Argentina). I express my appreciation to the Office of Grants and Felloships staff, especially to Diane Bynum and Maria Dickson. At the Department of Mammalogy (AMNH), I thank Pat Brunauer, Rob Voss, Neil Duncan, Darrin Lunde, Teresa Pacheco, John Wahlert, Richard Monk, Robert Anderson, Norberto Giannini, Mariko Kageyama, Valeria Tavares, Ruth O'Leary, Erica Pannen, Adrian Tejedor, Nancy Simmons, and Eileen Westwig for assistance in everything and for kindness during my work at the AMNH. Thanks to Rob Voss, Sergio Solari, Adrián Tejedor, Mónica Díaz, Julián Faivovich, José Tello, Norberto Giannini, Sara Bertelli, and Enrique Penalver for their discussions and suggestions on the earlier version of this work. I am especially grateful to Rob Voss for his trust and support on this project. Thanks to Ines Horovitz, Rob Voss, and an anonymous reviewer for their valuable comments that improved the quality of this work.

Thanks to the curators and staff of museums and institutions for providing valuable assistance on visits and loans: Rubén Bárquez (CML), Daphne Hills (BMNH), Bruce Patterson (FMNH), Jim Patton (MVZ), Mónica Díaz (MMD), Phil Myers (UMMZ), and Hein Van Grow (RMNH). Sharon Jansa kindly provided DMP-1 sequences. Andrea del Moral helped with the English correction. Finally, I also extend my thanks to Luis Luna and Martin Dury for their friendship and support during my days in Westminster (London), and to all my close friends in New York, that is, Sara Bertelli, Adrián Tejedor, Valeria Tavares, Norberto Giannini, Juan Sosa, Enrique Panalver, Kenny Kozol, Pepe Tello, Marcelo Weksler, Guillermo Cárdenas, Paul Sweet, and Tony Perlstein, for their inestimable help during my unforgettable time there.

REFERENCES

Abdala, V., S. Moro, and D. Flores. 2006. The flexor tendons in the didelphid manus. Mastozoología Neotropical 13: 193–204.

Alpin, K.P., and M. Archer. 1987. Recent advances in marsupial systematics with a new syncretic classification. *In* M. Archer (editor), Possums and opossums: studies in evolution., Vol. 1: 15–72. Sydney: Surrey Beatty.

Argot, C. 2001. Functional-adaptive anatomy of the forelimb in the Didelphidae, and the paleobiology of the Paleocene marsupials *Mayulestes ferox* and *Pucadelphys andinus*. Journal of Morphology 247: 51–79.

Argot, C. 2002. Functional-adaptive analysis of the hindlimb anatomy of extant marsupials and paleobiology of the Paleocene marsupials *Mayulestes ferox* and *Pucadelphys andinus*. Journal of Morphology 253: 76–108.

Argot, C. 2003a. Functional-adaptative anatomy of the axial skeleton of some extant marsupials and the paleobiology of the Paleocene marsupials *Mayulestes ferox* and *Pucadelphys andinus*. Journal of Morphology 255: 279–300.

Argot, C. 2003b. Functional adaptations of the postcranial skeleton of two Miocene borhyaenoids (Mammalia, Metatheria), *Borhyaena* and *Prothylacinus*, from South America. Palaeontology 46: 1213–1267.

Argot, C. 2004a. Functional-adaptive features and paleobiologic implications of the postcranial skeleton of the late Miocene sabretooth borhyaenoid *Thylacosmilus atrox* (Metatheria). Alcheringa 28: 229–266.

Argot, C. 2004b. Functional-adaptive analysis of the poscranial skeleton of a Laventan Borhyaenoid, *Lycopsis longirostris* (Marsupialia, Mammalia). Journal of Vertebrate Paleontology 24: 689–708.

Asher, R.J., I. Horovitz, and M. Sánchez-Villagra. 2004. First combined cladistic analysis of marsupial mammal interrelationships. Molecular Phylogenetics and Evolution 33: 240–250.

Barnett, C.H., and J.R. Napier. 1953. The form and mobility of the fibula in metatherian mammals. Journal of Anatomy 87: 207–213.

Bensley, B.A. 1903. On the evolution of the Australian Marsupialia, with remarks on the relationships of the marsupials in general. Transactions of the Linnean Society of London, Zoology 9: 83–217 + pls. 5–7.

Bezuidenhout, A.J., and H.E. Evans. 2005. Anatomy of the woodchuck (*Marmota monax*). Special Publication American Society of Mammalogists 13: 1–180.

Bremer, K. 1994. Branch support and tree stability. Cladistics 10: 295–304.

Campbell, J.A., and D.R. Frost. 1993. Anguid lizards of the genus *Abronia*: revisionary notes, description of four new species, a phylogenetic analysis, and key. Bulletin of the American Museum of Natural History 216: 1–121.

Clemens, W.A. 1968. Origin and early evolution of marsupials. Evolution 22: 1–18.

Coues, E. 1869. The osteology and myology of Didelphyidae *Didelphis virginiana*. Memoires of the Boston Society of Natural History 2: 41–154.

Creighton, G.K. 1984. Systematic studies on opossums (Didelphidae) and rodents (Cricetidae). Ph.D. dissertation, University of Michigan, Ann Arbor.

Crompton, A.W. 1989. The evolution of mammalian mastication. *In* D.B. Wake and J. Roth (editors), Complex organismal function: integration and volution in vertebrates: 23–40. New York: John Wiley.

Crompton, A.W., and K. Hiiemae. 1970. Molar occlusion and mandibular movements during occlusion in the American opossum, *Didelphis marsupialis*. Zoological Journal of the Linnean Society 49: 21–47.

Crompton, A.W., and W. Hylander. 1986. Changes in mandibular function following the acquisition of a dentary–squamosal jaw articulation. *In* N. Hotton III, P.D. MacLean, J.J. Roth, and E.C. Roth (editors), The ecology and biology of mammal-like reptiles: 263–282. Washington, D.C.: Smithsonian Institution Press.

Elftman, H.O. 1929. Functional adaptations of the pelvis in marsupials. Bulletin of the American Museum of Natural History 58(5): 189–232.

Evans, H.E. 1993. Miller's Anatomy of the dog. 3rd ed. Philadelphia: W.B. Saunders.

Filan, S.L. 1990. Myology of the head and neck of the bandicoot (Marsupialia: Peramelemorphia). Australian Journal of Zoology 38: 617–634.

Flores, D.A. 2003. Estudio taxonómico y zoogeográfico de los marsupiales de Argentina. Unpublished Ph.D. dissertation., Universidad Nacional de Tucuman, Argentina.

Flores, D.A., R.M. Bárquez, and M. Díaz. 2008. A new species of *Philander* Brisson, 1762 (Didelphimorphia, Didelphidae). Mammalian Biology 73: 14–24.

Flower, W.H. 1885. An introduction to the osteology of Mammalia. 3rd ed. London: Macmillan.

Gardner, A. 2005. Order Didelphimorphia. *In* D.E. Wilson and M. Reeder (editors), Mammals species of the world. 3rd ed.: 3–18. Baltimore, MD: John Hopkins University Press.

Gebo, D.L. 1989. Locomotor and phylogenetic consideration in anthropoid evolution. Journal of Human Evolution 18: 201–233.

Giannini, N.P., and S. Bertelli. 2004. A phylogeny of extant penguins based on integumentary characters. Auk 121: 422–434.

Gilbert, S. 1994. Pictorial anatomy of the cat. 3rd ed. Toronto: University of Toronto Press.

Goin, F.J. 1993. Living South American opossums are *not* living fossils. Abstracts of the 6th International Theriological Congress: 112–113. Sydney, Australia.

Goin, F.J. 1995. Los Marsupiales. *In* M.T. Alberdi, G. Leone, and E.P. Tonni (editors), Evolución Biológica y climática en la región pampeana durante los últimos cinco millones de años, un ensayo de correlación con el mediterráneo occidental: 162–179. Madrid: Museo Nacional de Ciencias Naturales.

Goloboff, P., J.S. Farris, M. Källersjö, B. Oxelman, M. Ramírez, and C. Szumik. 2003. Improvements to resampling measures of group supports. Cladistics 19: 324–332.

Goloboff, P., J.S. Farris, and K. Nixon. 2004. T.N.T.: tree analysis using new technologies. Program and documentation. Available in www.cladistics.org.

Goslow, G.E., H.J. Seeherman, C.R. Taylor, M.N. McCutchin, and N.C. Heglund. 1981. Electrical-activity and relative length changes of dog limb muscles as a function of speed and gait. Journal of Experimental Biology 94: 15–42.

Grand, T.I. 1983. Body weight: its relationships to tissue composition, segmental distribution of mass, and motor function. III. The Didelphidae of French Guyana. Australian Journal of Zoology 31: 299–312.

Gregory, W.K. 1910. The orders of mammals. Bulletin of the American Museum of Natural History 27: 1–524.

Gruber, K.F., R.S. Voss, and S.A. Jansa. 2007. Base-compositional heterogeneity in the RAG1 locus among didelphid marsupials: implications for phylogenetic inference and the evolution of GC content. Systematic Biology 56: 1–14.

Herbin, M., V. Jeanne, J.P. Gasc, and P.P. Vidal. 2000. Geometrie du squelette cervical durant la transition repos-locomotion: eneralisation aux caracteristiques du repertoire moteur des rongeurs. Compte Rendues de l'Academie des Sciences Serie III Sciences de la Vie 324: 45–50.

Hershkovitz, P. 1999. *Dromiciops gliroides* Thomas, 1894, last of the Microbiotheria (Marsupialia), with a review of the Family Microbiotheriidae. Fieldiana Zoology New Series 93: 1–60.

Horovitz, I., and M.R. Sánchez-Villagra. 2003. A morphological analysis of marsupial mammal higher-level phylogenetic relationships. Cladistics 19: 181–212.

Howell, A.B. 1965. Speed in animals: their specialization for running and leaping. New York: Hafner Publishing Company.

Jansa, S.A., J.F. Forsman, and R.S. Voss. 2006. Different patterns of selection on nuclear genes IRBP and Dmp1 affect the efficiency but not the outcome of phylogeny estimation for didelphid marsupials. Molecular Phylogenetics and Evolution 38: 363–380.

Jansa, S.A., and R.S. Voss. 2000. Phylogenetic studies on didelphid marsupials. I. Introduction and preliminary results from nuclear IRBP gene sequences. Journal of Mammalian Evolution 7: 43–77.

Jansa, S.A., and R.S. Voss. 2005. Phylogenetic relationships of the marsupial genus *Hyladelphys* based on nuclear gene sequences and morphology. Journal of Mammalogy 86: 853–865.

Jenkins, F.A., Jr., 1970. Anatomy and function of expanded ribs in certain edentates and primates. Journal of Mammalogy 51: 288–301.

Jenkins, F.A., Jr., and S.M. Camazine. 1977. Hip structure and locomotion in ambulatory and cursorial carnivores. Journal of Zoology 181: 351–370.

Jenkins, F.A., Jr., and D. McClearn. 1984. Mechanisms of hind foot reversal in climbing mammals. Journal of Morphology 182: 197–219.

Jenkins, F.A., Jr., and W.A. Weijs. 1979. The functional anatomy of the shoulder in the Virginia opossum (*Didelphis virginiana*). Journal of Zoology 188: 379–410.

Johnson, S.E., and L.J. Shapiro. 1998. Positional behavior and vertebral morphology in atelines and cebines. American Journal of Physical Anthropology 105: 333–354.

Kirsch, J.A.W., and M. Archer. 1982. Polythetic cladistics, or, when parsimony's not enough: the relationships of carnivorous marsupials. *In* M. Archer (editor), Carnivorous Marsupials., Vol. 2: 595–620. Mosman, NSW: Royal Society of New South Wales.

Kirsch, J.A.W., A.W. Dickerman, and O.A. Reig. 1995. DNA/DNA hibridization studies of Carnivorous Marsupials IV. Intergeneric relationships of the opossum (Didelphidae). Marmosiana 1: 57–78.

Kirsch, J.A.W., and R.E. Palma. 1995. DNA/DNA hybridization studies of carnivorous marsupials. V. A further estimate of relationships among opossums (Marsupialia, Didelphidae). Mammalia 59: 403–425.

Klima, M. 1987. Early development of the shoulder girdle and sternum in marsupials (Mammalia, Metatheria). Advances in Anatomy, Embryology and Cell Biology 109: 1–91.

Kurz, C. 2005. Ecomorphology of opossum-like marsupials from the Tertiary of Europe and a comparison with selected taxa. Darmstädter Beiträge zur Naturgeschichte 14: 21–26.

Lanyon, L.E. 1980. The influence of function on the development of bone curvature an experimental study on the tibia rat. Journal of Zoology 192: 457–466.

Larson, S.G. 1993. Functional morphology of the shoulder in primates. *In* D.L. Gebo (editor), Postcranial adaptation in nonhumans primates: 45–69. DeKalb: Northern Illinois University Press.

Lew, D., R. Pérez-Hernández, and J. Ventura, J. 2006. Two new species of *Philander* (Didelphimorphia, Didelphidae) from northern South America. Journal of Mammalogy 87: 224–237.

Lunde, D.P., and W.A. Shutt. 1999. The peculiar carpal tubercles of male *Marmosops parvidens* and *Marmosa robinsoni* (Didelphidae: Didelphinae). Mammalia 63: 495–504.

Mabee, P.M., and J. Humphries. 1993. Coding polymorphic data: examples from allozymes and ontogeny. Systematic Biology 42: 166–81.

MacLeod, N., and K.D. Rose. 1993. Inferring locomotor behavior in Paleogene mammals via Eigenshape analysis. American Journal of Science 293-A: 300–355.

MacPhee, R.D.E., and L.L. Jacobs. 1986. *Nycticeboides simpsoni* and the morphology, adaptations, and relationships of Miocene Siwalik Lorisidae. *In* K.M. Flanagan and J.A. Lillegraven (editors), Contributions to geology: 131–161. Laramie: University of Wyoming Press.

Mann-Fischer, G. 1953. Filogenia y función de la musculatura en *Marmosa elegans* (Marsupialia, Didelphydae). Investigaciones Zoológicas Chilenas 1: 3–15.

Mann-Fischer, G. 1956. Filogenia y función de la musculatura en *Marmosa elegans* (Marsupialia, Didelphydae). 2 da. Parte. Investigaciones Zoológicas Chilenas 3: 3–28.

Marshall, L.G., J.A. Case, and M.O. Woodburne. 1990. Phylogenetic relationship of the families of marsupials. *In* H.H. Genoways (editor), Current mammalogy: 433–505. New York: Plenum Press.

Marshall, L.G., and D. Sigogneau-Russell. 1995. *Pucadelphys andinus* (Marsupialia, Mammalia) from the early Palaeocene of Bolivia. Part 3. The postcranial skeleton. Mémoires du Muséum National d'Histoire Naturelle 165: 91–164.

Martin, K.E.A., and S. Mackay. 2003. Postnatal development of the fore- and hindlimbs in the grey short tailed opossum, *Monodelphis domestica*. Journal of Anatomy 202: 143–152.

Maynard Smith, J., and R.J.G. Savage. 1955. Some locomotory adaptations in mammals. Zoological Journal of the Linnean Society 42: 603–622.

Muizon, C. de. 1998. *Mayulestes ferox*, a borhyaenoid (Metatheria, Mammalia) from the early Paleocene of Bolivia: phylogenetic and paleobiologic implications. Geodiversitas 20: 19–142.

Muizon, C. de, and C. Argot. 2003. Comparative anatomy of the Tiupampa didelphimorphs: an approach to locomotory habits of early marsupials. *In* M.E. Jones, C.R. Dickman, and M. Archer (editors), Predators with pouches: the biology of carnivorous marsupials: 43–62. Collingwood, VIC: CSIRO Publishing.

Oxnard, C.E. 1963. Locomotor adaptations in the primate forelimb. *In* J. Napier and N.A. Barnicot (editors), The primates: 165–182. London: Symposium Zoological Society of London.

Patterson, B., and R. Pascual. 1972. The fossil mammal fauna of South America. *In* A. Keast, F.C. Erk, and B.P. Glass (editors), Evolution, mammals and southern continets: 247–309. Albany: State University of New York Press.

Patton, J.L., S.F. dos Reis, and M.N.F. da Silva. 1996. Relationships among Didelphid Marsupials based on secuence variation in the mitochondrial cytochrome b gene. Journal of Mammalian Evolution 3(1): 1–29.

Pridmore, P.A. 1992. Trunk movements during locomotion in the Marsupial *Monodelphis domestica* (Didelphidae). Journal of Morphology 211: 137–146.

Reig, O.A., J.A.W. Kirsch, and L.G. Marshall. 1987. Systematic relationships of the living and neocenozoic American ''opossum-like'' marsupials (Suborder Didelphimorphia), with comments on the classification of these and of the Cretaceous and Paleogene New World and European metatherians. *In* M. Archer (editor), Possums and opossums: studies in evolution. Vol. 1: 1–89. Sydney: Surrey Beatty.

Roberts, D. 1974. Structure and function of the primate scapula. *In* F.A. Jenkins (editor), Primate locomotion: 171–200. New York: Academic Press.

Rockwell, H., F. Gaynor Evans, and H. Pheasant. 1938. The comparative morphology of the vertebrate spinal column its form as related to function. Journal of Morphology 63: 87–117.

Sánchez-Villagra, M., S. Ladevèze, I. Horovitz, C. Argot, J.J. Hooker, T. Macrini, T. Martin, S. Moore-Fay, C. de Muizon, T. Schmelzle, and R. Asher. 2007. Exceptionally preserved North American Paleogene matatherians: adaptations and discovery of a major gap in the opossum fossil record. Biology Letters 3: 318–322.

Sanders, W., and B. Bodenbender. 1994. Morphometric analysis of lumbar vertebra UMP 67-28: implications for spinal function and phylogeny of the Miocene Moroto hominid. Journal of Human Evolution 26: 203–237.

Sargis, E.J. 2001. A preliminary qualitative analysis of the axial skeleton of tupaiids (Mammalia, Scandentia): functional morphology and phylogenetic implications. Journal of Zoology 253: 473–483.

Sargis, E.J. 2002. Functional morphology of the hindlimb of tupaiids (Mammalia, Scandentia) and its phylogenetic implications. Journal of Morphology 254: 149–185.

Sears, K. 2004. Constraints on the morphological evolution of marsupial shoulder girdles. Evolution 58: 2353–2370.

Shapiro, L.J. 1993. Functional morphology of the vertebral column in primates. *In* D. Gebo (editor), Poscranial adaptation in nonhuman primates: 121–149. DeKalb: Northern Illinois University Press.

Shapiro, L.J. 1995. Functional morphology of indrid lumbar vertebrae. American Journal of Physical Anthropology 98: 323–342.

Shapiro, L.J., and W.L. Jungers. 1994. Electromyography of back muscles during quadrupedal and bipedal walking in Primates. American Journal of Physical Anthropology 93: 491–504.

Simpson, G.G. 1971. The evolution of marsupials in South America. Anais da Academia Brasileira de Ciencias 43(Suppl.): 103–118.

Solari, S. 2004. A new species of *Monodelphis* (Didelphimorphia, Didelphidae) from southeastern Peru. Mammalian Biology 69: 145–152.

Solari, S. 2007. New species of *Monodelphis* (Didelphimorphia: Didelphidae) from Peru, with notes on *M. adusta* (Thomas, 1897). Journal of Mammalogy 88: 319–329.

Szalay, F.S. 1982. A new appraisal of marsupial phylogeny and classification. *In* M. Archer (editor), Carnivorous marsupials: 621–640. Mosman, NSW: Royal Society of New South Wales.

Szalay, F.S. 1994. Evolutionary history of the marsupials and an analysis of osteological characters. New York: Cambridge University Press.

Szalay, F.S., and E.J. Sargis. 2001. Model-based analysis of poscranial osteology of marsupials of Palaeocene of Itaboraí (Brazil) and the phylogenetics and biogeography of Metatheria. Geodiversitas 23: 139–302.

Tardieu, C. 1983. L'articulation du genou analyse morpho-fonctionelle chez les primates et les hominides fossiles. Cahiers de Palèoanthropologie. Paris: Presses du CNRS.

Taylor, M.E. 1974. The functional anatomy of the forelimbs of some African Viverridae (Carnivora). Journal of Morphology 143: 307–336.

Taylor, M.E. 1976. The functional anatomy of the hindlimbs of some African Viverridae (Carnivora). Journal of Morphology 148: 227–254.

Voss, R.S., A. L Gardner, and S.A. Jansa. 2004. On the relationships of *Marmosa formosa* Shamel, 1930 (Marsupialia: Didelphidae), a phylogenetic puzzle from the Chaco of northern Argentina. American Museum Novitates 3442: 1–18.

Voss, R.S., and S. Jansa. 2003. Phylogenetic studies in didelphid marsupials II. Nonmolecular data and new IRBP sequences: separate and combined analyses of didelphine relationships with denser taxon sampling. Bulletin of the American Museum of Natural History 276: 1–82.

Voss, R.S., D.P. Lunde, and S.A. Jansa. 2006. On the contents of *Gracilinanus* Gardner and Creighton, 1989, with the description of a previously unrecognized clade of small didelphid marsupials. American Museum Novitates 3482: 1–34.

Voss, R.S., T. Tarifa, and E. Yensen. 2004. An Introduction to *Marmosops* (Marsupialia: Didelphidae), with the description of a new species from Bolivia and notes on the taxonomy and distribution of other Bolivian forms. American Museum Novitates 3466: 1–40.

Walker, A. 1974. Locomotor adaptations in past and present prosimian primates. *In* F.A. Jenkins (editor), Primate locomotion: 349–381. New York: Academic Press.

Washburn, S., and J. Buettner-Janush. 1952. The definition of thoracic and lumbar vertebrae. American Journal of Physical Anthropology 10: 251–252.

Weisbecker, V., and M.R. Sánchez-Villagra. 2006. Carpal evolution in Diprotodontian Marsupials. Zoological Journal of the Linnean Society 146: 369–384.

Weksler, M. 2006. Phylogenetic relationships of oryzomyine rodents (Muroidea: Sigmodontinae): separate and combined analyses of morphological and molecular data. Bulletin of the American Museum of Natural History 296: 1–149.

White, T.D. 1989. An analysis of epipubic bone function in mammals using scaling theory. Journal of Theoretical Biology 139: 342–357.

White, T.D. 1990. Gait selection in the brush-tail possum (*Trichosurus vulpecula*), the northern quoll (*Dasyurus hallucatus*), and the Virginia opossum (*Didelphis virginiana*). Journal of Mammalogy 71: 79–84.

Whitehead, P.F., W.K. Sacco, and S.B. Hochgraf. 2005. A photographic atlas of physical anthropology. Englewood, CO: Morton Publishing Company.

Wible, J.R. 1990. Petrosals of late cretaceous marsupials from North America, and a cladistic analysis of the petrosal in therian mammals. Journal of Vertebrate Paleontology 10: 183–205.

Wiens, J. 1999. Polymorphism in systematics and comparative biology. Annual Review of Ecology and Systematics 30: 327–362.

Wiens, J.J. 2000. Coding morphological variation withn species and higher taxa for phylogenetic analysis. *In* J.J. Wiens (editor), Phylogenetic analysis of morphological data: 115–145. Washington, DC: Smithsonian Institution Press.

Wroe, S., M. Ebach, S. Ahyong, C. de Muizon, and J. Muirehead. 2000. Cladistic analysis of dasyuromorphian (Marsupialia) phylogeny using cranial and dental characters. Journal of Mammalogy 81: 1008–1024.

APPENDIX 1

Postcranial Material Examined

The skeletons analyzed for this study are deposited in the following systematic collections, listed in alphabetical order by their acronyms: AMNH, American Museum of Natural History (New York); BMNH, Natural History Museum (London); CML, Colección Mamíferos Lillo (Tucumán, Argentina); FMNH, Field Museum of Natural History (Chicago); MMD, Voucher Collection of Mónica Díaz (will be deposited at the MUSM, Museo de Historia Natural de la Universidad Nacional Mayor San Marcos, Lima, Perú); MSB, Museum of Southwestern Biology (Albuquerque, New Mexico); MVZ, Museum of Vertebrate Zoology (University of California, Berkeley); MZUSP, Museu de Zoologia (Universidade de São Paulo, Brazil); RHMH, Rijksmuseum van Natuurlijke Historie (Leiden, Netherlands); ROM, Royal Ontario Museum (Toronto); RSV, Voucher Collection of R.S. Voss (will be deposited at the AMNH); UMMZ, University of Michigan Museum of Zoology (Ann Arbor); UWZM, University of Wisconsin Zoological Museum (Madison).

Caluromys lanatus: AMNH 133199, 133200, 215001
Caluromys philander: AMNH 95761, 267001, 267002, 267337, 95974, RMNH uncataloged, 12866, 10790, 19646, 20664
Caluromysiops irrupta: AMNH 208101, 244364
Chironectes minimus: AMNH 97319, 148720, 212909, 264571, RMNH uncataloged
Cryptonanus unduaviensis: AMNH 210369, 262401
Didelphis albiventris: AMNH 13102, 148320, 170653, 170654, 170664, 204406, 205301, 205382, 205385, 238006
Didelphis marsupialis: AMNH 13448, 97318, 132784, 209164, 210427, 210428, 210439, 210447, 235003, 255854
Didelphis virginiana: AMNH 70082, 146551, 35908, 235278, 70375, 21599, 215193, 240516, 240517, 240519, 240520, 242658
Glironia venusta: MMD 607
Gracilinanus agilis: AMNH 133234, 209157
Gracilinanus microtarsus: MVZ 182057
Hyladelphys kalinowskii: RSV 1572
Lestodelphys halli: UWZM 224223, BMNH 21.6.7.19
Lutreolina crassicaudata: AMNH 133250, 205378, 210421, 210425, CML 2895
Marmosa mexicana: AMNH 189483, 189485, ROM 96090, 99608
Marmosa murina: AMNH 99983, 136159, 254508
Marmosa robinsoni: AMNH 206596, 206597, 206766, 207766, 257209, 257210
Marmosa rubra: FMNH 124612
Marmosops impavidus: AMNH 139226
Marmosops incanus: MVZ 182768, 182769
Marmosops noctivagus: AMNH 136157, 231952
Marmosops parvidens: AMNH 267348, 267344
Marmosops pinheiroi: AMNH 267004, 267005
Metachirus nudicaudatus: AMNH 97320, 136151, 136155, 244617, 267009, CML 7342
Micoureus demerarae: AMNH 257211, 257212, RMNH 12871, 998, 18228
Micoureus regina: AMNH 61391, 148757
Micoureus paraguayanus: CML 7343, 2867, AMNH 42289, 42911
Monodelphis adusta: AMNH 136158, 139227
Monodelphis brevicaudata: AMNH 48133, 257203, RMNH 18079, 12851, 17907
Monodelphis theresa: MVZ 182775
Philander frenatus: MVZ 182066, 182067
Philander mcilhennyi: MVZ 190342
Philander opossum: AMNH 61396, 61864, 97332, 133074, 190446, 210406, 210410, 248703, 254509, 261273, 261276, 262415, RMNH 12835, 12838, 12834, MMD 3737, 1995, 835, 2972
Thylamys macrurus: MZUSP 32094, 32095, 32096, MSB 70700
Thylamys pallidior: AMNH 262405, 262406, 262408, CML 3189, 3192, 3574, 3575
Thylamys pusillus: AMNH 246442, 246446, 275445, 275446, CML 3198, 3573
Thylamys venustus: AMNH 261245, 261253
Tlacuatzin canescens: UMMZ 94604, 94605

APPENDIX 2

Postcranial Data Matrix

Polymorphic entries are coded as {01} = A; {12} = B.

Caluromys lanatus: 1111111201 0110002100 1110000143 0101A10111 00031--200 2101020110 1011001102 0113101010 1100100110 1011010110 0111100111 0010
Caluromys philander: 1101111201 0110002100 1110000243 0101110111 00031--200 2101020110 1011001102 0113101000 1100100110 1011010110 0111100111 0010
Caluromysiops irrupta: 1111101201 0010A02100 1110010151 0101110111 0013330200 2A01120110 00110–1102 0112102010 1100101110 1011010110 0111100110 0010
Chironectes minimus: 1101311101 1000102101 1100103201 0001A11111 1113231211 1000120001 10A1110100 0112111001 000000A101 110110A100 0110110110 0011
Cryptonanus unduaviensis: 0001211201 1101100000 0A00101342 1001100111 0100---010 1011120110 1000100011 0112101000 1000100000 1011001110 110?000001 0010
Didelphis albiventris: 1011100000 0110002111 1110110012 0000A10111 0110–2A111 0111011001 11011A0100 1102111000 1000000100 1101100110 0011110111 0010
Didelphis marsupialis: 1011100000 0110002111 1110110012 0000A10111 0110–2A111 01110110A1 11011A0100 1102111000 1000000100 1101100110 001111011A 0010
Didelphis virginiana: 1011100000 0110002111 1110110012 0000A10111 0110–2A111 0111011001 1101110100 1102111000 1000000100 1101101110 001111011A 0010

Glironia venusta: 1001111101 0101101100 0110101210 1101100000 -0003--010 2101120110 1111001102 0113101000 1100100001 1011011010 0111000110 0010

Gracilinanus agilis: 0A01311211 110010A000 0100100332 1000100111 0112–20111 0011110111 1AA0100A21 011311A000 1000000000 1011000110 1101100001 0010

Gracilinanus microtarsus: 0001211211 ??0?100001 0100101311 10001001?? ?112–?0?1? 0011120110 1000100011 0113101000 0000000000 101100?100 11???00000 0010

Hyladeplhys kallinowskii: 0000110200 1?00001001 0000103222 1001101001 1102---110 1000120100 1010000112 0013101010 0100000110 1011011110 1011100101 1010

Lestodelphys halli: 0001211101 1001102000 0000102220 1000100101 0110–11110 0110120111 1000101021 0112011010 1100000100 100100?110 01???????? ????

Lutreolina crassicaudata: 1001111201 1111002000 110010-232 0000111111 1111-2A111 1001120001 1101110000 1112111010 1000101100 110110?110 001??10111 0010

Marmosa mexicana: 0001210211 1100101001 0110000312 1000000111 0113021111 0011120110 00001–0010 0112100000 0000100100 1011110110 1111100001 A010

Marmosa murina: 0101211201 ??00102001 0100100301 1000A00111 011302A110 ?011120111 10001A0121 011210A000 0000100100 1011010110 0101100001 0010

Marmosa robinsoni: 0A01211201 10A1102000 0A10101312 1001A00111 01A1-2A110 10011201A0 10001AAA21 0112101000 0000100100 1011100110 0111100001 0010

Marmosa rubra: 1101310201 1101111100 0110100211 1000110101 01030--111 ??01100110 1100111112 0112101011 0000100010 101101?110 0111100001 0010

Marmosops impavidus: 0001210201 1001001001 0A00100302 1000A00111 0110-21110 0111120100 1000100121 0112101000 1000110100 1011100110 110?100001 0010

Marmosops incanus: 0001210201 0101001001 0100101211 1001100110 –110–0AA10 0111120111 1000110111 0112111100 1000110100 1011001110 1101100001 0010

Marmosops noctivagus: 0A01210201 100100A001 0100101302 1001A0011A -110-21110 011112A011 1000100111 0112101000 1000110100 1011000110 110?100001 0010

Marmosops parvidens: 0001210201 1001101000 0100101321 1010100110 –110–21110 1101120101 1000111111 0010012110 1000110110 1011101110 0101100001 0010

Marmosops pinheiroi: 0001210211 1001101000? 0100101331 101010011A 1110-21110 111112011A 1000110111 0112101000 1000110100 1011101110 0101100001 0010

Metachirus nudicaudatus: 1A01310201 1011102A01 1101100212 0010111111 1113221111 0101011001 2101110100 1001011000 0011001001 1101101111 0010101110 0100

Micoureus demerarae: 0001111101 1100001A01 0100100231 1001100111 0113021110 001112010A 100010012B 0113101010 0000100100 1011010110 0111100001 0010

Micoureus paraguayanus: AA01211101 1100001001 0100100231 1001100111 0113021110 00111201AA 1A001A012B 011310A000 0000100100 1011010110 01???????? ????

Micoureus regina: 0001111201 100010AA0A 0100100432 100A100111 0113021110 0011120100 1000100011 0112101000 0000100A00 1011010110 01?1100001 0010

Monodelphis adusta: 0001211201 1101101101 0000100211 1000100111 0113010010 0010110100 1100110111 0112110110 0000100100 1001001110 0011?????? ????

Monodelphis brevicaudata: 0101111101 1101101001 0101100201 1000100111 0112-20110 0010110100 1100110111 0112100110 0000100100 1001001110 0011?10001 0010

Monodelphis theresa: 0001211201 1101101001 0001100342 1000100111 01030--010 1010110100 1100110111 0113101110 0000100100 1001001110 0011110001 0010

Philander frenatus: 1A01211101 1010002100 1100101132 0000111111 1110-21111 0101110011 1101110000 0113101001 000000A100 1101111110 0011110111 0010

Philander mcilhennyi: 1001111201 1000002000 1100100233 0000110111 1110-21111 0101110010 1101110000 0112001001 0000000??0 110111?110 0001110111 0010

Philander opossum: 10A1211001 1010001100 1100100132 0000110111 0110-2A111 01011100A1 1101110000 0113111001 0000000100 1101111110 0011110111 0A10

Thylamys macrurus: 0001?11201 0101101001 0010100231 1000100111 1110-00010 0011100101 1000100011 0112110000 0000100100 0011001110 0011100001 0010

Thylamys pallidior: 0000210211 1000101001 0A10100321 1000100111 0110-20110 0011121110 1000100011 0112110000 0000100100 1000001110 0111100000 0010

Thylamys pusillus: AA01211211 1101100000 0000100231 1000100111 0110-20110 001112A110 11001A0011 0112110000 0000101100 101100?110 0100100001 0010

Thylamys venustus: 000A210211 100110000A 0A00100321 100010011A -110-20110 0011120100 1000100011 0112110000 0000100?00 10??001110 0111100001 0010

Tlacuatzin canescens: 0000111201 A102100000 0100102331 1000100111 011332A011 0001120110 1000100011 0113101000 0000100001 0001101100 010??00001 0010

APPENDIX 3

Nodal synapomorphies in strict consensus of total combined evidence tree (i.e., all morphology and IRBP, DMP-1, and RAG-1 sequences), with polymorphism analyzed as composites entries (fig. 37). BS indicates Bremer support values; JK, Jackknife resampling support. The morphological synapomorphies come from Voss and Jansa (2003, external and craniocaudal) and from characters described in this report (postcranial). Character numbers (and states) are indicated for postcranial characters. Outgroups are not indicated.

Node	Composition	BS	JK	Description of morphological synapomorphies	Molecular synapomorphies
1	Didelphinae	>7	99	Unfurred ventral surface of tail base covered with smooth scales. Postorbital process of frontals absent or indistinct. Posterior palate abruptly inflected ventrally, with straight lateral margins and prominent lateral corners.	IRBP: 3 DMP-1: 18 RAG-1: 19
2	Didelphinae minus *Hyladelphys*	>7	99	Manual digit III longer than other manual digits. P3 with only posterior cutting edge. Preprotocrista and anterolabial cingulum separate, not forming a continuous shelf. Axis, dens strongly cranially extended (ch. 11[1]). C7 transverse process laterally oriented (ch. 23[0]). Craniocaudal extension of hemal arches in T1 and T2 similar (ch. 32[0]). Ventral foramina on S1 body present (ch. 42[1]). Spinous process vertical in Ca1, but caudally oriented in Ca2–Ca3 (ch. 45[2]). Second sternebrae laterally compressed (ch. 51[1]). Humerus with similar proximal extension of capitulum and trochlea (ch. 63[0]). Humerus shaft curved (ch. 65[1]). Proximal process of the supinator ridge of humerus absent (ch. 67[0]). Radius without a bony plate posterolaterally extended on the diaphysis (ch. 82[0]). Femur with distal epiphysis not anteroposteriorly compressed (ch. 96[0]).	IRBP: 4 RAG-1: 7
3	Node F	>7	100	Pouch present. Caudal integument blackish basally and abruptly whitish distally. Nasals tips posterior to I1, exposing nasal orifice dorsally. Postorbital processes present but not flattened or associated with supraorbital crests. Sagittal crest large and extending to frontals. Extracranial course of mandibular nerve usually enclosed by posteromedial bullar lamina. Anterior limb of ectotympanic indirectly attached via malleus. Paraoccipital process as a large erect process usually directed ventrally. P3 distinctly taller than P2. P3 erupts before M4. Lower incisors without lingual cusp. Robertsonian equivalents {acr1 + acr5, met1} as two acrocentric chromosomes. Robertsonian equivalents {acr3 + acr10, met3} as two acrocentric chromosomes.	IRBP: 22 DMP-1: 24 RAG-1: 42

APPENDIX 3
(*Continued*)

Node	Composition	BS	JK	Description of morphological synapomorphies	Molecular synapomorphies
				S1 spinous process taller than S2 (ch. 41[1]).	
				Internal border of the first rib almost straight on distal half (ch. 50[1]).	
				Scapular notch extended less than half of the scapula (ch. 58[0]).	
				Capitulum of humerus cylindrical (ch. 60[1]).	
				Anconeal process of ulna well developed (ch. 76[1]).	
				Angle formed by the two posterior rami of ischium in caudal view of 90° or scarcely more (ch. 85[0]).	
				Caudal portion of ischium body curved laterally (ch. 92[1]).	
				Femur with greater trochanter surpassing the level of the head (ch. 95[1]).	
	Node E	>7	100	Palatine fenestrae present.	IRBP: 3
				Dorsal margin of foramen magnum formed by exoccipitals only.	DMP-1: 4
				Axis neural arch and cranial notch narrow (ch. 15[0]).	RAG-1: 8
				First vertebra where the accessory process is differentiated from the transverse process placed on T8 (ch. 30[2]).	
				Spinous process only in first caudal vertebra (ch. 44[1]).	
				Deltopectoral crest of humerus reaching distal half (ch. 62[1]).	
	Node D	>7	99	Spinous process on anterior caudal vertebrae absent (ch. 44[0]).	IRBP: 4
				Sternebrae not laterally compressed (ch. 51[0]).	DMP-1: 3
				Keel of manubrium well developed (ch. 52 [1]).	RAG-1: 9
	Didelphis	>7	100	Dorsal underfur white.	DMP-1: 2
				Dorsal pelage with guard hairs conspicuously longer and coarser than underfur.	RAG-1: 1
				Transverse process of atlas caudally extended (ch. 3[1]).	
				Caudal articular fovea of atlas not posteriorly extended (ch. 6[0]).	
				Caudal articular fovea of atlas oval in shape (ch. 7[0]).	
				Transverse process of atlas more extended craniocaudally than the hemal arches (ch. 8[0]).	
				Spinous process of axis not posteriorly extended (ch. 10[0]).	
				C3–C7 spinous process similar in size than the axis spinous process (ch. 19[1]).	
				C6 and C7 spinous process of similar size (ch. 20[1]).	
				C7 transverse process ventrolaterally oriented (ch. 23[1]).	
				T1 body craniocaudally extended in dorsal view (ch. 26[1]).	
				Diaphragmatic vertebra placed on T8 (ch. 28[0]).	
				Anticlinal vertebra placed on T11 (ch. 29[1]).	
				S1 and S2 spinous process of similar size (ch. 41[0]).	
				Coracoid process of the scapula small (ch. 53[1]).	

APPENDIX 3
(*Continued*)

Node	Composition	BS	JK	Description of morphological synapomorphies	Molecular synapomorphies
				Witdth of the scapular infraspinous and supraspinous fossae subequal (ch. 56[1]). Caudal angle of the scapula rounded (ch. 57[1]). Crest on the anterior side of the ulna absent (ch. 73[0]).	
	D. albiventris-D. marsupialis	3	69	Without sesamoids in the articular area between tibia, fibula, and astragalus (ch. 97[0]).	IRBP: 4 DMP-1: 1 RAG-1: 1
	Philander	6	95	Conspicuous pale spot above each eye present. Caudal atricular fovea of axis rounded in shape (ch. 12[0]). Medial relief for m. teres major on humerus present (ch. 59[1]). Radius with articular facet for humerus anteroposteriorly compressed (ch. 80[1]). Distal epiphysis of femur anteroposteriorly compressed (ch. 96[1]).	IRBP: 2 DMP-1: 2
	P. mcilhennyi-P. opossum	>7	99	None	IRBP: 1 DMP-1: 4 RAG-1: 11
	Node L	1	<50	Centrocrista of M1–M3 strongly V-shaped, its apex high above the trigon basin. Atlantal foramen absent (ch. 1[0]). C7 transverse foramen absent (ch. 18[0]). C3 transvese process with one head (ch. 21[0]). Postzygapophysis of thoracic vertebrae 2–8 caudally enlarged (ch. 31[1]). Lumbar vertebrae with dorsal intervertebral space (ch. 36[0]). Humerus, lateral extension of capitulum absent (ch. 64[0]). Astragalus without ridge between medial and lateral astragalotibial facets (ch. 108[0]). Astragalus without ridge between lateral astragalotibial and astragalofibular facets (ch. 109[0]).	DMP-1: 2 RAG-1: 3
	Chacodelphys + Monodelphis	1	<50	Tail scales in predominantly annular series. m3 hypoconid lingual to salient protoconid. Entoconid very small or indistinct.	None
	Monodelphis	>7	99	Fur surrounding eye not distinctively colored. Pedal digit III distinctly longer than adjacent digits II and IV. Maxilloturbinals small and unbranched. Maxillary and alisphenoid in contact on orbital floor. P3 distinctly taller than P2. p2 and p3 subequal in height.	None

APPENDIX 3
(*Continued*)

Node	Composition	BS	JK	Description of morphological synapomorphies	Molecular synapomorphies
	(*M. theresa* (*M. adusta-M. brevicaudata*))	1	<50	None	RAG-1: 3
	M. adusta-M. brevicaudata	1	<50	Ulna without longitudinal groove in its lateral surface (ch. 77[0]).	DMP-1: 1 RAG-1: 5
	Tlacuatzin + node I	3	<50	Manual digits III and IV subequal and longer than other manual digits. Postorbital processes of frontals flattened, with winglike extensions of supraorbital crests. Preprotocrista and anterolabial cingulum joined to form a continuous shelf along the anterior margin of M3. Deciduous lower third premolar with incomplete trigonid.	IRBP: 2 RAG-1: 9
	Node I	7	100	Premaxillae forming a distinct shelflike rostral process. Spinous process vertical in Ca1–Ca3 (ch. 45[0]). Femur with distal epiphysis anteroposteriorly compressed (ch. 96[1]). Sesamoids in the articular area between tibia, fibula, and astragalus absent (ch. 97[0]).	IRBP: 9 DMP-1: 5 RAG-1: 45
	(*Marmosa rubra* (*M. mexicana-M. robinsoni*))	7	100	Conspicuous medial carpal tubercle supported internally by the prepollex. C7 transverse process ventrolaterally oriented (ch. 23[1]).	IRBP: 1 DMP-1: 4 RAG-1: 40
	M. mexicana-M. robinsoni	7	100	Gular gland present. Vertebra where the transverse process is differentiated from the accesory proces placed on T8 (ch. 30[2]). Femur with greater trochanter surpassing the level of the head (ch. 95[1]).	IRBP: 7 DMP-1: 15 IRBP: 53
	(*Marmosa lepida* (*M. murina* (*Micoureus*))	>7	99	None	IRBP: 2 RAG-1: 12
	M. murina-Micoureus	>7	100	None	DMP-1: 3 RAG-1: 22
	Micoureus	>7	100	Humerus without medial relief for m. teres major (ch. 59[0])	IRBP: 3 DMP-1: 4 RAG-1: 40
	Micoureus demerarae-M. paraguayanus	>7	98	Atlas with similar craniocaudal lenght of transverse process with respect to hemal arches (ch. 8[1]). Diaphragmatic vertebra placed on T11 (ch. 28[2]). Ulna with fossa for the exterior ligament extended beyond the trochlear notch (ch. 74[3]).	DMP-1: 2 RAG-1: 7
	(*Tlacuatzin*-node I) node C))	1	<50	External lateral carpal tubercle supported by pisiform present in adult males.	RAG-1: 9

APPENDIX 3
(*Continued*)

Node	Composition	BS	JK	Description of morphological synapomorphies	Molecular synapomorphies
	Node C	1	<50	Extracranial courser of mandibular nerve enclosed by an anteromedial strut of alisphenoid bulla.	IRBP: 5 DMP-1: 6
				First three caudal vertebrae without spinous process (ch. 44[0]).	RAG-1: 6
	(*Marmosops incanus* (*M. impavidus-M. noctivagus*))	4	93	Middle hair of each caudal scale triplet thicker than the lateral hairs. Axis with neural arch and cranial notch narrow (ch. 13[0]). C6 and C7 spinous process of similar size (ch. 20[1]). Posteroventral extension on the ischium present (ch. 86[1]). Tibia with posterior crest for the insertion of m. *flexor digitorum tibialis* (ch. 101[1]).	IRBP: 11 DMP-1: 6 RAG-1: 5
	Marmosops impavidus-M. noctivagus	6	99	Anticlinal vertebra placed on T10 (ch. 29[0]). First vertebra where the accessory process is differentiated from the transverse process placed on T8 (ch. 30[2]). Sesamoids in the articular area between tibia, fibula, and astragalus absent (ch. 97[0]).	IRBP: 9 DMP-1: 12 RAG-1: 27
	(*Metachirus* (*Marmosops parvidens-M. pinheiroi*))	3	96	Spinous process posterior to the anticlinal vertebra cranially oriented (ch. 33[1]). S1 spinous process taller than S2 (ch. 41[1]). Femur with greater trochanter surpassing the level of the head (ch. 95[1]).	IRBP: 1 DMP-1: 2 RAG-1: 352
	Marmosops parvidens-M. pinheiroi	>7	100	Gular gland absent. Middle hair of each caudal scale triplet thicker than the lateral hairs. Premaxillae forming a distinct shelflike rostral process. Upper canine with anterior and posterior accessory cusps. Second sternebra laterally compressed (ch. 51[1]). Posteroventral extension on the ischium present (ch. 86[1]).	IRBP: 14 DMP-1: 17 RAG-1: 34
	Node B	1	<50	Tail scales in predominantly annular series. Deciduous lower third premolar with incomplete trigonid. Deltopectoral crest of humerus slightly developed (ch. 68[0]).	IRBP: 7 DMP-1: 8 RAG-1: 5
	Node A	4	83	Dorsal body pelage "tricolored". Central palmar surface of manus densely covered with small convex tubercles. Plantar epithelium of tarsus densely covered with coarse fur. Mammae extending anteriorly beyond pouch region to thoracic region. Tail incrassate by fat seasonally deposited. External lateral carpal tubercles absent in both sexes. Posterolateral palatal foramina extending lingual to M4 protocones. Fenestra cochleae of petrosal concealed within a sinus formed by the caudal and rostral tympanic process. One head on C4 transverse process (ch. 22[0]).	IRBP: 5 DMP-1: 6

APPENDIX 3
(*Continued*)

Node	Composition	BS	JK	Description of morphological synapomorphies	Molecular synapomorphies
	Thylamys	4	77	Nasals uniformly narrow, with lateral margins subparallel. p2 and p3 subequal in height. Transverse processes of atlas extended laterally to the same level as cranial articular fovea (ch. 9[1]). First thoracic vertebra with a low and craniocaudally expanded spinous process placed on T10 (ch. 27[0]). Longitudinal groove in lateral surface of the ulna absent (ch. 77[0]). Bicipital tuberosity of radius scarcely marked (ch. 81[0]).	IRBP: 3 DMP-1: 2
	T. pusillus-T. macrurus-T. pallidior	4	78	None	RAG-1: 13
	Node N	2	60	Manual digits III and IV subequal and longer than other manual digits. Proximal size of epipubic bones short (ch. 88[0]). Tibia with posterior crest for the insertion of m. flexor digitorum tibialis (ch. 101[1]).	DMP-1: 2 RAG-1: 19
	Cryptonanus	4	93	Extracranial course of mandibular nerve not enclosed by bone.	IRBP: 8 DMP-1: 20 RAG-1: 54
	Gracilinanus	4	98	Premaxillae forming a distinct shelflike rostral process. Maxillary fenestrae present.	IRBP: 1 DMP-1: 2 RAG-1: 33
	(*G. microtarsus* (*G. aceramarcae-G. agilis*))	4	98	None	DMP-1: 5 RAG-1: 19
	G. aceramarcae-G. agilis	4	76	None	RAG-1: 8